DISSECTION OF RECEPTOR FUNCTIONS THROUGH THE GENERATION OF A TCU-PA CLEAVAGE RESISTANT U-PAR: A U-PA INDEPENDENT ACTIVE U-PAR

BY

EVELYN C. NIEVES

DISSERTATION

Submitted in partial fulfillment of the requirements
for the degree of Doctor of Philosophy in Biochemistry
in the Graduate College of the
University of Illinois at Urbana-Champaign, 2012

Urbana, Illinois

Doctoral Committee:
Professor Bradford S. Schwartz, Chair
Professor James H. Morrissey
Professor Emeritus George Ordal
Assistant Professor Rutilio A. Fratti

Abstract

The regulation of protease activity is essential for physiological events, such as angiogenesis, inflammation, wound healing, and tumor invasion. Urokinase plasminogen activator receptor (u-PAR) has been widely studied in both systemic and cellular processes. Systemic roles for u-PAR include angiogenesis, inflammation and cancer while cellular roles include cell proliferation, survival, adhesion, migration, and localizing activation of plasminogen (Pg) (Blasi, Behrendt et al. 1990; Ellis, Behrendt et al. 1991; Nguyen, Hussaini et al. 1998; Chapman, Wei et al. 1999). u-PAR exerts its effects through both proteolytic and non-proteolytic mechanisms that are inter-related. Both functions are directly affected by the activation of u-PAR through the binding of its cognate ligand, urokinase plasminogen activator (u-PA).

u-PAR is a glycosidylphosphatidylinsotol (GPI)-anchored receptor that has the ability to activate Pg through localization of u-PA to the cell surface. In malignant cells, the increased glycosylation of u-PAR confers resistance to cleavage by two-chain urokinase plasminogen activator (tcu-PA) (Montuori, Rossi et al. 1999). Interestingly, the presence of highly glycosylated receptor prevents the tcu-PA from cleaving domain 1 (D_1) by decreasing u-PA's affinity for u-PAR.

The central hypothesis of the work described here involves the sensitive balance that is created by the binding of u-PA to u-PAR for both the activation and functional regulation of these proteins. u-PAR has the ability to localize u-PA to the cell surface to initiate Pg activation. tcu-PA also has the ability to cleave D_1 of u-PAR from the rest of the protein, which prevents localization of u-PA on the cell-surface.

To explore and characterize this relationship, we engineered a mutant u-PAR that prevents cleavage of D_1, and studied the effects on the activation of Pg, u-PAR dependent cellular migration and proliferation. Mutation of residues Arg 83 and Arg 89 in u-PAR leads to conformational changes that resemble the active conformation of u-PAR previously observed in crystal structures (Llinas, Le Du et al. 2005; Barinka, Parry et al. 2006; Huai, Mazar et al. 2006). Although our studies indicate that the initiation of the Pg activation cascade of our u-PAR mutants is essentially indistinguishable from wild type wt u-PAR, we also show an acceleration of the rate at which u-PA-PAI-1 complexes are cleared by α_2-macroglobulin receptor/ low-density lipoprotein receptor-related protein (LRP) through u-PAR binding. In addition, we observe an increase in cell proliferation, cell migration and changes in cell morphology that correlates with an increase in ERK signaling.

The u-PAR:LRP interaction we identified was remarkably novel, although one publication related u-PAR to LRP via binding the u-PA-PAI-1 complex, with u-PAR with minimal interaction via domain 3 of u-PAR (Czekay, Kuemmel et al. 2001). The u-PAR:LRP interaction we observed was supported by an increase in u-PAR detection when the mutant receptor was co-immunoprecipitated with an antibody against LRP. A similar increase was not observed with wt u-PAR. We also observed a direct impact on cell migration, adhesion and proliferation that are known to be u-PA dependent.

The ability of u-PAR to aid in cellular motility in response to local environment is intriguing, in light of the fact that there is a correlation between plasma levels and the amount of intact su-PAR found in cancer patients (Bifulco, Longanesi-Cattani et al. 2011). The ability of highly glycosylated u-PAR molecules to increase proliferative

events is also of interest. Over-glycosylation of u-PAR leads to resistance to cleavage by its cognate ligand, tcu-PA (Sier, Nicoletti et al. 2004). In addition, this effect is pronounced in highly metastatic anaplastic thyroid carcinoma (Montuori, Rossi et al. 1999). Studying the mechanisms used by u-PAR *in vitro* and *in vivo* provides great insight into which u-PAR activities are important in cancer. The expression of u-PAR in both neoplastic cells and tumor-associated cells from ovary, colon, lung, breast, endometrium, macrophages, endothelial cells, and fibroblasts indicates that u-PAR may be a useful therapeutic target since researchers have been able to correlate prognosis and u-PAR expression levels (Mazar 2001; Wang, Mao et al. 2001; Ge and Elghetany 2003; Sidenius and Blasi 2003; Mazzieri and Blasi 2005). Furthermore, u-PAR may be useful as a prognostic marker for cancer and to detect metastasis at an early stage. Generation of a non-cleavable u-PAR provides information regarding what relative roles are played by the intact and cleaved forms of the receptor.

To Sean, June and AJ

Acknowledgment:

After so many grueling and arduous years I can finally say: This dissertation is dedicated to everyone that throughout these years knowingly and unknowingly have helped me, molded me, or guided me to get where I am today. It is hard to fit or remember everyone, however, I will try and fit as many as I can in to these next few pages and do my utmost best to thank them.

I want to thank first and foremost my husband Dr. Shih-Hon Li (aka. Sean). I have to admit that I am blessed and lucky to have a person like you in my life. Without your everlasting, undoubted confidence in me I would have never written these words. Your enlightening words of wisdom and genuine love for research made many hours to Chicago into brainstorm sessions that I will always cherish. Thank you for the vast pool of knowledge, for your love and support, for the not giving up on me and my dream. These past few years have been of significant sacrifices but you taught me to believe in myself as a scientist, to trust my instincts and to take risks. This is a testament on what both of us, together, have accomplished as a team, colleagues, best-friends and husband and wife. I never thought that the day I met you, you would be the sense of reason for the rest of my scientific life. Thank you for taking care of June and A.J. during this long process.

I need to also thank my beautiful daughters, June and Audrey, for sacrificing time so I can finish this work, for understanding at quite a young age when mommy was busy. Thank you for sacrificing time with mommy so she can finish her dream. You both have taught me that unconditional love and passion for what you are doing in rewarding on itself.

To my parents, Agustin Nieves and Evelyn Torres, and to my sister and brother, thank you for understanding and supporting my ideas when I was growing up, for letting me be stubborn and challenge myself to the best of my abilities. Papi y mami, gracias por todas las veces que me llevaron a la biblioteca a escoger libros, por enseñarme todo sobre ciencia, por escucharme y apoyarme todos estos años. Aprecio el sacrifico que han hecho por mi y por darme la seguridad de que todo es posible en la vida. Siempre les agradeceré esta oportunidad. Para mis amistades de la Univ de Puerto Rico Marieliz, Charlene, Tito, Vimary, Manuel. Gracias por los apoyos y el soporte desde tan lejos, por tantos años. Siempre estarán en mi corazón.

I want to thank my advisor Dr. Naveen Manchanda for handing me handing over this project and letting me to run with my ideas. To Dr. Bradford Schwartz, I want to thank you for putting up with me, for encouraging me all these years. It was a long road and I thank you for always having a few minutes to listen to me. Thank you for being honest, straightforward and the voice of reason during the times I needed it most. You taught me a lot about how to be a good scientist and guided me even though my choices sometimes were not as well communicated to you. To the Schwartz lab (Christina, Karen, Lucienne, Sean and Julie), thank you for their constant and everlasting support and making the lab a pleasure to work in. I cannot stop before thanking the Biochemistry department in Univ of Illinois. From the beginning everyone has been completely understanding and helpful. Louise Cox, Colin Wraight, Jim Morrissey, Susan Martinis and everyone in the graduate college. Thank you for the positive feedback and the strong support I received when I had to make the difficult choices in my degree.

I also need to thank all my friends from all walks of life that I met in Champaign-Urbana. Paul, Willie, Franklin, Keki, Brad, Katharina, the Ordal Lab. So much to be grateful that all of you were in my life as a graduate student.

Last but definitely not least, I need to thank Dr's Pavan Reddy, Sophie Paczensy, Yi Zhang and everyone from the Univ of Michigan BMT program and Internal Medicine. Thank you for cheering me on throughout these years and shining a light at the end of the tunnel so I did not give up in the darkest moments.

Table of Content:

Abbreviations xii

List of Figures xiv

List of Tables xvi

CHAPTER 1: INTRODUCTION 1

1.1. Regulation of u-PAR mRNA 1
1.2. u-PAR protein and structure 2
1.3. Proteolytic functions of u-PAR 5
1.3.1. Plasminogen activation cascade 5
1.3.2. Internalization of u-PAR and clearance of u-PA-PAI-1 7
1.3.3. Resurfacing and receptor degradation 9
1.4. Non-proteolytic role of u-PAR 10
1.4.1. Adhesion 10
1.4.2. Signaling 13
1.4.3. Cell migration 16
1.4.4. Cell proliferation 18
1.4.5. Cell apoptosis 19
1.5. The role of u-PAR in cancer 20
1.6. Overview of project 23
1.7. Figures and Tables 25

CHAPTER 2: MATERIALS AND METHODS 34

2.1. Materials 34
2.2. Methods 35
2.2.1. Site-directed mutagenesis of u-PAR variants 35
2.2.2. Stable transfection into 293 37
2.2.3. Antibody purification 37
2.2.4. u-PAR immunoblotting 38
2.2.5. u-PAR cleavage assay 38
2.2.6. Reverse transcriptase PCR 39
2.2.7. Flow cytometry 41
2.2.8. Inactivation of tcu-PA 41
2.2.9. ^{125}I Protein labeling 41
2.2.10. Competition binding assay 42
2.2.11. Fibrinolytic assay 42
2.2.12. Cell-surface bound u-PA in plasminogen activation and inhibition 43
2.2.13. Internalization assay 44
2.2.14. Receptor recycling assay 45
2.2.15. Co-immunoprecipitation of u-PAR with LRP 45

2.2.16. Chymotrypsin cleavage assay 46
2.2.17. Cell morphology 46
2.2.18. Immunofluorescence 47
2.2.19. Proliferation assay 47
2.2.20. Dissociation assay 47
2.2.21. Adhesion assay 48
2.2.22. Migration assay 48
2.2.23. Cell signaling 49
2.2.24. Cell death 50
2.2.25. Caspase assay 50
2.2.26. Apoptosis assay 50
2.3. Figures and Tables 51

Chapter 3: CHARACTERIZATION OF WILD TYPE U-PAR AND MUTANT U-PAR VARIANTS 52

3.1. Introduction 52
3.2. Results 53
3.2.1. Site-directed mutagenesis of u-PAR: Generation of a cleavage resistant receptor 53
3.2.2. Generating stable-transfected 293 cells expressing the u-PAR variants 54
3.2.3. u-PAR with Arg^{83} and Arg^{89} mutated proves to be an effective cleavage resistant variant 56
3.2.4. The cleavage resistant receptor has high affinity interactions with its ligands, and is over-expressed in 293 cells 58
3.2.5. Binding of tcu-PA to the u-PAR variants promotes plasminogen activation 59
3.2.6. Specificity of u-PAR based plasminogen activation 60
3.2.7. cr-uPAR has a decreased rate of fibrin clot lysis than its wt u-PAR counterpart 60
3.3. Discussion 61
3.4. Figures and Tables 64

Chapter 4: CR-UPAR IS IN A CONFORMATION THAT IS PREDOMINANTLY U-PA INDEPENDENT 77

4.1. Introduction 77
4.2. Results 79
4.2.1. Cell surface regulation of scu-PA and tcu-PA 79
4.2.2. Cells expressing cr-uPAR internalize u-PA-PAI-1 complexes more rapidly than those cells expressing wt u-PAR 80
4.2.3. cr-uPAR recycling is increased following internalization of u-PAR:u-PA-PAI-1 complexes 82

4.2.4. cr-uPAR binds LRP in the absence of u-PA-PAI-1 complex 83
4.2.5. Chymotrypsin cleaves cr-uPAR at a different rate than wt u-PAR 84
4.3. Discussion 85
4.4. Figures and Tables 90

CHAPTER 5: EFFECTS OF CR-UPAR ON CELL MORPHOLOGY AND BIOLOGY 98

5.1. Introduction 98
5.2. Results 99
5.2.1. Expression of u-PAR alters the cells by elongating their processes 99
5.2.2. Localization of u-PAR to focal adhesion points 101
5.2.3. u-PAR variants promote enhanced adhesiveness and delay cellular dissociation on a Vtn based matrix 102
5.3. Discussion 103
5.4. Figures and Tables 106

CHAPTER 6; CELLULAR RESPONSES CHANGE DRAMATICALLY WHEN CR-UPAR IS EXPRESSED 112

6.1. Introduction 112
6.2. Results 114
6.2.1. cr-uPAR expressing accelerates cellular proliferation independent of u-PA 114
6.2.2. The presence of cell-surface cr-uPAR enhances basal activation of ERK similar to active wt u-PAR 115
6.2.3. Both wt u-PAR and cr-uPAR cell variants use additional signaling pathways 116
6.2.4. Decreased apoptosis contributes to the enhanced cell number seen in 293 cr-uPAR cell cultures 117
6.2.5. Expression of cr-uPAR promotes migration paralleling the effects of activated wt u-PAR 118
6.2.6. Migration via the GPCR pathway is unaffected by the presence of cr-uPAR 119
6.3. Discussion 120
6.4. Figures and Tables 123

CHAPTER 7: Summary and New Directions 132

References 137

Abbreviations:

ATF: amino terminal fragment of urokinase plasminogen activator

c-uPAR: cleaved urokinase plasminogen activator receptor

Co-IP: co-immunoprecipitate

CHX: cycloheximide

CMK: Glu-Gly-Arg-chloromethyl ketone

complexes: u-PA-PAI-1 complexes

D_1: domain 1

D_2D_3: domain 2 and domain 3

FCS: fetal calf serum

GPI: glycosylphosphatidylinositol

GFD: growth factor domain

GPCR: G-protein coupled receptor

FBS: fetal bovine serum

HEK293, 293: human embryonic kidney-293

LDLR: low density lipoprotein receptor

LRP: α-macroglobulin receptor / low density lipoprotein receptor-related protein

PAI-1: plasminogen activator inhibitor type-1

Pg: plasminogen

PMA: phorbol myristate acetate

Pn: plasmin

PTX: pertussis toxin

RAP: receptor associated protein

scid: severe combined immunodeficiency

scu-PA: single-chain urokinase plasminogen activator

serpin: serine protease inhibitor

su-PAR: soluble urokinase plasminogen activator receptor

SMB: somatomedin B domain

SF: serum free

cr-uPAR: tcu-PA cleavage-resistant urokinase plasminogen activator receptor

tcu-PA: two-chain urokinase plasminogen activator

TNF-α: tumor necrosis factor- alpha 1

u-PA: urokinase plasminogen activator

u-PAR: urokinase plasminogen activator receptor

Vtn: vitronectin

List of Figures:

1.1. mRNA structure for u-PAR 25
1.2. u-PAR domain 1 schematic and crystal structure. 26
1.3. Schematic of u-PAR structure 27
1.4. Crystal structure of u-PAR with the ATF and the linker region 28
1.5. Structures of Plasminogen forms 29
1.6. Urokinase type plasminogen activator forms 29
1.7. Plasminogen activation cascade 30
1.8. Schematic of Vitronectin 31
3.1. Generation of u-PAR mutants 64
3.2. DNA and protein sequence alignment 65
3.3. Expression of different u-PAR variants 66
3.4. u-PAR mRNA detection in 293 cr-uPAR but not in 293 cells 67
3.5. Detection of u-PAR by flow cytometry 68
3.6. Cleavage profiles of u-PAR expressing cells 69
3.7. Cleavage profiles for u-PAR expressing single point mutants 70
3.8. Competitive binding for u-PAR variants expressed in 293 cells 71
3.9. Both cell surface u-PAR variants bind specifically to u-PA and initiate Pg activation 72
3.10. Cells expressing the single point u-PAR mutants can generate Pn 73
3.11. Cell surface u-PAR variants undergone receptor cleavage limits Pn generation 74
3.12. Generation of fibrin degradation fragments is deterred in cr-uPAR expressing cells 75
4.1. u-PA inhibition by PAI-1 is unaffected by the presence of cr-uPAR 90
4.2. Internalization and receptor resurfacing is dramatically faster in the presence of cr-uPAR. 91
4.3. Presence of RAP prevents internalization of tcu-PA-PAI-1 bound to u-PAR 92
4.4. Addition of biotinylated complex promotes internalization of u-PAR 93
4.5. Unoccupied cr-uPAR resurfaces more rapidly 94
4.6. cr-uPAR co-immunoprecipitates with LRP in the absence of u-PA-PAI-1 complexes 95
4.7. LRP interaction by cr-uPAR is not significantly disrupted by addition of complex 96
4.8. Impaired cleavage of cr-uPAR by chymotrypsin as compared to wt u-PAR 97
5.1. Expression of u-PAR alters the 293 cell morphology 106
5.2. Removal of GPI-anchored receptors shows reversal of cell morphology changes 107
5.3. Distribution and cell-surface localization of u-PAR on 293 cells 108
5.4. Expression of u-PAR variant on 293 cells leads to changes in processes 109
5.5. Expression of u-PAR leads to changes in adhesion and dissociation in 293 cells 110

6.1. cr-uPAR expressing cells proliferate more rapidly than their untransfected counterparts 123
6.2. cr-uPAR cells proliferate similar to uPA-bound wt u-PAR cells, which are regulated by multiple pathways 124
6.3. Expression of cr-uPAR induces hyper-activation of ERK 125
6.4. 293 cells expressing uPAR have reduced apoptosis 126
6.5. Expression of u-PAR diminishes induction of cell death 127
6.6. 293 cr-uPAR expressing cells promote u-PA-independent migration 128
6.7. Migration of cr-uPAR on serum-coated membranes is similar to that of Vtn coated membranes 129
6.8. 293 cells show no random chemotaxis 129
6.9. Inhibition of GPCR pathway prevents migration of u-PAR expressing cells 130

List of Tables:

Table I: Functional binding partners of u-PAR 32
Table II: The u-PA -u-PAR activated signaling pathways and its biological relevance. 33
Table III: u-PAR primers for site-directed mutagenesis.....51
Table IV: Binding of CMK-uPA to 293 cells.....76
Table V: Elongation of cellular processes 111
Table VI: Proliferation of 293 cells under normal conditions 131

CHAPTER 1. INTRODUCTION

1.1.Regulation of u-PAR mRNA

Urokinase plasminogen activator receptor (u-PAR), is a species-specific, cognate cell-surface receptor for urokinase plasminogen activator (u-PA). The human u-PAR gene (PLAUR) has been localized to chromosome 19q13.2. It spans 23 kb of genomic DNA and contains seven exons and six introns (Borglum, Byskov et al. 1992). The u-PAR gene shares approximately 76 % sequence homology between mouse, bovine and rat u-PAR (Reuning, Little et al. 1993). Expression levels for u-PAR range from 50,000 to 200,000 receptors per cell in normal cells, with a 4-5 fold increase in expression in cancer cells (Plow, Freaney et al. 1986).

Regulation of u-PAR expression occurs at both the transcriptional and post-transcriptional levels. The u-PAR gene contains a promoter region -141 to +47 bp relative to the transcription initiation site (Fig. 1.1.1) (Wang 2001). The TATA and CAAT boxes are missing from the upstream region of u-PAR, but it does have a GpC-rich region containing both cis- and trans-acting factor binding sites that regulate u-PAR gene expression (Soravia, Grebe et al. 1995). These include a proximal AP-1, a distal AP-1, an AP-2 and NF-κB response elements (Soravia, Grebe et al. 1995; Dang, Boyd et al. 1999; Wang, Dang et al. 2000). Wang *et al*., observed an increase in u-PAR expression on colon cancer cells with either tumor necrosis alpha-1 (TNF-α) or phorbol-12 myristate acetate (PMA) stimulation. Post-transcriptional regulation is carried out by several different sequence elements that promote mRNA decay or stability, including an AU-rich element in the 3' untranslated region that is highly conserved among u-PAR from several species (Wang, Collinge et al. 1998; Nau, Guerin-Dubiard et al. 2003; Kotzsch,

Sieuwerts et al. 2008). Degradation through the 3' AU-rich element occurs as the 3'-Poly(A) tail is shortened (Chen and Shyu 1995). In addition, both stabilizing and destabilizing regulatory elements have been found in the coding region (Shetty, Kumar et al. 1997; Montuori, Mattiello et al. 2001; Montuori, Mattiello et al. 2003; Shetty, Muniyappa et al. 2004).

u-PAR's cognate ligand, u-PA, has the ability to upregulate u-PAR expression. Promotion of u-PAR expression by u-PA occurs at the transcriptional level due to increased activity of the transcription factor Sp1, while post-transcriptional regulation by u-PA is due to changes in activity and concentration of stabilizing factors, such as the embryonic lethal, abnormal vision (ELAV) RNA-binding protein, Hu antigen R (HuR) (Tran, Maurer et al. 2003), and heterogeneous nuclear ribonucleoprotein C (hnRNPC) (Shetty 2005). These stabilizing factors bind to the coding region of u-PAR mRNA, preventing messenger degradation (Montuori, Mattiello et al. 2001).

1.2. u-PAR protein and structure

u-PAR is a heavily and heterogeneously glycosylated glycosylphosphatidylinositol-anchored (GPI) cell-surface protein. The apparent molecular weight of u-PAR is 50-65 kD. Forty percent of the molecular weight is attributed to glycosylation (Blasi, Stoppelli et al. 1986; Moller, Pollanen et al. 1993; Ploug 1998), and enzymatic deglycosylation of u-PAR results in a 35 kD protein. Widely distributed in the body, u-PAR is expressed by human monocytes (Miles and Plow 1987), kidney, vascular endothelium (Miles, Levin et al. 1988; Barnathan, Kuo et al. 1990), fibroblasts, and sperm cells. It is also expressed by several types of malignant cells (Needham, Nicholson et al. 1988; Cohen, Xi et al. 1991;

Ossowski, Clunie et al. 1991). In addition, a soluble form of u-PAR (su-PAR) which lacks the GPI-anchor, circulates in the plasma of humans and mice (Kasperska-Zajac and Rogala 2005).

The nascent u-PAR protein consists of 313 residues that encode a 21-residue signaling peptide, three Ly-6 domains, a 14-residue linker region, a C-terminal GPI-anchor, and five potential glycosylation sites (Moller, Pollanen et al. 1993) (Figure 1.1.2). The 21-residue signaling peptide is not included in the nascent protein, since it is removed from the N-terminal region during post-translational modification. In addition, the 30-residue peptide on the C-terminal, beginning with Gly^{283}, is removed for incorporation of the GPI-anchor (Moller, Ploug et al. 1992). The extent of glycosylation varies between different cell types, and may account for the differences in affinity for u-PA. Substitution analysis of the five potential glycosylation sites (Asn^{52}, Asn^{162}, Asn^{172}, Asn^{200}, and Asn^{233}) in u-PAR determined that glycosylation at residue Asn^{52} is required both for high affinity to u-PA and for secretion of the protein (Figure 1.1.3) (Moller, Pollanen et al. 1993; Ploug, Rahbek-Nielsen et al. 1998). Glycosylation of the other four sites aid in high affinity interactions with u-PA (Nielsen, Kellerman et al. 1988; Estreicher, Wohlwend et al. 1989; Ploug, Rahbek-Nielsen et al. 1998).

u-PAR has three highly homologous cysteine-rich domains, each consisting of 90 residues that are linked by a total of 28 cysteines (Ploug, Kjalke et al. 1993). These domains have a finger-like shape with three adjacent loops that form a planar anti-parallel β-sheet with four highly conserved disulfide bonds in domains 1 (D_1) and 2 (D_2), and three disulfide bonds in domain 3 (D_3). Ly-6, snake venom α-neurotoxin, and polycythemia rubra vera 1 (PRV-1) are proteins with internal sequence homology, based

on cysteine residue patterns similar to u-PAR (Temerinac, Klippel et al. 2000). u-PAR's three domains form a concave shape with a maximal diameter of 52 Å and a height of 27 Å (Barinka, Parry et al. 2006). The growth factor domain (GFD) of u-PA interacts with the cavity of u-PAR, making contact with all three domains. Although D_1 was originally identified as primarily responsible for the high affinity binding of u-PAR to u-PA, (Ronne, Behrendt et al. 1991) it was more recently observed that both D_2 and D_3 also contribute. Domain 2 contacts key residues of the amino terminal fragment (ATF), forming most of the hydrogen bonds between u-PAR and ATF. Domain 3 interacts with the ATF through helix $\alpha 3$ and forms part of the su-PAR cavity by interacting with D_1, closing the cavity (Huai, Mazar et al. 2006).

Binding of u-PA to u-PAR causes conformational changes that convert the receptor from an inactive to an active form. This conversion allows for new interactions with other proteins such as vitronectin (Vtn) and some integrins (Hoyer-Hansen, Behrendt et al. 1997; Wei, Czekay et al. 2005). Several researchers have identified regions in u-PAR that move upon the binding of u-PA (Huai, Mazar et al. 2006; Gardsvoll and Ploug 2007). Crystallization studies indicate that u-PAR undergoes major changes in inter-domain alignment upon ATF binding, potentially exposing new epitopes on the receptor surface (Barinka, Parry et al. 2006). One such area that is altered upon ligand-binding is the 14-residue linker region, which is a flexible unstructured loop between D_1 and D_2. It does not directly contribute to u-PAR's affinity for u-PA (Fig. 1.1.4). Within this linker region is a key five-residue sequence, ^{88}SRSRY^{92}, called the "chemotactic epitope". This epitope is exposed when u-PA binds to u-PAR, as are residues essential for Vtn-binding. While the only crystal structure available of unliganded u-PAR contains a disulfide bond

that links D_1 to D_3, comparison of the structures of u-PAR, complexed to either a small inhibitory peptide or to ATF, suggests that the different ligands induce different amounts of conformational change in u-PAR. The linker region is more completely resolved and the diameter of the central cavity is smaller when u-PAR is co-crystallized with ATF, rather than a small peptide. This suggests that binding of u-PA causes changes not only to the cavity, but also to the linker region of the receptor (Barinka, Parry et al. 2006).

1.3.Proteolytic functions of u-PAR

1.3.1. Plasminogen activation cascade

u-PAR is involved in the initiation of pericellular plasminogen (Pg) activation, which generates the broad-specificity serine protease, plasmin (Pn), from its zymogen precursor, Pg (Fig. 1.1.5). Pg activation leads to the dissolution of fibrin clots and the digestion of extracellular matrices and basal membranes. In addition, there is strong evidence implicating the Pg activation cascade in cancer, i.e. colorectal cancer, breast cancer and prostate cancer (Duffy, Reilly et al. 1990; Pyke, Kristensen et al. 1991; Zhang, Sud et al. 2011). Currently, the proteins in the cascade are being used as prognostic markers and biomarkers. Plasminogen is a 92 kD single-chain glycoprotein that is synthesized primarily in the liver and circulates in plasma at a concentration of 1.5-2 μM with a plasma half-life of approximately two days. It has five N-terminal kringle domains, with the first and fourth kringle domains lending to high-affinity and low-affinity fibrin-binding, respectively, and a C-terminal serine protease domain. The kringle domains allow Pg to interact with fibrin, cell-surface receptors, and permit rapid binding of the

cognate inhibitor α_2-antiplasmin to Pn. Activation of Pg occurs by a single cleavage event of the zymogen protease domain, Arg^{560}-Val^{561}.

The serine protease u-PA is a 54 kD protein that is secreted by the endothelium and kidneys in the zymogen single-chain form (scu-PA) (Fig. 1.1.6). The active protease is a two-chain form (tcu-PA) that is generated by cleavage of the peptide bond, Lys^{158}-Ile^{159}. u-PA is comprised of 411-residues that create the serine protease domain, a kringle domain and an epidermal growth factor (EGF) domain. u-PA may also undergo a secondary cleavage at Lys^{136}-Lys^{137} to produce two new fragments, the ATF and low-molecular weight u-PA (LMW-uPA). The ATF has no catalytic activity, since it contains only the EGF domain and most of the kringle domain, whereas LMW-uPA contains the serine protease domain. Intact u-PA binds to u-PAR with high affinity (K_D 0.5 pM - 2 nM) (Hoyer-Hansen, Ronne et al. 1992; Behrendt, Ronne et al. 1996). The half-life of the u-PA:u-PAR complex is several hours (Stoppelli, Corti et al. 1985; Vassalli, Baccino et al. 1985), and the receptor-enzyme complex has not been observed to be taken up by the cell. u-PAR amplifies the Pg activation cascade (Fig. 1.1.7) by localizing scu-PA on the cell-surface and augmenting the intrinsic activity of scu-PA 10^3-fold, thus accelerating the generation of Pn from the widely present precursor protein, Pg (Manchanda and Schwartz 1991; Ellis, Whawell et al. 1999). Pn cleaves scu-PA to the active protease tcu-PA, causing feedback activation and resulting in further augmentation of Pn generation. Cleavage of u-PA by Pn in the GFD of u-PA generates a 33 kDa u-PA, which lacks u-PAR affinity helping to regulate the Pg activation cascade (Saksela and Rifkin 1988).

Enzymatic activity of free u-PA or u-PAR-bound u-PA is inhibited by the serine protease inhibitor (serpin), plasminogen activator inhibitor-1 (PAI-1). PAI-1 is a 45 kD single chain glycoprotein consisting of 319 residues that contains a reactive peptide bond Arg^{346}-Met^{347} (Ginsburg, Zeheb et al. 1986). PAI-1 is found in plasma, platelets, adipose tissue, and in endothelial cells. It is also expressed pathologically by several types of neoplastic cells (e.g. hepatoma, fibrosarcoma) (Erickson, Schleef et al. 1985; Blasi, Vassalli et al. 1987; Juhan-Vague, Alessi et al. 1991). PAI-1 is a rapid and efficient inhibitor of u-PA. PAI-1 can reversibly inhibit scu-PA, but irreversibly inhibits tcu-PA, due to formation of a 1:1 molar ratio of SDS-stable covalent complexes. PAI-1 is also a rapid physiologic inhibitor of tissue-type plasminogen activator (t-PA), and can inactivate Pn *in vitro* (Declerck, De Mol et al. 1992).

1.3.2. Internalization of u-PAR and clearance of u-PA-PAI-1

The u-PA-PAI-1 covalent complex is found in solution and bound to the cell surface. The enzyme-inhibitor complex is cleared via protein degradation. u-PAR plays a secondary role in aiding the clearance of the u-PA-PAI-1 complex by forming a tertiary complex, u-PAR:u-PA-PAI-1. The receptor-bound protease-serpin complex is cleared from the cell surface by the endocytic receptor, α_2-macroglobulin receptor / low density lipoprotein receptor-related protein (LRP) (Nykjaer, Kjoller et al. 1994; Conese, Nykjaer et al. 1995; Czekay, Kuemmel et al. 2001). LRP, also known as LRP1, is a member of the LDL receptor family and is a multifunctional scavenger that plays a role in lipid metabolism. LRP internalizes target ligands via clathrin-mediated endocytosis with subsequent ligand clearance and degradation. LRP is essential for survival, as homozygous knock-out mice are not viable (Jedrychowski, Gartner et al. 2010)). LRP is

a transmembrane protein with molecular weight of 600 kD that contains a light chain (85 kD) and a heavy chain (515 kD), which contains four clusters of cysteine-rich complement repeats and a cytoplasmic tail with NPxY motifs. The receptor interacts with at least 30 different ligands, including t-PA-PAI-1, u-PA-PAI-1, fVII:TF:TFPI, integrins, and u-PAR (Kounnas, Church et al. 1996; Rodenburg, Kjoller et al. 1998; Zhang, Sakthivel et al. 1998). The major ligand-binding regions are within either cluster II or IV.

Receptor-associated protein (RAP) is a molecular chaperone for LDLR family members. It is a 39 kD membrane anchored protein localized to the endoplasmic reticulum and is recognized by LRP clusters I and III (Horn, van den Berg et al. 1997). RAP antagonizes the binding of all other known LRP ligands, thus preventing premature association of ER proteins to the receptor. Recombinant soluble RAP has served as an invaluable tool in the study of LRP biology, since it also blocks the binding of ligands on the cell surface (Williams, Ashcom et al. 1992).

u-PA-PAI-1 complexes are recognized by LRP, but pre-binding to u-PAR is required for internalization and degradation to occur, unless u-PA-PAI-1 complexes are present at high concentrations. The quaternary complex, once formed, rapidly undergoes clathrin-mediated endocytosis. Internalization results in movement of the quaternary complex from the cell-surface into early-endosomes (Czekay, Kuemmel et al. 2001). Within the early-endosomes, the u-PA-PAI-1 complexes dissociate from both u-PAR and LRP, and are directed into late-endosomes. The u-PA-PAI-1 complexes are transferred to end-lysosomes for degradation, while u-PAR and LRP resurface (Nykjaer, Conese et al. 1997). u-PAR has only been identified in late lysosomes in one study (Nykaer 1998).

Bridging via the u-PA-PAI-1 complex appears to be primarily responsible for the tight interaction between u-PAR and LRP, although one study found a direct interaction between the endocytic receptor and D_3 of u-PAR. Because internalization decreases the concentration of u-PAR on the cell-surface, it provides an efficient mechanism for immediate downregulation of the cell surface proteolytic processes mediated by the u-PA:u-PAR complex. Receptor internalization may also assist cells in modulating several key functions such as adhesion and migration, since u-PAR interacts with high affinity to the extracellular matrix by Vtn (Nykaer 1998; Cao, Lawrence et al. 2006).

1.3.3. Resurfacing and receptor degradation

Recent studies show that u-PAR and LRP are internalized and recycled in the same vesicles. LRP-mediated internalization can result in the redistribution of u-PAR to focal adhesion sites, where u-PAR subsequently aids in the activation of proteolysis and/or engagement of cell-matrix contact (Czekay and Loskutoff 2009). u-PAR can also be internalized and recycled in specialized lipid rafts called “caveolae” (Cortese, Sahores et al. 2008). Caveolae are flask-shaped invaginations of the plasma membrane containing the protein caveolin, a 22 kD protein (Rothberg, Heuser et al. 1992) that plays a role in signaling, migration, cholesterol uptake, and internalization via a non-clathrin mechanism (Stan 2007). Clustering of u-PAR to calveolae augments pericellular Pg activation and a wide array of cellular signaling (Stahl and Mueller 1995; Wei, Yang et al. 1999; Cavallo-Medved, Mai et al. 2005). u-PAR also clusters with β_1-integrins in the presence of caveolin, promoting kinase recruitment, ERK signaling, and cell adhesion (Wei, Yang et al. 1999; Tang, Burke et al. 2009)

1.4.Non-proteolytic role of u-PAR

u-PAR interacts with several proteins [e.g. Vtn, integrins, and epidermal growth factor receptor (EGFR)], and strongly influences cell adhesion, signaling, proliferation, migration and cell differentiation in both normal and neoplastic cells (Wei, Tang et al. 2007; Madsen and Sidenius 2008). u-PAR-mediated activities modulate physiologic processes such as wound healing, inflammation, and stem cell mobilization, as well as pathophysiological processes such as metastasis and tumor invasion. More recently, *in vivo* studies showed that u-PA:u-PAR interaction suppresses fibrin-associated chronic inflammation (Connolly, Choi et al. 2010).

Since u-PAR lacks a transmembrane domain and a cytoplasmic domain, it is unable to signal directly. Thus, GPI-anchored proteins, such as u-PAR, interact with transmembrane proteins through lateral binding to affect intracellular signaling (Korty, Brando et al. 1991; Stefanova, Horejsi et al. 1991; Anderson 1994) The *cis*-ligands for u-PAR are EGFR, LRP, caveolin, integrins, and FPRL1 (Table I). As discussed above, the binding of u-PA to u-PAR leads to receptor activation and promotes the interaction with other cell-surface or matrix proteins (Table I). Liberation of u-PAR from its GPI-anchor by proteases or phospholipases, and the subsequent generation of soluble u-PAR, shifts its role from a receptor to that of a soluble ligand capable of initiating ERK and FAK signaling events (Piccolella, Festuccia et al. 2008).

1.4.1. Adhesion

Cell surface u-PAR is found in close proximity to proteins that mediate adhesion and expression of u-PAR increases cellular adhesion. Direct interactions between u-PAR, Vtn, and members of the integrin superfamily have been extensively investigated in a

wide variety of cell types (i.e. H1299, MCF-7, MDA-MD-231) (Dass, Ahmad et al. 2007). u-PAR-dependent adhesion is regulated by u-PA, PAI-1, and the endocytic receptors, utilizing u-PA-induced u-PAR activation and endocytosis-mediated downregulation to control the affinity and availability of cell-surface u-PAR for its binding partners.

Vitronectin is primarily synthesized in the liver as a 456-residue single-chain polypeptide and 19-residue signaling sequence. It predominantly circulates in human plasma as a 75 kD protein. The N-terminal 44-residue is known as the somatomedin B domain (SMB). The SMB domain of Vtn binds to u-PAR and PAI-1 in a mutually exclusive manner. At the C-terminal of the SMB domain is the RGD sequence that is critical to the binding of Vtn with integrins and mediates adhesion (Chillakuri, Jones et al. 2010). An area adjacent to the RGD region contains two sulfated tyrosines that bind extracellular matrix (ECM) proteins, such as collagen. Near the C-terminus, spans basic residues that binds heparin and other glycosaminoglycans, and may contain a lower-affinity, secondary binding site for PAI-1.

u-PA promotes the binding of Vtn to u-PAR (Madsen, Ferraris et al. 2007). The dissociation constant for u-PAR and Vtn in the absence of u-PA is approximately 1.9 μM. When u-PA is pre-bound to u-PAR, the affinity for Vtn increases about 4-fold to 0.4 μM. *In vitro*, the u-PA effect is nullified when u-PAR is over-expressed, potentially due to avidity (Wei, Waltz et al. 1994; Wei, Lukashev et al. 1996; Cunningham, Andolfo et al. 2003). Vitronectin binding does not alter the affinity of u-PAR for u-PA.

Recent mutational analysis of the interaction between u-PAR and Vtn showed that this interaction is distant from the u-PA binding site of u-PAR. Because proteolytic

removal of D_1 disrupts the interaction between Vtn and u-PAR (Sidenius and Blasi 2000), cleavage of D_1 can mediate cell-adhesion (Montuori, Carriero et al. 2002). Alanine scanning analysis identified five residues in u-PAR that contribute to Vtn binding. These consist of three residues from D_1 (Trp^{32}, Arg^{58} and Ile^{63}) and two residues from the linker region (Arg^{91} and Tyr^{92}) (Gardsvoll and Ploug 2007; Madsen, Ferraris et al. 2007). Crystal structures of the ATF:u-PAR:SMB complex indicate that SMB interacts with the D_1-D_2 region of u-PAR, which is found on the opposite side of the u-PA binding cavity. Vtn binds PAI-1 with high affinity (K_D < 100nM) at a site that adjacent to the u-PAR binding site. Because the binding sites on Vtn for u-PAR and PAI-1 are located so closely together, PAI-1 can effectively block the association of the receptor with Vtn, thus nullifying the contribution of this interaction to cellular adhesion (Preissner, Kanse et al. 1999).

Adhesion is also mediated through the interaction of u-PAR and integrins. Integrins are ubiquitous transmembrane adhesion molecules that are involved in cell-cell or cell-ECM contacts. Integrins are α/β heterodimeric receptors that interact with many extracellular matrix and cell-surface proteins and regulate cellular adhesion, migration, growth, survival and differentiation. u-PAR and integrins co-localize at focal adhesion points at the leading edge of migrating cells (Estreicher, Muhlhauser et al. 1990). Binding of u-PAR to integrins is distinct from that with Vtn or u-PA, since peptides blocking integrin:u-PAR interactions do not affect either the formation of u-PAR:Vtn complexes or u-PAR:u-PA complexes (Simon, Wei et al. 2000). However, the manner in which u-PAR binds to integrins remains unknown.

u-PAR interacts with β_1, β_2 and β_3 integrins, but associates most strongly with members of the β_1 family (Wei 1996). On 293 cells, expression of u-PAR redirects adhesion from a β_1 integrin-fibronectin mechanism to a u-PAR:Vtn mechanism (Wei 1996) The β_2 family plays an important role in inflammation, specifically in leukocyte migration and adhesion. u-PAR, in the presence of u-PA, co-localizes with $\alpha_v\beta_3$ in the membrane ruffles of smooth muscle cells (Degryse, Resnati et al. 1999), the presence of Vtn promotes clustering of u-PAR and $\alpha_v\beta_3$ (Stepanova and Tkachuk 2002). Expression levels of u-PAR and $\alpha_v\beta_3$ appear to be co-regulated, and migration can be inhibited by either anti-u-PAR or anti-$\alpha_v\beta_3$ antibodies (Degryse, Resnati et al. 1999).

1.4.2. Signaling

Interaction of u-PAR with a number of proteins can activate kinase cascades, these include integrins, epidermal growth factor receptor (EGFR), the GPCR FPR-like receptor-1 / lipoxin A4 receptor (FPRL-1), caveolin, gp130, and kininogen (Smith and Marshall 2010). This wide signaling specificity is attributed to the dynamic composition of the u-PAR-receptor signaling complex (Jo, Thomas et al. 2003). A recent crystal structure indicates that a large interface on u-PAR is available for interaction with these proteins (Huai, Mazar et al. 2006).

Though much has been uncovered on u-PAR's structure-function relationships, the mechanism by which u-PAR accomplishes intracellular signaling remains unclear. u-PAR affects cellular behavior and functions in ways that are both u-PA-dependent and -independent. u-PAR contains a unique linker region between D_1 and D_2 that is sensitive to proteolysis by tcu-PA, Pn, and matrix metalloproteases (MMP) (Hoyer-Hansen, Ronne et al. 1992; Hoyer-Hansen, Ploug et al. 1997; Montuori, Rossi et al. 1999). u-PA-

mediated cleavage of u-PAR in the linker region is only observed in GPI-anchored u-PAR since it requires the enzyme to be concurrently bound to a second membrane-bound u-PAR molecule, facilitating protease-substrate recognition (Hoyer-Hansen, Pessara et al. 2001). This trans-cleavage dissociates D_1 from the rest of the anchored receptor that results in a loss of affinity for u-PA and Vtn. The generation of a new N-terminal region in u-PAR exposes the previously buried chemotactic epitope, ^{88}SRSRY^{92}, which leads to changes in migration and signaling (Fig. 1.1.3) (Fazioli, Resnati et al. 1997). A pentapeptide, based on the chemotactic epitope, induces signaling events and reduces adhesion (Gargiulo, Longanesi-Cattani et al. 2005). While receptor cleavage is a powerful trigger for changes in cellular behavior, alterations in proliferation, adhesion, migration, and differentiation can also be induced by enzymatically inert forms of urokinase, such as the zymogen scu-PA, chemically inactivated tcu-PA, and ATF. These observations led to the hypothesis that binding of u-PA to u-PAR leads to conformational changes that increase interactions with the adapter protein listed above, ultimately enhancing signaling events (Mukhina, Stepanova et al. 2000).

Since the effects of u-PA-binding and u-PA-mediated cleavage on u-PAR-dependent cellular events are at least partially overlapping, the physiological relevance of these two modes of u-PAR activation has been difficult to delineate. The roles of u-PAR in cell signaling have also been difficult to dissect because the cellular response varies depending on the ligand to which u-PAR is exposed, the cell line studied, and the make-up of the membrane receptor signaling complex. Despite these challenges, several different u-PAR-influenced signaling pathways have been isolated (Table II), including ERK/MAPK, Src, GPCR, and JAK/STAT.

ERK/MAPK signaling activation is required for cell differentiation, adhesion, migration, and proliferation. u-PAR-dependent ERK activation occurs primarily though non-exclusively via EGFR. EGFR activation simultaneously upregulates ERK while down-regulating the pro-apoptotic p38 mitogen-activating protein kinase pathway, thus promoting cell proliferation. Over-expression of u-PAR activates $\alpha_5\beta_1$ integrins and EGFR, sustains ERK activity, and upregulates genes necessary for cells to enter S-phase to promote cell growth (Weber, Hu et al. 1997; Murphy, Smith et al. 2002; Jo, Thomas et al. 2003). The relationship between u-PA:u-PAR in signaling also plays a role in apoptosis. u-PAR has an anti-apoptotic effect in MDA-MB-231 breast cancer cells; α-u-PA antibody leads to a decrease in ERK phosphorylation and an increase in apoptosis (Ma, Webb et al. 2001; Alfano, Iaccarino et al. 2006). ERK activation is necessary for expression of both u-PA and u-PAR. This positive-feedback loop shows the tight regulation found in the u-PA:u-PAR system, where the maintenance of ERK activation can lead to suppression of apoptosis and promote cancer progression.

u-PAR can activate the GPCR signaling pathway via exposure of the receptor's chemotactic region since u-PA has no effect on signaling events when FPRL1 is expressed in the absence of u-PAR (Resnati, Pallavicini et al. 2002; Jo, Thomas et al. 2003) Cleaved su-PAR behaves only as a partial agonist similar to, but not as effective as, its membrane bound u-PAR:u-PA counterpart. These studies suggest that the signaling potential of u-PAR is dependent on the form that is present on the cell: either unliganded/latent, u-PA–bound/active, or cleaved/active.

u-PAR-dependent β_1 integrin signaling leads to activation of Src kinase and focal adhesion kinase (FAK). Activation of Src family tyrosine kinases is required for

adhesion mediated by the fibronectin and Vtn receptors, $\alpha_5\beta_1$ integrin and $\alpha_V\beta_5$ integrin, respectively. In addition, phosphorylation of FAK leads to Src-binding and promotes cellular proliferation, migration, and survival (Giancotti and Ruoslahti 1999; Aguirre Ghiso 2002; Mitra and Schlaepfer 2006). u-PAR-mediated enhancement of FAK activation is u-PA-dependent, and this is accompanied by increased co-immunoprecipation of u-PAR and β_1 integrins, which is consistent with the hypothesis that u-PA induces a conformational change in its receptor that augments integrin-binding (Yebra, Goretzki et al. 1999; Nguyen, Webb et al. 2000).

u-PAR can also be co-immunoprecipitated with JAK/STAT proteins (Koshelnick, Ehart et al. 1997). In smooth muscle cells (SMC), the association of JAK1 and u-PAR phosphorylates STAT1, which in turn translocates to the nucleus and alters gene expression (Dumler, Weis et al. 1998). The activation of this signal transduction pathway may be involved in cell migration regulation. For pathways involving at least two of the STAT proteins, STAT3 and STAT5b, activation by u-PA-bound u-PAR is independent of u-PA's proteolytic activity (Jo, Thomas et al. 2005; Shetty, Rao et al. 2006).

1.4.3. Cell migration

Cell migration involves a complex balance between focused proteolysis (the dynamic interaction with extracellular matrix proteins), and the ability to reorganize the cytoskeleton. The proteolytic activity of the u-PA/u-PAR system aids in matrix invasion and tissue remodeling. As discussed previously, the u-PA-dependent activation of u-PAR promotes lateral binding to several molecules that can induce signaling pathways, leading ultimately to changes in migration and proliferation. *In vitro* studies implicate several signaling pathways in u-PAR-mediated cell migration. These include

ERK/MAPK, tyrosine- and serine-protein kinases, FAK, and Src. Ongoing studies continue to identify new participants.

The pro-migratory effects observed with u-PAR are specific to individual cell types and ECM components. Accumulating evidence suggests that integrin activation is involved in u-PAR-mediated migration, cell adhesion, proliferation, and cell survival (Ossowski and Aguirre-Ghiso 2000; Chapman and Wei 2001). In leukoctyes, u-PAR-mediated migration involves β_1 and β_2 integrins and occurs in a manner dependent on the concentration of u-PA (Gyetko, Todd et al. 1994; Aguirre Ghiso, Kovalski et al. 1999; Liu, Aguirre Ghiso et al. 2002; Montuori, Carriero et al. 2002). u-PA-induced cytoskeletal reorganization and cell migration is halted in the presence of signaling pathway inhibitors such as pertussis toxin (PTX), calphostin, and PD98059, demonstrating the involvement of GPCR, PKC, and MEK1, respectively. In MCF-7 cells, increased u-PAR occupancy by u-PA activates ERK1/2 and leads to migration mediated through the JAK kinase family (Nguyen, Hussaini et al. 1998).

The induction of pathways may also depend on the manner in which u-PAR is activated. Chymotrypsin-cleaved su-PAR exhibits pro-chemotactic activity similar to that of u-PAR bound by inactive u-PA in p56/59hck activation and signals via the FRPL1/LXA4R (Resnati, Pallavicini et al. 2002). Non-cleavable u-PAR enhances migration via signaling pathways differently from those of the wild-type receptor (Mazzieri, D'Alessio et al. 2006). These mutations display the inability to activate ERK or engage FRPL1 and GPCR, leaving EGFR as the major cell-surface receptor induced by non-cleavable u-PAR (Mazzieri, D'Alessio et al. 2006).

1.4.4. Cell proliferation

Signaling responses mediated via u-PAR also impact cell proliferation. The proliferative effect of u-PAR correlates with the expression levels in tumor cells, and is a strong predictor of malignant behavior. u-PAR:integrin interactions promotes neoplastic cell proliferation, tumor growth, and invasion (Ossowski 1988; Liu, Aguirre Ghiso et al. 2002). Proliferation of u-PAR-expressing cells involves the activation of the ERK/MAPK pathway and deactivation of the p38 MAPK pathway (Liu, Liu et al. 1997). In HEp3 cells, high expression levels of u-PAR leads to tumor growth whereas the down-regulation of u-PAR causes cell dormancy (Yu, Kim et al. 1997). ERK activation in u-PAR-expressing HEp3 cells is dependent on the $\alpha_5\beta_1$-integin:u-PAR interaction, which is optimal when u-PA is bound to u-PAR and Fn is bound to $\alpha_5\beta_1$-integin.

u-PAR cross-talks with growth factor receptors such as EGFR and PDGFR (Liu, Aguirre Ghiso et al. 2002; Kiyan, Kiyan et al. 2005). EGFR is known to interact with u-PAR and remains activated when u-PAR is overexpressed. The regulation of proliferation by u-PAR requires ERK activation, which is FAK-dependent but EGFR-ligand independent (Aguirre-Ghiso, Liu et al. 2001)). EGFR signaling is $\alpha_5\beta_1$ integrin dependent and leads to constitutive ERK pathway activation which is necessary for *in vivo* growth. High levels of u-PAR create a positive feedback loop, with high ERK activity inducing expression of u-PA and u-PAR (Lengyel, Stepp et al. 1995). EGFR is the most influential receptor leading to ERK activation, and is essential for u-PAR-initiated ERK up-regulation (Jo, Thomas et al. 2003). In the absence of EGFR, the presence of u-PA leads to a G-protein dependent migration (PTX sensitive) migration (Resnati, Guttinger et al. 1996; Fazioli, Resnati et al. 1997; Degryse, Orlando et al.

2001). u-PAR can also cross-talk with PDGFR in vascular smooth muscle cells, wherein activation of u-PAR by u-PA-binding induces PDGF-independent PDGFR-beta phosphorylation and cell proliferation (Kiyan, Kiyan et al. 2005).

As expected, down-regulation of u-PAR in cell lines affects signaling pathways involved in the cell cycle. Decreases in u-PAR expression lead to inhibition in invasion, adhesion, proliferation and migration (D'Alessio, Margheri et al. 2004; Dass, Nadesapillai et al. 2005). The use of antisense oligodeoxynucleotide (asODN) leads to a dramatic decrease in ERK1/2 activation in melanoma cells (D'Alessio, Margheri et al. 2004) and a dramatic decrease in FAK/JNK/Jun activation in prostate cancer cells (Margheri, D'Alessio et al. 2005). u-PAR down-regulation *in vivo* by u-PAR anti-sense ODN or short-interference RNA (shRNA) reduces tumor growth and metastases in at least two different cancers (i.e. Meningiomas and MDA-MB-231) (Mohan, Lakka et al. 1999; Lakka, Rajagopal et al. 2001; Wang, Ma et al. 2001; D'Alessio, Margheri et al. 2004; Gondi, Lakka et al. 2004; Dass, Nadesapillai et al. 2005; Margheri, D'Alessio et al. 2005; Kunigal, Lakka et al. 2007; Tummalapalli, Gondi et al. 2007).

1.4.5. Cell apoptosis

Deregulation of apoptosis and enhancement of proliferation is crucial for neoplastic cell survival. Cell death via apoptosis is tightly regulated in normal cells, whereas in cancer cells, this regulation has been interrupted by as yet poorly defined mechanisms. Recent studies of u-PAR down-regulation show an increase in cellular apoptosis, whereas over-expression promotes cellular growth. u-PAR downregulation is associated with a heightened response to TNF-α mediated ligand-induced apoptosis (Alfano, Franco et al. 2005), while use of shRNA u-PAR in glioblastoma cells increases caspase-mediated

apoptosis (Yanamandra, Konduri et al. 2000). In HEK293 cells, expression levels of u-PAR are positively correlated with resistance to apoptosis after ECM detachment. Downregulation of u-PAR leads to substantial cell death via apoptosis by p53 activation, which is independent of ERK or FAK signaling in melanoma cells (Besch, Berking et al. 2007). ERK1/2 activation is enhanced, with a decrease in p38 (negative growth regulator) activation, leading to a halt in apoptosis and promotion of cell proliferation (Aguirre-Ghiso, Liu et al. 2001; Liu, Aguirre Ghiso et al. 2002). When cells undergo apoptosis, the presence of u-PA-bound to u-PAR reverses events leading to cell death (Alfano, Iaccarino et al. 2006). In mesangial cells, the u-PA/u-PAR system regulates cell survival and apoptosis via a stimulus-specific manner that signals through BAD (bcl-2/bcl-x antagonist causing cell death) (Tkachuk, Stepanova et al. 1998). These data suggest that u-PAR acts as a survival factor.

1.5. The role of u-PAR in cancer

Malignancy is a function of the ability of tumor cells to invade tissue spaces and metastasize. Clinical studies associate the Pg activation cascade with a poor prognosis in breast cancer (Janicke, Schmitt et al. 1991), and over-expression of u-PAR in particular cell lines correlates with malignancy (Andreasen, Kjoller et al. 1997). It is not surprising that u-PAR has a role in cancer since approximately 20 years of studies have demonstrated u-PAR's role in Pg activation, internalization of u-PA-PAI-1 complexes, and the activation of signaling pathways. When these functions are improperly regulated, they can lead to oncogenic cell transformation, enhanced proliferation, migration, invasion, and resistance to apoptosis (Hanahan and Weinberg 2000). Expression of u-PAR has been observed in neoplastic cells and tumor-associated cells from ovary, colon,

lung, breast, endometruim, macrophages, endothelial cells, and fibroblasts, suggesting that u-PAR might be a useful therapeutic target (Mazar 2001; Wang 2001; Ge and Elghetany 2003; Sidenius and Blasi 2003; Mazzieri and Blasi 2005). The proteolytic role of the u-PA/u-PAR system modulates cell invasion and metastasis via its ability to disrupt the ECM, and promote adherence (Carmeliet 2000; Jain and Carmeliet 2001). In patients with colon and breast cancer, high levels of u-PAR correlates with metastasis and poor outcome (Dano K., Behrendt et al. ; Ge and Elghetany 2003). u-PAR over expressing cells tend to be located at the leading outer edge of tumors and may provide enhanced angiogenesis and infiltration of surrounding normal tissues (Skriver, Larsson et al. 1984; Yamamoto, Sawaya et al. 1994; Lindberg, Larsson et al. 2006).

The ability of u-PAR to interact with many ligands and membrane-anchored partners plays a key role in cell-cell interaction and cytoskeleton rearrangement (Table I). For instance the interaction between u-PAR and integrin induces cell signaling events that can be optimal for growth, invasion and dissemination of tumor cells. The broad range of potential ligands and interactions for u-PAR and integrins may represent useful therapeutic targets because of the significance of downstream signaling events (Degryse 2011).

Other strong prognostic markers for survival are the presence of su-PAR and the cleavage products D_2-D_3 and D_1 in the plasma of cancer patients. The soluble and cleaved form of u-PAR has been found in the fluid of human malignant ovarian cysts, the urine of cancer patients and also blood from patients with myeloid leukemia (Wahlberg, Hoyer-Hansen et al. 1998; Mustjoki, Sidenius et al. 2000; Sidenius, Sier et al. 2000). Proliferation of cancer cells can be interrupted by reducing the available intact u-PAR via

cleavage and dissociation of D_1. On the other hand, cancer cells derived from anaplastic thyroid carcinoma and PMA-stimulated U937 cells often express a form of u-PAR that is heavily glycosylated and confers resistance to cleavage by tcu-PA (Picone, Kajtaniak et al. 1989; Montuori, Rossi et al. 1999). There seems to be a correlation between increased glycosylation, resistance to tcu-PA cleavage, and tumor aggressiveness in various types of thyroid tumor cells, suggesting that tight regulation of u-PAR is essential to maintain a balance between pericellular proteolysis, cell signaling, and downstream effectors.

Measurement of u-PA, u-PAR and PAI-1 is useful in predicting patient outcome. Quantitative immunoassays have been developed to measure levels in both solid tumors and in blood (Pedersen, Brunner et al. 1994). Levels of circulating u-PAR in blood correlate with expression levels on solid tumors but it seems that both can predict outcome. Elevated quantities of u-PAR in breast tumor tissue indicated a poor relapse-free survival and overall survival (de Witte, Foekens et al. 2001). There are some setbacks in the quantitation of u-PAR levels for prognostic value since its prognostic indicator is diminished by the addition of PAI-1 to the multivariate model (Grondahl-Hansen, Peters et al. 1995). However, Christensen *et al.*, imply that a more homogenous sample, blood, should be taken while measuring the levels of u-PAR. These results were reproduced in colorectal cancer by analyzing the levels of su-PAR in plasma samples (Stephens, Nielsen et al. 1999; Fernebro, Madsen et al. 2001; Riisbro, Christensen et al. 2005). In non-small cell lung cancer, u-PAR D_1 levels were determined rather than intact su-PAR levels, with the reasoning that cleavage reflects an active plasminogen activation cascade and should correlate with a better prognosis. These studies show that u-PAR has potential as a biomarker and therapeutic target but more studies need to be performed.

1.6. Overview of project

u-PAR has been widely shown to be involved in cancer, angiogenesis and inflammatory diseases. The evidence for the roles of u-PAR in neoplasia and the multiple regulatory mechanisms associated with u-PAR suggests that cleavage of the receptor may be important for regulation of specific cell functions. However, the complexity of u-PAR interactions makes it extremely difficult to associate individual u-PAR forms with specific u-PAR functions. Many of the receptor's functions have been hypothesized to be associated with both u-PA binding and a potential conformational change in the receptor. However, it has been difficult to delineate whether the downstream effects of u-PAR activation are regulated by a cell-surface bound u-PA through u-PAR, by a u-PA induced conformational change in u-PAR, or by the generation of cleaved u-PAR via tcu-PA. All three circumstances require the presence of tcu-PA.

In this work, we created a mutant form of u-PAR that allows for better discrimination between the potential mechanisms of action of u-PAR. Since various forms of u-PAR have been widely used that affect cell function and cancer progression, we chose to explore the importance of receptor cleavage in Pg activation, clearance of u-PA-PAI-1 complexes, cell migration, receptor signaling and cellular growth. In order to isolate a single receptor form, we exploited the two u-PA cleavage site creating a mutant cleavage resistant u-PAR (cr-uPAR) that confers resistance exclusively to tcu-PA associated cleavage. The differences between cr-uPAR and wt u-PAR allows us to discriminate between the functions previously linked to both the u-PA-bound u-PAR and the cleaved forms of u-PAR. This mutant allowed us to identify a potential regulatory role for intact

u-PAR. We show that cr-uPAR closely interacts with LRP. This gain of function appears to regulate clearance of complexes bound and its re-surfacing. It also promotes u-PAR-dependent cell migration.

In addition, exposure of the chemotactic epitope in the linker region of u-PAR is a potential link in receptor regulation. u-PAR's interaction with lateral cell-surface bound molecules may regulate migration, proliferation, adhesion and apoptosis. Our goal was to identify the non-proteolytic functions of u-PAR when a prominent intact receptor is on the cell-surface that is u-PA-independent. The presence of u-PAR appears to contribute to a delicate balance in cell functions. If this balance is tilted toward a highly active receptor, we hypothesized that the cell might gain oncogenic features similar to those observed in cells expressing a cleavage resistant u-PAR (ARO cells). Our novel tcu-PA cleavage resistant receptor has a direct effect on internalization, created through direct binding to LRP that is independent of u-PA-PAI-1 complex binding. We also demonstrate that cr-uPAR has functions that correlate with the highly aggressive thyroid carcinoma ARO, with enhanced signaling, migration, proliferation and apoptosis.

1.7 Figures and Tables

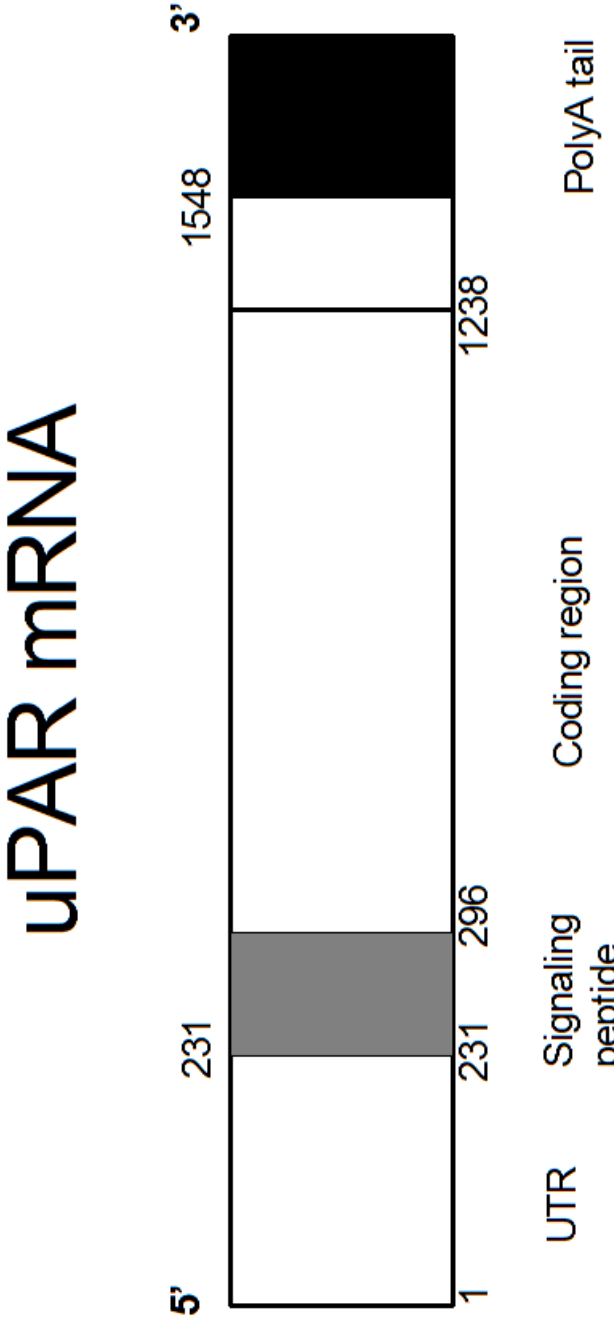

Figure 1.1. mRNA structure for u-PAR. u-PAR has a UTR region with a signal peptide 231 bases downstream. This is followed by the coding region and a polyA tail.

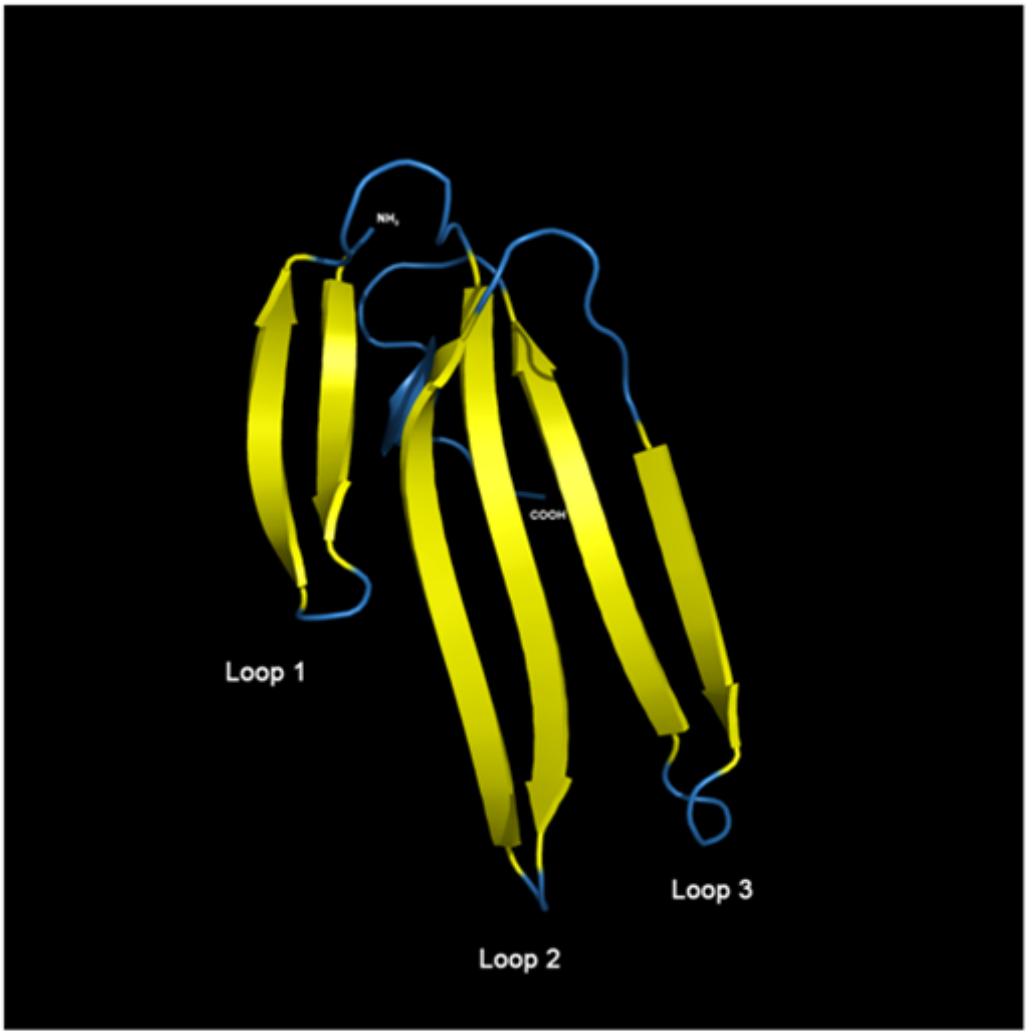

Figure 1.2. u-PAR domain 1 schematic and crystal structure. The crystal structure of u-PAR here is shown with the finger (yellow)-loop (blue) structure with the N-terminal on the top left and the C-terminal in the center.

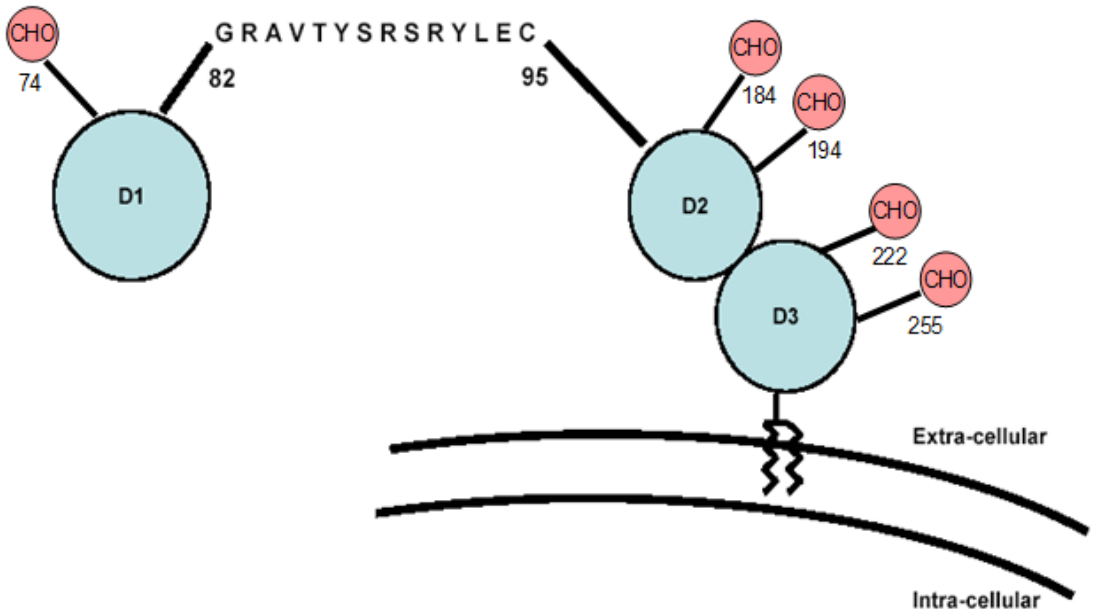

Figure 1.3. Schematic of u-PAR structure. Domains 1, 2 and 3 are shown with their respective glycosylation sites (pink). D_1 has one site at Asn^{52} whereas D_2 and D_3 have two potential sites each, Asn^{184}, Asn^{194} for D_2 and Asn^{222}, Asn^{255} for D_3. The linker region connecting D_1 to D_2 is detailed. D_3 also contains the GPI-anchor at the C-terminus.

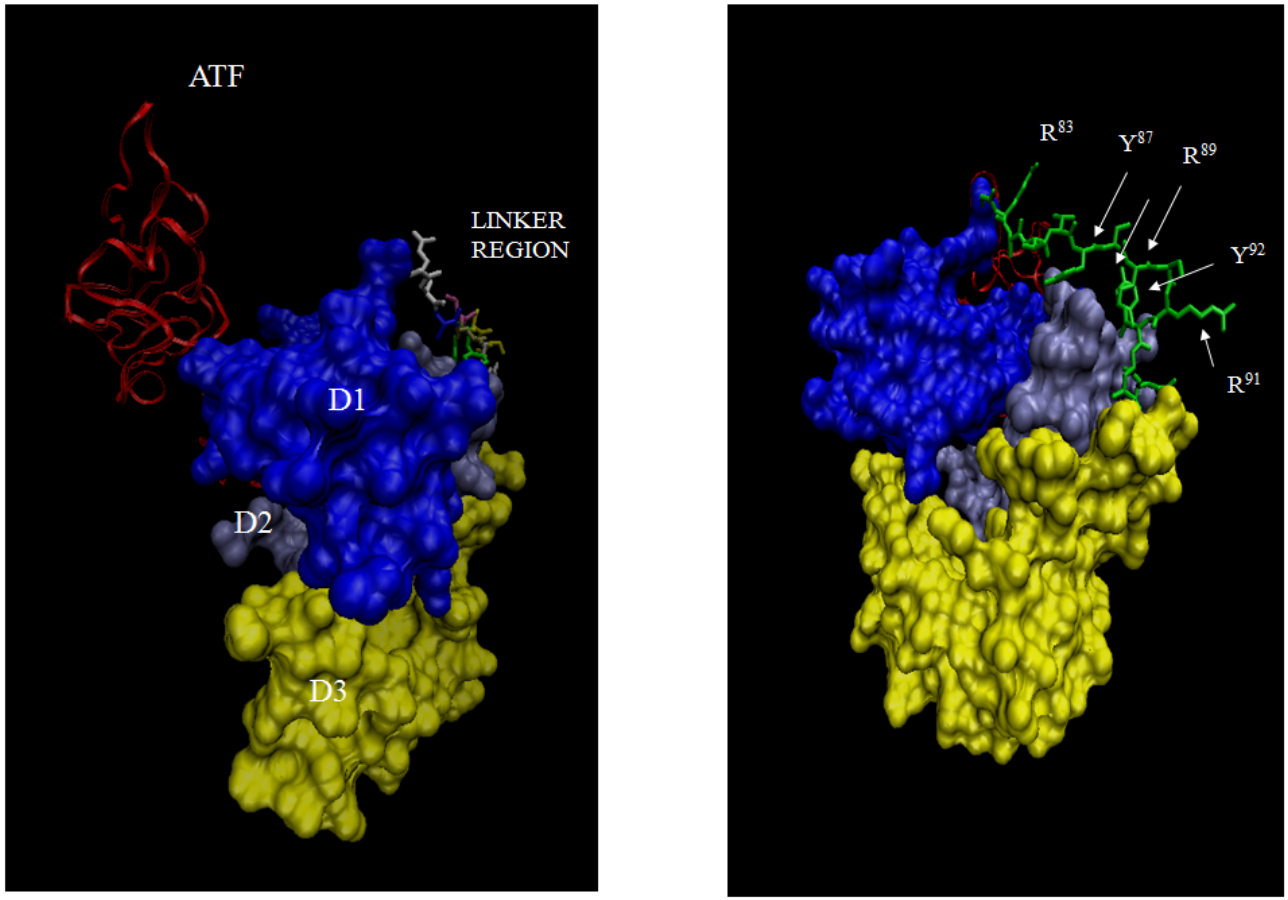

Figure 1.4. Crystal structure of u-PAR with the ATF and the linker region. The finger-like regions for D_1 (blue), D_2 (purple) and D_3 (yellow) are shown above. The ATF region of u-PA (red) binds to u-PAR on the opposite site of the linker region. The linker region (Lund, Green et al.) is exposed when bound to u-PA, Arg ^{83} is fully exposed and the chymotrypsin site inaccessible. Accession number: 2I9B

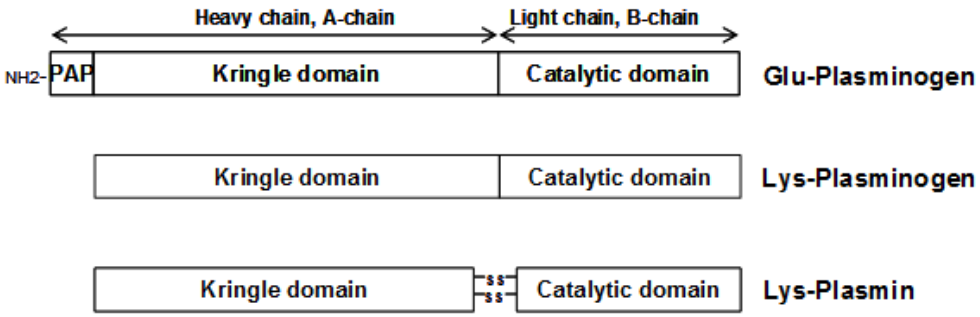

Figure 1.5. Structures of Plasminogen forms. The zymogen Glu-plasminogen is depicted as a single chain protein (at top). The pre-activating peptide (PAP) is cleaved off generating Lys-plasminogen (middle). When tcu-PA is generated it cleaves plasminogen converting it into a two-chain active form, plasmin, which is held together by disulfide bonds (at bottom).

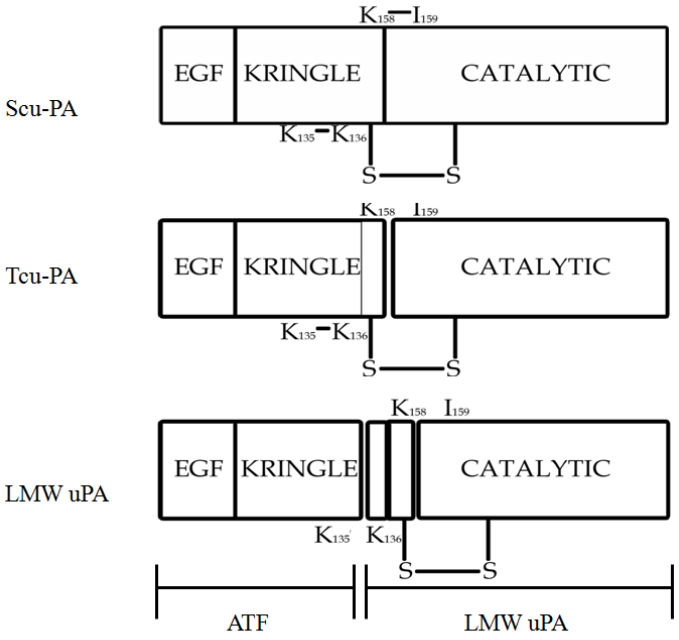

Figure 1.6. Urokinase type plasminogen activator forms. The zymogen single chain u-PA, shown on top. The activated two-chain form of u-PA is depicted here with the cleavage site and the protein domains linked by the disulfide bond. A secondary cleavage site generates the low molecular weight u-PA that separates the catalytic domain from the EGF and kringle domain.

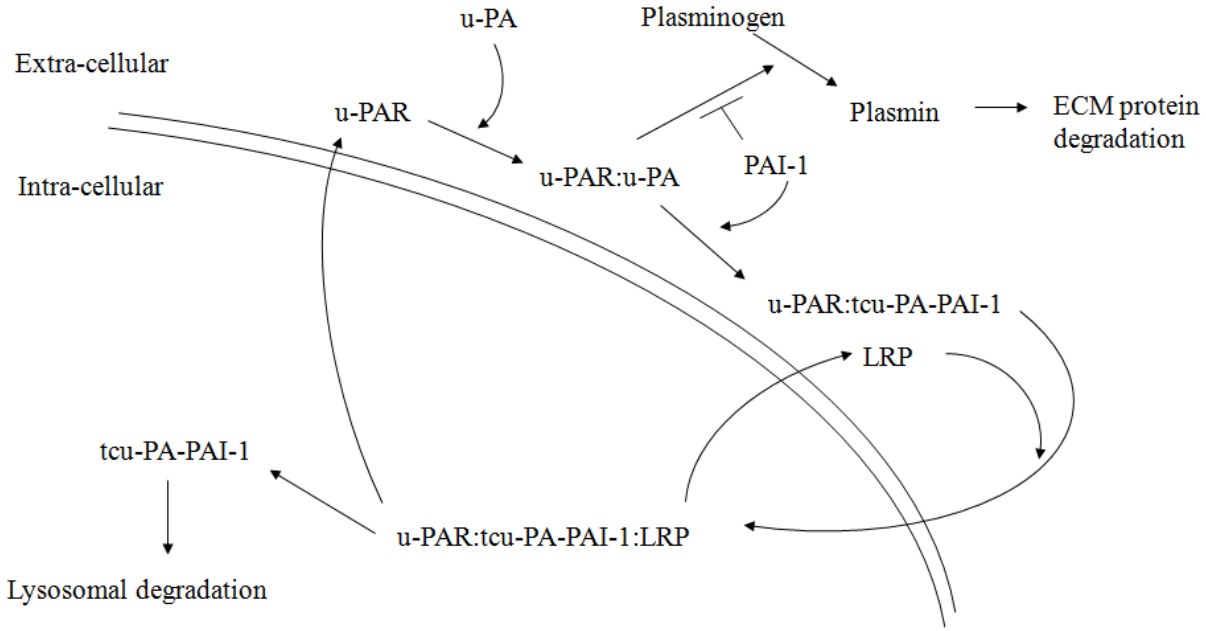

Figure 1.7. Plasminogen activation cascade. Initiation of the Pg activation cascade occurs with pericellular localization of scu-PA by u-PAR. The augmented activity of bound scu-PA generates Pn from Pg. Pn activates the zymogen scu-PA into the active protease tcu-PA, this tcu-PA can generate even more Pn. The amplification is regulated by serpins, in this case PAI-1. PAI-1 inhibits tcu-PA activity preventing more Pn generation. PAI-1 also has some inhibitory activity against Pn although it is less specific then for u-PA. The covalent complex tcu-PA-PAI-1 is still bound to u-PAR and can then be cleared from the system by interacting with LRP, an endocytic receptor, undergoing internalization and endosomal degradation. LRP and u-PAR get recycled back to the cell surface unoccupied and ready to bind a new ligand.

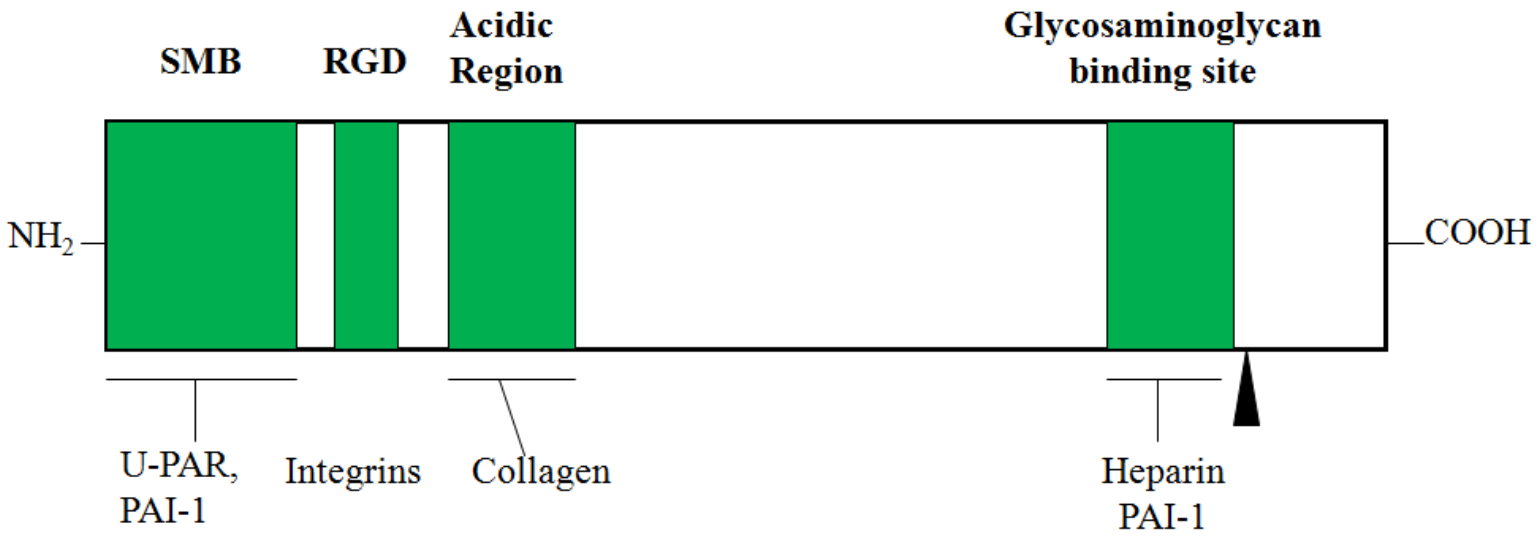

Figure 1.8. Schematic of Vitronectin. The SMB domain and the RGD domains are at the N-terminal followed by the acidic region. At the C-terminal there is a glycosaminoglycan binding region. Underlining the diagram are the proteins that interact with each particular domain.

Table I: Functional binding partners of u-PAR

Functional Group	Binding Partners	Cell Function	Reference
GPI-anchored receptor	u-PAR	Plasminogen activation, pericellular proteolysis, adhesion, migration, proliferation	Blasi et al. 1990, Cohen *et al*. 1991, Ellis *et al*. 1999, Mazar *et al*. 2008, Smith *et al*. 2010
Serine protease	scu-PA/ tcu-PA	Plasminogen activation, adhesion, migration, proliferation	Patthy L *et al*. 1985, Cubellis *et al*. 1986
Inhibitory complex	tcu-PA-PAI-1	Inhibition of plasminogen activation, Inhibition of u-PA dependent functions, Internalization	Czekay *et al*. 2001, Binder *et al*. 2007
Extracelular matrix protein	Vitronectin	Adhesion, Migration	Madsen et al. 2007, Deng et al. 1996
Integrins	α3β1, α4β1, α5β1, α6β1, α9β1 αMβ2, αLβ2, αXβ2 αvβ3, αvβ5, αvβ6	Adhesion, Migration	Chapman et al. 1999, Tarui et al. 2003
Receptor protein tyrosine kinases	EGFR, PDGFR, IGF-1-R	Proliferation, Migration	Mazzieri et al. 2006, Schiller et al. 2009
Endocytic receptor	LRP, LRP1B VLDL-R Mannose-6-phosphate receptor UPARAP	Internalization	Czekay et al. 2001, Conese et al. 1995, Godar et al. 1999
Scaffolding	Caveolin	Signaling	Chapman et al. 1999, Wei et al. 2001
Cytokine	Gp130	Migration	Shushakova *et al*. 2005, Liang *et al*. 2003
Adhesion	L-selectin	Adhesion	Petty *et al*. 2001
Seven-transmembrane domain receptor	FRPL1, FPR, FPRL2	Migration	Mazzieri *et al*. 2006, Resnati *et al*. 2002

Table II: The u-PA-u-PAR activated signaling pathways and its biological relevance.

Signaling molecules	Cell type studied	Biological response	Ref.
Ras-ERK	human gastric cancer (AGS), 293, MCF-7, MEF	migration, proliferation, chemotaxis	Ma Z *et al.* 2001, Guerrero *et al* 2004, Baek, 2008, Blasi *et al* 2002, Vial *et al.* 2003
FAK, Src, ERK	LNCaP, EC, MCF-7, 293	adhesion, migration	Aguirre-Ghiso 2002, wei et al 2001
PKC-ERK	hepatocarcinoma, PC12	Motility, differentiation	Bessard et al 2007; Farias-Eisner R., J Neurosci 2000
PI3K-AKT	papillary thyroid carcinoma	migration, invasion, proliferation, senescence	Nowicki, et al, 2011
Mek-ERK, Mek-ERK-MLCK	MCF-7, MCF-7/uPAR, HEp3, 293	adhesion, migration, tumor growth *in vivo*	Nguyen et al 1998, Nguyen 1999
Rho family small GTPase Rac	MCF-7/uPAR, Hct-116 and BE colon carcinoma	cytoskeleton rearrangement, cell motility, migration	Mueller 2000; Vial et al 2003; Kjoller et al., 2001
Hck-Fgr, Hck-G$\alpha\beta\gamma$	U937, THP-1, VSMC	chemotaxis, adhesion, differentiation, cytoskeleton rearrangement	REsnati 1996, Fazioli, Degryse 1999
Hck-ERK/p38, P38	HT-1080, HEp3, PC-3	tumor growth *in vivo*	Korakova 1998, Aguirre-Ghiso 1999
JAK/Stat family	VSMC, EC	Transcription, DNA binding, distribution to cell processes	Koshelnick 1999, Dumler 1998

CHAPTER 2. MATERIALS AND METHODS

2.1. *Materials*

Scu-PA was a kind gift from Dr. Jack Henkin (Abbot Labs, Rockford IL). Active tcu-PA was generated by incubating scu-PA with Pn-sepharose beads, as previously described (Manchanda and Schwartz 1991). Pg, Pn and chymotrypsin were purchased from EMD Bioscience (San Diego, CA). Soluble u-PAR (su-PAR) was a kind gift from Dr. Andrew Mazar (Attenuon, San Diego, CA). The monoclonal antibodies directed against the C-terminus of LRP, 11H4, and RAP were kind gifts from Dr. Dudley Strickland (Univ. of Maryland, MD). The SMB domain of Vtn was a kind gift from Dr. Michael Ploug (Finsen Lab, Denmark). Peptide 7 (AEPVYQYELDSYLRSYY), peptide 25 (AESTYHHLSLGYMYTLN) and prothrombin peptide (peptide Pt) were all synthesized (Biopeptides, San Diego, CA). Glu-Gly-Arg Chloromethyl ketone (CMK) (EMD Bioscience, San Diego, CA) was used to inactivate tcu-PA (CMK-uPA) (Kettner and Shaw 1979). DFP was used, in some instances, to inactive residual u-PA in our scu-PA as described (Manchanda and Schwartz 1991). Active wt PAI-1 and the stable PAI-$1_{14\text{-}1B}$ were kind gifts from Dr. Daniel Lawrence (Univ. of Michigan, Ann Arbor, MI).

The ECL substrate used for immunoblotting was from Pierce (Rockford, IL) and goat α-rabbit HRP antibody and streptavidin-HRP were purchased from Jackson Immunoresearch (West Grove, PA). DMEM, high glucose was purchased from the Cell Media facility in UIUC. Trypsin-EDTA, penicillin/strep, L-glutamine, fetal bovine serum (FBS) and RPMI 1640 were purchased from Invitrogen (Carlsbad, CA). G418 sulfate (Gemini Bio, West Sacramento, CA), Hank's balances salt solution (HBSS) (Invitrogen, Carlsbad, CA), non-enzymatic dissociation buffer (Invitrogen, Carlsbad,

CA), HEPES (Lonza), and cyloheximide (CHX) (Sigma, St. Louis, MO) were of highest quality available. PBS -Ca^{+2}/-Mg^{+2} was made using the standard protocol (Sambrook and Russell 2006) Triton X-100 and deoxycholate were purchased from Sigma. Sulfo-NHS-LC-biotin, NHS-S-S-LC-biotin, immobilized Protein G and streptavidin-agarose beads (Pierce, Rockford, IL) were used to label and isolate proteins. Protein concentrations were determined using the BCA protein assay (Pierce).

2.2.Methods:

2.2.1. <u>Site-directed mutagenesis of u-PAR variants:</u>

Wild-type human u-PAR cDNA was obtained through RT-PCR of mRNA from U937 lymphoma cells (CRL-1593.2) (ATCC, Manassas, VA). The u-PAR cDNA was then inserted into pBSIISK(+). u-PAR variants were generated using the Quikchange® site-directed mutagenesis kit (Stratagene, La Jolla, CA) and sequenced. The u-PAR sequence was compared to the sequence found in NCBI, NM 002659. The immediate non-coding 5' and 3' region of u-PAR was mutated to insert EcoRI (5'-TCGATCGGAATTCCATGGGTCACCCGCCGCTG-3') and EcoRV (5'-CTGCATGGATATCCTCAGGTTTAGGTCCAGAG-3') sites, respectively (Table III). Several different mutational combinations were constructed at the two tcu-PA cleavage sites in u-PAR, Arg^{83} and Arg^{89}. Double point mutation combination to the residues were generated as follows: $R^{83}A$ / $R^{89}A$, $R^{83}E$ / $R^{89}E$, $R^{83}A$ / $R^{89}E$, and $R^{83}E$ / $R^{89}A$. Single point mutations were also generated on the individual residues: $R^{83}A$, $R^{89}A$, $R^{83}E$ and $R^{89}E$. The primary mutant u-PAR used in these experiments was the $R^{83}A$ / $R^{89}A$, termed "cr-uPAR." Primers for generating $R^{83}A/R^{89}A$ were 5'-GCA ACT CTG GCG CAG CTG TCA CCT ATT CCG CAA GCC GTT ACC-3', and its complementary set (IDT

Inc, Coralville, IA). Table III shows all primers used for the generation of all other u-PAR variants. The primers that were constructed had a high GC content. To aid in the success of mutation, multiple reactions were performed with increasing concentrations of DMSO from 0 - 5%. The reaction was assembled using 10x reaction buffer, 10 mM dNTP, 10 µM of forward primer, 10 µM of reverse primer, 100 ng of wt u-PAR pcDNA3.1(+), increasing amounts of DMSO, and 2.5 units of KOD polymerase. The final total volume was brought to 50 µl with ddH_2O, and the reaction was layered with mineral oil.

Once the reactions were assembled amplification was initiated with a "hot start" step. After the "hot start" step, 25 cycles of the denaturing (30 sec at 94°C), annealing (5 sec at 65°C), and elongation (6 min at 70°C) steps were performed, followed by a final elongation step (10 min at 74°C). Amplified samples were electrophoresed on a 1% agarose gel, imaged using a digital camera (Cannon) with UV filter and the 1D Kodak imaging system. Since the goal was to express the u-PAR variants in a mammalian cell line, standard subcloning procedures and manufacture's recommendations were followed for the restriction digest. EcoRI and EcoRV digested DNA fragments were inserted into the cDNA and ligated the u-PAR fragments into the pcDNA3.1(+) (Invitrogen, Carlsbad, CA) plasmid using T4 ligase. Once the variant u-PAR cDNA sequences were in pcDNA3.1(+), the mutations were verified before proceeding (high-throughput sequencing and genotyping unit, Univ. of Illinois-Urbana, IL). All variant u-PAR cDNAs were transformed into TG1 cells following isolation for transfection into HEK293 (293) cells.

2.2.2. Stable transfection into 293:

Two cell lines, HEK293 (293, CRL-1573) and U937, were purchased from ATCC. 293 transfection of plasmids carrying the cDNA of the u-PAR variants (wt u-PAR, cr-uPAR, the double point u-PAR mutations, and the single point u-PAR mutations) was accomplished using the Superfect® transfection reagent as per the manufacturer's protocol (Qiagen, Valencia, CA). Transfected 293 cells were cultured in DMEM with 10% FBS and 400 µg/mL G418. Cell colony selections were then performed (range 12-24 colonies per cell line) on all the u-PAR variants, and repeated two weeks after.

2.2.3. Antibody purification:

Protein A sepharose beads (Protein A Sepharose CL-4B, Pharmacia) were equilibrated in 10 ml of $NaPO_4$ pH 8.2 buffer prior to use. The bead slurry was nutated for 10 min at room temperature (RT), following centrifugation for 5 min at 2000 rpm. This was repeated a total of five times. Rabbit serum was adjusted to pH 7.0, and 1 mL was added to the Protein A beads, and incubated for 2 h at RT. The beads were centrifuged at 2000 rpm for 5 min, and the supernatant was removed. The antibody bound protein A beads were transferred to a Na_3PO_4 pre-wet column (Bio-Rad). The eluate was tested for unbound antibody until the absorbance (A_{280}) reached 0. Antibody fractions were then eluted using 0.1 M NaCitrate, and the pH adjusted using a neutralizing buffer. The two fractions with highest A_{280} were pooled and examined for purity using SDS-PAGE with immunoblotting.

2.2.4. u-PAR immunoblotting:

Cells were lysed for 30 min on ice using RIPA (150 nM NaCl, 50 mM Tris-HCl pH 7.5, 1% deoxycholate, 0.1% SDS, 1% Triton X-100) buffer with protease inhibitor cocktail (Roche). The total protein content was determined using a BCA assay, so that equal quantities of protein were loaded on SDS-PAGE. Gels were typically 10% polyacrylamide, unless otherwise specified(Laemmli 1970). Electrophoresis was performed at 200 V for 1 h. The samples were transferred to an activated PVDF membrane with 100 V current for 1 h in ice-cold transblotting buffer (25 mM Tris pH 8.0, 192 mM glycine and 20% methanol) per the manufacturer's recommendations (Bio-Rad). The membranes were blocked for 1 h at RT (alternatively overnight at 4°C) using TBS/ 0.01% Tween-20/ 1% gelatin, and then incubated with polyclonal rabbit anti-human u-PAR (purified as described above) diluted 1:5000 in TBS/ 0.01% Tween-20/ 1% gelatin for 2 h at RT. Excess antibody was removed by repeated washing in TBS/ 0.01% Tween-20. The membrane was incubated for 1 h at RT with secondary antibody (goat α-rabbit HRP, diluted to 1:5000 in TBS/ 0.01% Tween-20/ 1% gelatin), then washed 6 times in TBS/ 0.05% Tween-20. The presence of the target protein was detected using SuperSignal ECL buffer (Pierce).

2.2.5. u-PAR cleavage assay:

Target cells ($1x10^6$ of non-transfected 293, 293 wt u-PAR or cr-uPAR) were dissociated using non-enzymatic dissociation buffer, then resuspended in DMEM with 0.1% BSA (Calbiochem, San Diego, CA). As a control, $5x10^6$ PMA-stimulated U937 cells (3-day culture) cells were resuspended in RPMI with 0.1% BSA (Picone, Kajtaniak et al. 1989). Cells were acid-washed once to remove surface-bound proteins by addition

of 0.1 M Glycine, 0.15 M NaCl (pH. 3.0) for 3 min at RT followed by neutralization using 0.5 M Hepes, 0.15 M NaCl (pH. 7.5) (Manchanda and Schwartz 1991). Tcu-PA was generated from scu-PA as previously described (Manchanda and Schwartz).

Cells were incubated either with 100 nM tcu-PA or 250 nM Pn for 20 h at 37°C. Cells incubated with chymotrypsin at different concentrations (0 nM - 100 nM) were incubated for 30 min at 37°C. Cell membrane proteins were solubilized for analysis with RIPA buffer (150 mM NaCl, 50 mM Tris-HCl pH 7.5, 1% deoxycholate, 0.1% SDS, 1% Triton X-100) (Wei, Lukashev et al. 1996) and protease inhibitor cocktail™ (Roche, Indianapolis, IN). Cell lysate (5 µgs) was subjected to SDS-PAGE (Pierce, Rockford, IL) and equivalent loading of proteins was achieved by quantitating samples using a BCA assay (Pierce, Rockford IL). Samples were immunoblotted using polyclonal rabbit α-u-PAR and goat α-rabbit HRP. In some instances, purified su-PAR and endogenous u-PAR were used for comparison.

2.2.6. Reverse transcriptase PCR:

Cells (5×10^5) were lysed and homogenized in freshly prepared mixture of 99.4 µM β-mercaptoethanol (β_2-ME) and Lysis Buffer obtained from the Absolute RNA Microprep Kit® (Stratagene). An equal volume of 70% ethanol was added to the cell lysate followed by thorough mixing. The lysate was transferred into an RNA-binding spin column (Absolutely RNA® Microprep Kit, Stratagene), and the unbound portion was removed. Contaminating DNA was removed by treatment with DNase I (1 U/µg of RNA) (Invitrogen, Carlsbad, CA) for 15 min at 37°C. Residual DNA was removed with a high salt exchange followed by a low salt wash. Afterwards, the RNA bound to the

matrix was eluted with 60°C elution buffer. The concentration of RNA was calculated from A_{280}.

First-strand cDNA was prepared using the StrataScript™ First-Strand Synthesis System (Stratagene). For the control reactions, control mRNA was mixed with either oligo(dT) primer (100 ng/µl) or random primer (100 ng/µl). For the experimental reaction, 10 µg of total RNA was combined with random primers (100 ng/µl). The reactions were incubated at 65°C for 5 min then slowly cooled to RT (10 min) for the primers annealing to the RNA.

First-strand cDNA was performed by the addition of 10X first-strand buffer, RNase Block Ribonuclease Inhibitor (40 U/µl), 100 mM dNTPs, and StrataScript™ reverse transcriptase (50 U/µl) following an incubation at 42°C for 1 h. The control and experimental reactions were incubated at 90°C for 5 min and transferred to 4°C for subsequent use in the PCR amplification protocol.

Amplification of cDNA was performed by assembling the reactions with cDNA from the first cDNA strand. The reaction was assembled using 10X reaction buffer, 10 mM dNTP, 10 µM of the ATG forward primer, 10 µM of the TGA reverse primer, template cDNA, and 2.5 units of KOD polymerase. The total volume was brought to 50 µl with ddH2O, the reaction centrifuged, then layered with mineral oil. The set-up of the PCR amplification was performed as previously described, following assembly of the reactions. The mutations were verified prior to DNA sequencing (high-throughput sequencing and genotyping unit, U. of Illinois-Urbana, IL).

2.2.7. Flow cytometry:

U937 (human leukemic monocyte lymphoma) cells, suspended 293 non-transfected cells, 293 wt u-PAR cells or cr-uPAR cells were washed three times with PBS to remove any Ca^{+2} and Mg^{+2} present. The cell surface ligands were eluted off these various cell types as described above. Unbound protein was removed by repeated suspension and centrifugation for 5 min at 1200 rpm in PBS. Cells were resuspended at a final concentration of $1x10^6$ cells/ 0.1 ml (U937), or $2x10^6$ cells/ 0.1 ml (293 cell variants), and incubated with either polyclonal rabbit α–uPAR (1:250 dilution), normal rabbit IgG (1:100 dilution) or PBS (control) for 30 min at 4°C. Next samples were diluted ten-fold with PBS and re-pelleted to remove any unbound antibody. Cells were then resuspended into a final volume of 400 µl, and passed through a 40 µm cell strainer to obtain single cell suspension. Samples were run through a flow cytometer (Beckman Coulter Epics) which was gated for live cells.

2.2.8. Inactivation of tcu-PA:

tcu-PA was inactivated by two consecutive incubations (each at RT for 20 min) of 1 mM ERG-CMK (EMD, San Diego CA) in PBS. To remove the excess EGR-CMK, the reaction was dialyzed against six exchanges of PBS. The degree of enzyme inactivation was evaluated by measuring the residual amidolytic activity of tcu-PA against 10 mM SpecUK (American Diagnostica, Greenwich CT) at 37°C for 30 min.

2.2.9. ^{125}I protein labeling:

Glass tubes were coated with 20 µl of 100 µg/ml Iodogen reagent (Pierce, Rockford IL) in CH_2Cl_2, evaporated to dryness under of N_2, and stored with desiccation at -20°C.

CMK-uPA (50 μg) was incubated with I^{125} (Perkin Elmer) in an Iodogen-coated tube at RT for 4 min. The reaction was quenched with 5 mM saturated tyrosine and 6 mM KI solution. The quenched reaction was transferred onto a G-25 Sephadex column (BioRad) and eluted with TBS. Excess free radioisotope was removed by dialysis using six exchanges of ice-cold TBS. Protein concentration and protein integrity were evaluated by TCA precipitation, autoradiography, and Coomassie stained SDS-PAGE analysis.

2.2.10. Competition binding assay:

Cells ($2.5x\ 10^4$) were seeded in a 24-well microplate and incubated for 14 h at 37°C with DMEM/ 10% FCS. Media was then replaced with freshly made pre-chilled DMEM, 0.1% BSA, 10 mM Hepes and 10 μg/ml CHX. Cells were pre-chilled for 30 min, followed by incubation with 200 nM unlabeled CMK-uPA at 4°C for 30 min. Cells were then incubated with increasing concentrations (0 nM - 100 nM) of I^{125}CMK-uPA for 4 h at 4°C. Unbound I^{125}CMK-uPA was removed by washing the cells with PBS. Cells were then lysed in 0.1 N NaOH/1% SDS.

2.2.11. Fibrinolytic assay:

Fibrinogen was radiolabeled with ^{125}I, and prior to the experiment was clotted in 48-well microplates as previously described. Either (Manchanda and Schwartz 1990)dissociated cells (0.1M Tris pH 8.1), U937 cells, or 293 cells expressing u-PAR (0.1M Tris-EDTA pH 8.1) were added to the pre-formed I^{125}-fibrin clot. Cells were incubated with 1 nM scu-PA for 30 min at 37°C, after which Pg (4 μg/ml) was added. Gamma counts were collected on the samples, and data was analyzed to generate the percentage of clot lysis, utilizing scu-PA only as 100% clot lysis (GraphPad Prism).

2.2.12. Cell surface bound u-PA in plasminogen activation and inhibition:

293 cell variants ($5x10^4$) were seeded overnight with DMEM/ 10% FCS in 24-well microplates. Cells were washed three times with Hanks' balanced saline solution (HBSS) before the addition of reaction buffer (DMEM with 0.1% BSA) alone or preincubated with CMK-tcu-PA, tcu-PA, or chymotrypsin followed by an incubation with 10 nM tcu-PA for 30 min at 37 °C.

Cell surface generation of Pn at 37 °C was monitored with a SpectroMax Gemini XS microplate spectrofluorometer (Molecular Devices, Sunnyvale, CA) as described (Ellis, Behrendt et al. 1991), with the modification of 56 nM Pg and 600 µM of the Pn substrate, H-D-Ala-Leu-Lys-AMC (Bachem, Torrance, CA) in PBS and 0.1% BSA. Excitation and emission wavelengths were 360 and 460 nm, respectively.

Cell samples were pre-incubated with 100 nM CMK-uPA, to block specific binding between active tcu-PA and receptor. The effect of limited proteolysis of u-PAR on its ability to support Pg activation was studied by pre-incubating cell samples with either 100 nM tcu-PA or 100 nM chymotrypsin.

Pre-formed complexes of tcu-PA and PAI-1 were generated by incubation of 3 µM tcu-PA with 7 µM PAI-1 for 30 min at 37°C. The ability of u-PAR to bind these pre-formed complexes was tested by treatment of cells with 10 nM u-PA-PAI-1 complexes and washed prior to the addition of 10 nM tcu-PA. The ability of u-PAR to allow receptor-bound tcu-PA to be inhibited was tested by allowing binding of 10 nM tcu-PA followed by a 30 min incubation with 20 nM PAI-1 at 37°C before the addition of Pg and Pn substrate. The residual activity of the protease-serpin complex was assayed for

amidolytic activity using SpecUK (American Diagnostica, Greenwich CT) for 30 min at 37°C.

The rates of Pn generation were determined from parabolic plots of RFU versus time, fitted to a second-order polynomial, and then conversion to nanomolar Pn by reference to the amidolytic activity of purified Pn using the same fluorogenic substrate (Griffith, Breitkreutz et al. 1985; Fiore, Neuenschwander et al. 1992).

2.2.13. Internalization assay:

Cells ($1.5x10^5$) were harvested 18 h prior to labeling. Cell-surface u-PAR was biotinylated using 200 µM sulfo-NHS-SS-LC-biotin (Pierce, Rockford IL) as previously described (Wu and Gonias 2005). Cells were incubated with or without 10 nM u-PA-PAI-1 complex for 30 min at 4°C and were subsequently exposed to an increase in temperature (37°C) to initiate internalization. At specified times (0 – 30 min) cells were treated with 100 mM DTT (Fisher, Pittsburgh, PA) for 3 min at 37ºC followed by lysis in RIPA buffer. For controls, 500 nM RAP was added for each time point and incubated as described above. Lysates were exposed to streptavidin-agarose beads followed by β-ME reduction and denaturation to recover biotinylated u-PAR. Total crude cell lysate (10 µl) was reduced to quantify the total amount of u-PAR found in the samples. Samples were subjected to SDS-PAGE and detected using polyclonal rabbit α-uPAR (1:5000 dilution), washed blot with TBST and followed by goat α-rabbit HRP.

Alternatively, 293 cells expressing u-PAR were incubated with 10 nM biotinylated PAI-$1_{14\text{-}1B}$-tcu-PA complex for 30 min at 4°C. Cells were exposed to 37°C to initiate internalization. At specified times (0 – 30 min), cells were acid washed twice, and then lysed in RIPA buffer. All samples were subjected to SDS-PAGE and detected using

streptavidin-HRP (1:10,000) (Pierce, Rockford IL). Blots were analyzed by densitometry using the Kodak 1-D system. Control samples were prepared as described above and incubated with PAI-$1_{14\text{-}1B}$-tcu-PA for 30 min at 37°C, except that 500 nM RAP was added to each incubation solution.

2.2.14. Receptor recycling assay:

293 cells ($5x10^4$) were seeded with DMEM in 96 black microplates for 18 h at 37ºC prior to the experiment. Cells were then incubated with u-PA-PAI-1 complexes for 30 min at 4ºC. Unbound complex was washed off and the cells were incubated at 37ºC from 0 to 30 min. After which 10 nM tcu-PA was added for 30 min and further incubated at 37ºC. The amount of cell-surface u-PAR was measured via the Pg activation assay as described above. Cell surface-associated tcu-PA activity was normalized to the maximal amount of tcu-PA activity in the absence of u-PA-PAI-1 complexes. For the control samples, 500 nM RAP was added to all incubation solutions, as described.

2.2.15. Co-immunoprecipitation of u-PAR with LRP:

Immunoprecipitation experiments were performed as previously described (Czekay, Kuemmel et al. 2001). Suspensions of $1x10^6$ cells (293 wt u-PAR or cr-uPAR), were incubated in DMEM with 0.1% BSA only, or with additional 10 nM u-PA-PAI-1 complexes for 30 min at 4°C. Parallel samples of cells were incubated with either buffer or u-PA-PAI-1 complexes, with the addition of one of the following: 500 nM RAP, 4 µM SMB, 4 µM peptide 7, 4 µM peptide 25 or 4 µM peptide Pt. Treated cells were lysed in PBS/ 0.1% Triton-X 100 / 2 mM $CaCl_2$ for 30 min at 4°C. Lysates were then incubated

with 2.6 μg/ml and 20 μl/ml of mAb 11H4 and immobilized Protein G for 18 h at 4°C. Immunprecipitates were subjected to SDS-PAGE. Samples were immunoblotted using polyclonal rabbit α-uPAR antibody (1:5000 dilution) and goat α-rabbit HRP (1:5000 dilution) (Jackson ImmunoResearch). The immunoblots were analyzed using Kodak 1D and GraphPad Prism software.

2.2.16. Chymotrypsin cleavage assay:

Cells ($2.5x10^6$ cells/ml of 293 wt u-PAR or cr-uPAR) were suspended and incubated with DMEM, 0.1% BSA, and 100 μg/ml CHX in the absence or presence of 100 nM CMK-uPA for 30 min at 37°C. This was followed by incubation with 100 nM chymotrypsin (Fazioli, Resnati et al. 1997) at 37ºC for 0 to 30 min. Cells were then washed twice with PBS and lysed using RIPA buffer. Total crude lysate (10 μg) was loaded onto 10% SDS-PAGE gels and analyzed for u-PAR following immunoblotting as previously described.

2.2.17. Cell morphology:

Cells ($2.5x10^6$) were seeded in DMEM/ 10% FBS on Permanox™-treated slides (Nunc) and incubated at 37ºC / 7.5 % CO2 until 50% confluency was reached. On the day of the experiment, the cells were treated with 10 μM D-mannosamine or SF DMEM for 3 h at 37ºC, washed twice in PBS, and suspended in fresh SF DMEM on a slide. Then cells were sealed with a coverslip. Images were obtained with a SPOT camera at 20X and 40X magnifications. Images were measured by three separate blinds for all cells studied and with a minimum of three measurements per cell type.

2.2.18. Immunofluorescence:

Cells were harvested on Permanox™-treated slides (Nunc) as described above. The cells were rinsed in PBS followed by fixation with fresh 4% paraformaldehyde for 20 min. PBS was exchanged for the paraformaldehyde, followed by permeabilization with PBS/ 0.1% Triton X-100. Slides were then incubated with 10 nM $Alexa_{488}$-CMK-uPA, Hoechst and $Alexa_{560}$-Phalloidin (Invitrogen) for 1 h at 4°C. Images were obtained using a Spot Camera and a Zeiss Microscope at 40x magnification.

2.2.19. Proliferation assay:

Cells (2,000-50,000/ well) were seeded with DMEM/ 1% BSA into a 96 well microplate to generate a standard curve. Test wells were seeded at 5,000 cells/well. When necessary, 40 μM PD98059 (EMD), and/or 40μM JNKII inhibitor (Cell Signaling) were added daily. On the day of experiment, well media was exchanged with fresh DMEM/10% FCS. 20 μl CellTiter 96® AQueous One Solution Reagent (Promega) was incubated for 1.5 h at 37°C in humidified, 5% CO_2 atmosphere. A_{490} was measured on a Spectramax® microplate reader (Molecular Devices) and converted to cell number using the standard curve as a reference.

2.2.20. Dissociation assay:

Cells (100,000) were grown with DMEM/ 10% FCS in a 24 well plate for 18 h at 37ºC and 5% CO_2, then washed twice with HBSS (Bio-Whittaker). Cells were then incubated at RT for 0 - 30 min with enzyme-free dissociation buffer (Gibco). Dissociated

cells, from each time point, were centrifuged and resuspended in DMEM, 10% FCS (100 µl). Resuspended cells were transferred into a 96 well plate and cell counts were determined as described in the proliferation assay.

2.2.21. Adhesion assay:

Untreated wells of a 96 well microplate were pre-coated either overnight at 4°C, or for 3 h at 37°C, with 1 µg/ml Vtn or 1% FCS. Wells were then blocked with PBS/ 0.1% BSA for 1 h at 37°C. Previously dissociated cells were added (100,000 / well), then incubated for 1 h under normal growth conditions and washed three times to remove non-adherent cells. SF DMEM and Cell One™ proliferation reagent was added as previously described. Adherent cells were analyzed and compared to an untreated sample that represented the total cell number used to obtain the ratio of bound cells relative to the total.

2.2.22. Migration assay:

Resuspended cells ($2x10^5$) were incubated in either the presence or absence of 0.5 nM tcu-PA in SF DMEM for 15 min at 37ºC, and then placed on the top portion of Transwell™ chambers (Corning, Corning, NY) coated previously with 20% FCS or 10 µg/ml Vtn. For serum-coated matrix, the stimulus was performed in DMEM with 10% FCS added to the bottom chamber and incubated for 2 h at 37°C. For the Vtn-coated matrix, DMEM with 10% FCS was added to the bottom chamber and incubated for 4 h at 37°C. For the evaluation of G-protein interactions, 50 µg/ml PTX was incubated at 37ºC overnight prior to assay. The cells that were attached to either side of the Transwell

membranes were removed, fixed with methanol, stained with 1% Coomassie, and destained with acetic acid. Then absorbance at 506 nm was read using a SpectroMax® Plus 384 microplate spectrophotometer (Nguyen, Hussaini et al. 1998).

2.2.23. Cell signaling:

Cells were seeded with DMEM into a six well plate and incubated at 37ºC with 5% CO_2 until 80% confluence was reached. The day before the experiment, cells were washed three times with PBS, and the medium was replaced with SF DMEM for 18 h. After serum starvation, the medium was replaced with fresh SF DMEM in the presence of one of the following: undiluted fetal calf serum, 10 nM tcu-PA, 40 µM PD98059, 10 µM JNK II inhibitor or a combination of the all of the above. Cells were then stimulated for 5 min at 37°C, followed by quenching by washing three times with ice cold PBS/ 100 µM $NaVO_4$. Cells were then lysed in freshly made PBS/ 1% Triton X-100/ protease cocktail inhibitor (Roche). Lysates were subjected to BCA protein quantitation for equal loading. Samples were analyzed by immunoblotting and antibodies against phosphorylated ERK, JNK and p38 (Cell Signaling, San Diego CA) were used for cell signaling detection. Goat α-rabbit HRP (1:5000) (JackonImmunoReserch) was used for detection. Afterwards, blots were stripped using Pierce Stripping buffer for 30 min at 37°C. The samples were then re-analyzed using α-ERK (Zymed), α-JNK or α-p38 (all at 1:1000) antibodies, after which the standard immunoblotting procedure was performed.

2.2.24. Cell Death:

Cells (2,500 /well) were seeded into a 96 well plate, then treated either with SF DMEM, DMEM with 10% FCS, DMEM with 10% FCS and CO_2 deprivation or SF media and 10 nM TNF-α for 24 h at 37°C. The day of experiment, the media was exchanged with fresh DMEM/ 10% FCS following the addition of CellTiter 96® AQueous One Solution Reagent (Promega). The reactions were incubated for 1.5 h at 37°C/ 5% CO2. Cell density was determined using the proliferation assay outlined above.

2.2.25. Caspase assay:

293 cells, wt u-PAR cells and cr-uPAR cells were subjected to SF DMEM or DMEM containing 10 nM TNF-α (EMD Bioscience, San Diego CA) for 18 h at 37°C. Cells were lysed using TBS/1% Triton-x 100. Cell lystate (50 μg) was incubated for 4 h at 37°C with Ac-DEVD-AMC substrate following manufacturer's recommendations (Promega). Detection of caspase 3/7 was performed by reading the reaction for 60 min at 37°C at an excitation wavelength of 360 nm and emission wavelength of 460 nm.

2.2.26. Apoptosis assay:

293 cells were seeded onto a 24-well plate and subjected to DMEM (with or without serum) or SF DMEM with 10 nM TNF-α and 10 μg/ml CHX for 18 h at 37ºC. Media was removed and cells were trypsinized followed by washes with PBS. Cells were then incubated with PE-Annexin V, per manufacturers recommendations, for 15 min at 37°C. Samples were analyzed by flow cytometry and gated for both alive and dead.

2.3. Figures and Tables

Table III: u-PAR primers for site-directed mutagenesis

Residue mutated		Primer
EcoRI-ATG		ATCGATCGGAATTCCATGGGTCACCCGCCGCTG
EcoRV-TGA		CTGCATGGATATCCTCAGGTTTAGGTCCAGAG
R83A	forward	GCAACTCTGGCGCAGCTGTCACCTATT
	reverse	AATAGGTGACAGCTGCGCCAGAGTTGC
R89A	forward	CTGTCACCTATTCCGCAAGCCGTTACC
	reverse	GGTAACGGCTTGCGGAATAGGTGACAG
R83A/R89A	forward	GCAACTCTGGCGCAGCTGTCACCTATTCCGCAAGCCGTTACC
	reverse	GGTAACGGCTTGCGGAATAGGTGACAGCTGCGCCAGAGTTGC
R83E/R89A	forward	GCAACTCTGGCGAGGCTGTCACCTATTCCGCAAGCCGTTACC
	reverse	GGTAACGGCTTGCGGAATAGGTGACAGCCTCGCCAGAGTTAC
R83E/R89E	forward	GCAACTCTGGCGAGGCTGTCACCTATTCCGAGAGCCGTTACC
	reverse	GGTAACGGCTCTCGGAATAGGTGACAGCCTCGCCAGAGTTGC

CHAPTER 3. CHARACTERIZATION OF WILD TYPE U-PAR AND MUTANT U-PAR VARIANTS

3.1. Introduction:

In this chapter, we report the development and characterization of several u-PAR variants with increased resistance to proteolysis by tcu-PA. u-PAR contains a unique linker region between D_1 and D_2 of its multi-domain structure that is extremely sensitive to proteolysis by several proteases, including tcu-PA, Pn and matrix metalloproteases (Hoyer-Hansen, Ronne et al. 1992; Hoyer-Hansen, Ploug et al. 1997; Montuori, Rossi et al. 1999). The chemotactic epitope ^{88}SRSRY^{92} is found within this region and is exposed in the presence of u-PA by either a conformational change induced upon u-PA binding or by cleavage of D_1 (Fig. 3.1.1) (Fazioli, Resnati et al. 1997). The D_1 of u-PAR can be trans-cleaved by a u-PAR bound tcu-PA at two sites (Arg^{83} and Arg^{89}). The newly generated cleaved form of u-PAR (D_2D_3) is unable to bind u-PA (Hoyer-Hansen, Ronne et al. 1992), internalize u-PA-PAI-1 complexes, or efficiently bind Vtn (Montuori, Rossi et al. 1999). Cleavage of u-PAR is important in chemotaxis, cell migration and cell signaling, (Fazioli, Resnati et al. 1997; Montuori, Rossi et al. 1999; Montuori, Carriero et al. 2002; Mazzieri, D'Alessio et al. 2006) but the precise role of receptor cleavage in the regulation of cell-surface proteolysis is not clear. An extensively mutated u-PAR that provides cleavage resistance at all sites in the linker region exhibited increased alternative signaling-dependent migration compared to the wild type receptor (Mazzieri, D'Alessio et al. 2006). We hypothesized that u-PA regulates u-PAR by altering its function through the conformational states u-PAR can adopt. Heterogeneous glycosylation is an inherent

problem in studying u-PAR functions. Thus, we engineered a mutant u-PAR with Arg^{83} and Arg^{89} that confers cleavage resistance by tcu-PA.

3.2. Results:

3.2.1. Site-directed mutagenesis of u-PAR: Generation of a cleavage resistant receptor.

Cleavage of u-PAR by tcu-PA is thought to shift the functions of u-PAR from a proteolytic to a non-proteolytic role. To specifically study the effects of resistance to cleave by tcu-PA, all other linker region proteolytic sites were conserved including amino acids involved in receptor integrity, functionality of the chemotactic region, and maintenance of other protein interactions that contribute to chemotaxis. Figure 3.2.1, details the different combination of residues mutated for these studies. Alanine, a neutral residue, was selected as a major target for substitution in order to retain the overall structure of the receptor. An alternative residue to Arg was a Glu, since this residue has an opposite charge, retains its size but prevents tcu-PA cleavage. Additionally, we used combinatorial or individual mutations to optimize selection of a good candidate for the dissection of u-PAR functions. All mutations were confirmed by DNA sequencing (Fig. 3.2.2) prior to insertion into pDNA3.1 (+) for transfection into 293 cells. Wt u-PAR and cr-uPAR both expressed intact u-PAR at high levels The addition of exogenous Pn or chymotrypsin led to cleavage and degradation of the u-PAR variants. When tcu-PA was added this was not observed for cr-uPAR, supporting the double point mutational selection approach. Stable clones expressing high levels of u-PAR (similar to that observed in cancer cells) were selected.

3.2.2. Generating stable-transfected 293 cells expressing the u-PAR variants

293 cells expresses key proteins that initiate internalization (LRP), signaling (ERK, FPRL1, and EGFR), migration, proliferation and apoptosis, but does not express u-PAR or u-PA (Jo, Takimoto et al. 2009). The 293 cell line was used to identify functional abnormalities in the Pg activation system, and was characterized in the absence of u-PAR and in the presence of transfected intact full-length u-PAR or cleaved u-PAR. Wt u-PAR and the mutant u-PAR variants were stably transfected into 293 cells and selectively treated with 400 μg/ml of G418 for the incorporation of the human u-PAR pcDNA3.1(+) plasmid. Protein expression levels were evaluated following a double round of colony selection for all mutants by immunoblotting, then select representatives of u-PAR variants were chosen.

As expected, lysates from non-transfected 293 cells did not express u-PAR (Fig. 3.2.3 A). In cells expressing wt u-PAR and cr-uPAR, a band at approximately 55 kD represents the intact receptor. The additional band observed at approximately 40 kD in these two u-PAR variants may represent an underglycosylated or partially degraded u-PAR. Lysate from PMA-stimulated U937 cells were used as a positive control to delineate the approximate size of intact receptor (Fig. 3.2.3A). Stimulation with PMA increases u-PAR expression and glycosylation, resulting in a heterogeneous population of u-PAR. This increase in glycosylation, described previously, is most likely the explanation for the appearance of the PMA-stimulated U937 cell associated u-PAR at a higher molecular weight than 293 cell associated u-PAR (Behrendt, Ronne et al. 1990). In Figure 3.2.3 B, the u-PAR $R^{83}E/R^{89}E$ lane contains a minor band for the intact form, a major band representing the cleaved form, and a third major band of lower molecular weight. The

latter band likely represents a degradation product that formed due to cleavage by MMP-9, which is known to be expressed in 293 cells and has been shown to cleave at residue 86. The u-PAR mutant $R^{83}E/R^{89}A$ however, shows a band representing intact u-PAR and two lower bands: one of size similar to the cleaved form and the other similar to that observed in the $R^{83}E/R^{89}E$ u-PAR mutant. These combinational u-PAR variants ($R^{83}E/R^{89}E$ and $R^{83}A/R^{89}E$) did not express well in 293 cells. Whereas the single mutants expressed a significant amount of intact u-PAR, with a smaller additional form consistent with the cleaved form of u-PAR (Fig. 3.2.3 C and D). This additional band is likely a cleaved fragment of u-PAR that is more pronounced under conditions of high protein expression. Expression of $R^{83}E/R^{89}E$ and $R^{83}E/R^{89}A$ u-PAR mutants lead to a significant loss of adherent properties and were not used further in our studies. The $R^{83}A/R^{89}A$ mutant was utilized for further experiments to ensure stable protein production that would not be susceptible to cleavage by MMP-9. This mutant was further designated as cleavage resistant u-PAR (cr-uPAR).

After stable growth was achieved, cr-uPAR was subjected to reverse transcriptase PCR confirming the absence of additional unexpected mutations (Fig. 3.2.4). Non-transfected 293 cells did not transcribe u-PAR mRNA (lane 6), but the positive control for these cells (lane 5) and the 293 cr-uPAR positive control (lane 8) indicated that the PCR control, GADPH, was transcribed efficiently. 293 cr-uPAR and positive u-PAR cDNA control (lane 9) share a band of identical size. The cDNA was sequenced to confirm the presence of the expected mutations (data not shown). Flow cytometry was then used to determine the relative expression levels (Fig 3.2.5) of cell-surface u-PAR for a representative population of both wt u-PAR and cr-uPAR. 293 cells showed a higher

affinity for the isotopic control IgG, but the binding of α-human u-PAR polyclonal antibody did not show a significant enhancement in intensity, demonstrating a lack of u-PAR expression on the cell surface.

3.2.3. u-PAR with Arg^{83} and Arg^{89} mutated proves to be an effective cleavage resistant variant.

Specificity of cleavage resistance was confirmed by incubation with tcu-PA, another proteases known to cleave u-PAR in the linker region (Fig. 3.2.6 A). Overnight incubation of the cells in the absence of exogenous protease failed to produce cleavage products (Fig. 3.2.6, lane 2, all panels). The absence of a cleavage product indicated that any cleavage observed in the presence of exogenous proteases would be a result of the added enzyme. Exogenous tcu-PA generated a cleaved form of u-PAR in cells expressing wt u-PAR (Fig. 3.2.6 A; left and middle panel), with 70% of the receptor in the cleaved form indicating limited proteolysis of u-PAR. The observed pattern was not present in 293 cr-uPAR crude cell lysate (Fig. 3.2.6 A; right panel). In contrast, cleavage products were not observed when 293 cr-uPAR cells were incubated with excess tcu-PA for a prolonged time. As expected, the substitution of Ala at Arg^{83} and Arg^{89} lead to a u-PAR that cannot be proteolytically cleaved by tcu-PA.

Cell variants were then exposed to plasmin (Pn, 250 nM) to determine if u-PAR can be cleaved by a known protease that is also part of the Pg activation cascade. In 3-day PMA stimulated U937 cells (Fig. 3.2.6 B, left panel) Pn produced u-PAR cleavage products similar to those produced by tcu-PA. 293 wt u-PAR cells (middle panel) did not produce a cleavage product in the absence of protease, but in the presence of Pn a marked increase of cleavage product resulted. In 293 cr-uPAR cells (right panel), Pn produced a

similar cleavage pattern to that seen in wt u-PAR cells. However, the amount of observed cleavage product was significantly decreased, suggesting that there may be multiple cleavage sites in u-PAR. The cleavage profile was continued by using chymotrypsin. Both wt u-PAR (left panel) and cr-uPAR (right panel) were sensitive to limited and concentration-dependent proteolysis by chymotrypsin (Fig. 3.2.6 C). Lanes 2 and 3 contained bands representing intact u-PAR in both wt u-PAR and cr-uPAR panels. There was a decrease of the detected band that can be attributed to epitope loss by cleavage at secondary sites. However, a decrease in chymotrypsin concentration, as see in lanes 5 and 6 for both u-PAR variants, recovers the epitope loss of the cleaved product (Fig. 3.2.6 C). These experiments indicate that both wt u-PAR and cr-uPAR are susceptible to cleavage by proteases targeting residues in the linker region but not the two mutated Arg residues. Dano et al., reported that tcu-PA preferentially cleaves at residue 83, and that cleavage at residue 89 occurs to a lesser degree (Sidenius, Sier et al. 2000). Proteolytic digestion of single point mutants, $R^{83}A$ or $R^{89}A$ was evaluated to determine if tcu-PA cleavage resistance requires substitution at both Arg sites. Figure 3.2.7, demonstrates intact u-PAR with $R^{89}A$ and $R^{83}A$, lanes 1 and 4 respectively. In the presence of tcu-PA, the cleaved form of u-PAR was produced for the single mutants: $R^{89}A$ (lane 2) and $R^{83}A$ (lane 5). Full cleavage was not observed potentially due to incomplete digestion and time of exposure.

Both single point mutants were then subjected to limited proteolysis with chymotrypsin (10 nM). Incubation of 293 u-PAR $R^{89}A$ cells with chymotrypsin (lane 3) resulted in <50% cleavage, while incubation with cells expressing $R^{83}A$ resulted in 70-80% cleavage of the intact receptor. These results suggest that the two single mutation

sites may be different with respect to either conformation or the exposure of the linker region.

3.2.4. The cleavage resistant receptor has high affinity interactions with its ligands, and is over-expressed in 293 cells.

To compare the behavior of a mutant cell-surface molecule to its wild type counterpart, the binding-affinity for the cognate ligand needs to be similar. Thus, the binding affinities for 293 wt u-PAR and 293 cr-uPAR for an inactive form of u-PA, CMK-uPA were evaluated (Fig. 3.2.8). Triplicate of clones for each variant demonstrated differing expression levels by immunoblotting. Due to a tendency for over-expression, adherent cells were titrated to identify optimal saturation conditions (data not shown and Fig. 3.2.8). The cell titration identified the optimal cell number of 50,000 cells per well. This cell number was used to achieve receptor saturation. The dissociation constants obtained (1.1 nM to 1.5 nM) for three independent cell clones expressing either wt u-PAR or cr-uPAR (Fig. 3.2.8 A and Table IV) were similar to values observed by other groups (Stoppelli, Corti et al. 1985; Plow, Freaney et al. 1986; Estreicher, Wohlwend et al. 1989; Beaufort, Leduc et al. 2004). To determine ligand specificity, we exposed the non-transfected 293 cells to both CMK-uPA and radiolabeled CMK-uPA and observed no specific binding at the ranges studied (Fig. 3.2.8 A). Comparison of receptor number indicated that wt u-PAR expression levels (0.68 - 2.2 $x10^6$ receptors /cell) (Table IV, left panel) were lower than cr-uPAR expression levels (1.5 - 5.5 $x10^6$ receptors / cell) (Fig.3.2.8 A and Table IV, right panel). Immunoblotting of wt u-PAR and cr-uPAR confirmed the presence of a single intact protein, which was consistent with expression levels determined from the binding assays (Fig. 3.2.8 B). The similarity in binding

affinity between wt u-PAR and cr-uPAR demonstrated that cr-uPAR has a conformation similar to wt u-PAR, and that cr-uPAR has adequate post-translational modifications (glycosylation) to have a high affinity for u-PA.

3.2.5. Binding of tcu-PA to the u-PAR variants promotes plasminogen activation.

cr-uPAR has high affinity binding to u-PA (Table IV). In order to effectively use cr-uPAR, we questioned if it retained the ability to initiate the Pg activation cascade. The data presented previously demonstrated that cr-uPAR is able to bind u-PA with similar affinity to wt u-PAR. Next, we compared Pg activation between 293 cr-uPAR relative and 293 wt u-PAR. Unoccupied u-PAR was blocked with CMK-uPA, showing a significant decrease in Pg activation when supplementary tcu-PA was added, resembling the pattern observed with 293 cells incubated with tcu-PA (Fig. 3.2.9 A). 293 cr-uPAR cells and 293 wt u-PAR cells similarly initiated the cascade in the absence of CMK-uPA. The slight increase in Pn generation by wt u-PAR is likely a function of the higher level of expression of cell surface receptors.

The ability of the single point mutants, $R^{83}A$ and $R^{89}A$, to initiate the Pg activation cascade was tested since the single point mutations should not impact Pg activation. Plasmin generation by the u-PAR $R^{83}A$ mutant was similar to that of wt u-PAR and cr-uPAR. The individual clones were compared with regard to expression levels and Pn generation to discriminate between an effect due to the mutation and an effect of the individual clone's level of expression with clone 53 demonstrating slightly more Pn generation, which was attributed to its higher expression level identified by immunoblotting (Fig. 3.2.6 and 3.2.10). Plasmin generation by the $R^{89}A$ clones was also

similar to wt u-PAR and cr-uPAR with clone 43 demonstrating increased Pn generation that was associated with high expression levels, while clone 14 generated lower amounts of Pn in association with low expression levels (Fig. 3.2.10 and 3.2.6).

3.2.6. Specificity of u-PAR based plasminogen activation

Previous research coupled with results shown in section 3.2.3, shows that wt u-PAR but not cr-uPAR can be cleaved by tcu-PA, decreasing the amount of available intact receptors that can bind tcu-PA. The availability of intact receptor versus cleaved receptor can be observed in experiments where noticeable amounts of cleaved wt u-PAR are seen in the absence of extrinsically added protease, when compared to cr-uPAR (Fig. 3.2.6). Cleaved u-PAR generated by limited proteolysis with tcu-PA or chymotrypsin was used to ascertain the effect of D_1 removal from cell-surface u-PAR. Cleavage of wt u-PAR with either tcu-PA or chymotrypsin prior to binding tcu-PA (Fig. 3.2.11) resulted in a 50% decrease in Pn generation, similar to reports by other investigators (Hoyer-Hansen, Ronne et al. 1992; Hoyer-Hansen, Behrendt et al. 1997). Exposure of cr-uPAR to tcu-PA resulted in a 25% increase in Pn generation, which was attributable to the available cr-uPAR sites. Exposure of cr-uPAR to chymotrypsin resulted in a 50% decrease in Pn generation (Fig. 3.2.11). Cr-uPAR was expected to have equal or more tcu-PA-mediated Pn generation, but similar or less chymotrypsin-mediated Pn generation due to resistance to D_1 cleavage.

3.2.7. cr-uPAR has a decreased rate of fibrin clot lysis than its wt u-PAR counterpart.

Non-transfected, 293 wt u-PAR, and 293 cr-uPAR cells were evaluated for the ability to degrade fibrin clots. As a control, evaluation of acid washed 3-day PMA stimulated

U937 cells indicated that cells were not able to degrade fibrin, unless scu-PA was added (3.2.12 A). Under similar buffering conditions as U937 cells, 293 cells were able to degrade fibrin clot (data not shown), likely due to endogenous production of MMP-9 which has fibrinolytic activity. To limit cell-mediated fibrin degradation, EDTA, which is known to inhibit MMPs, was incorporated into the buffer. In the presence of EDTA, non-transfected 293 cells did not degrade fibrin clots, even with exogenous scu-PA added (Fig. 3.2.12 B). In comparison, 293 wt u-PAR cells were able to cause 50% degradation in the presence of scu-PA. Unexpectedly, 293 cr-uPAR cells delayed degradation at 20 min, with 50% degradation at 90 min (Fig. 3.2.12 C). Since both u-PAR variants bound u-PA with similar affinities we stipulate that a downstream effect or mechanism is altering fibrin clot lysis.

3.3. Discussion:

Prior to this study, the cleavage resistant u-PAR mutant available did not retained interactions with both u-PA and Vtn. Indeed, previously published mutational analysis studies have failed to provide useful insights into the differences between intact u-PAR and cleaved u-PAR. One study using a cleavage resistant u-PAR, termed hcr-uPAR, indicated a possible impact on signaling pathways (Mazzieri, D'Alessio et al. 2006). However, hcr-uPAR had the linker region extensively mutated altering all the proteolytic sites, including two of the five residues (R^{89} and R^{91}) in the chemotactic epitope. Studies performed using Ala scanning were used as means to identify protein interactions between u-PAR and Vtn or integrins and they noted that mutation to R^{91} of the linker region interferes with Vtn interactions (Madsen, Ferraris et al. 2007). Such a mutation

causes difficultly in isolating functional differences, since a Vtn binding site is also abolished.

tcu-PA trans-digests u-PAR, dissociating $D_{1,}$ and thus rendering it unable to bind u-PA. The interaction between u-PA and u-PAR is complementary, since cleavage cannot occur without binding. During the interaction between the ligand and receptor, both active site-dependent events and non-active site dependent occur. This is also true when generating a cleaved u-PAR changing the receptor from a proteolytic to non-proteolytic function. Limiting our mutations to the two Arg cleavage sites allowed for the generation of a tcu-PA cleavage-resistant receptor that retained significant function and preserved other known protein interactions that is important for chemotactic effectiveness.

In cancer studies, there is strong evidence of a role for soluble and cleaved forms of u-PAR, indicating a potential important role for u-PAR cleavage (Hoyer-Hansen review). However, there is little direct evidence implicating cleaved u-PAR in these events, since most of these effects are inducible by ligand-bound u-PAR (Ragno review 09). This leads to questions whether cleaved u-PAR is a regulatory step for the variety of functions. The only direct evidence of a specific role for cleaved u-PAR is an involvement in the differentiation of myofibroblast to fibroblast (Brenstein, 2009). However, these experiments were conducted using hcr-uPAR, as mentioned above, which also lacks Vtn binding.

Cells expressing the u-PAR variants $R^{83}E/R^{89}A$ or $R^{83}E/R^{89}A$ lost their adhesive properties or were prone to cell death, making the collection and isolation of these cell lines challenging. The effects observed with these mutants may be a result of an alternate conformation. Charge substitution in the linker region by exchanging the Arg to a Gln

could potentially disrupt the known multiple protein interactions. Thus, substitution of Arg to Ala may be key for these studies, since cr-uPAR retains the wt u-PAR functions and does not disrupt protein-protein interactions.

The cr-uPAR clones expressed similar high levels of u-PAR, and were comparable to the expression levels observed in cancer cells. The cleavage profile observed with the single point mutations supports the use of the double point mutant to confer resistance to tcu-PA cleavage while maintaining other proteolytic sites. For future experiments, single point mutants can aid in the dissection of residues important for specific functions.

3.4. Figures and Tables:

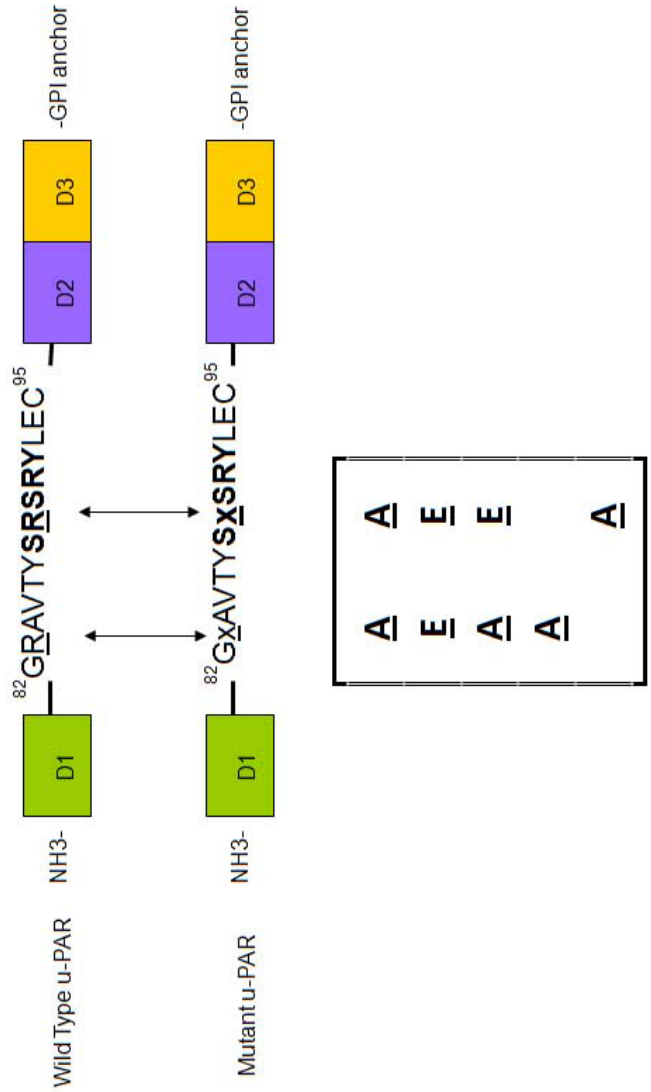

Figure 3.1. Generation of u-PAR mutants. The two tcu-PA cleavage sites, residue 83 and residue 89, shown at the top (wild type) are mutated to different residues, shown as an x (mutant). The bottom box outlines the mutational changes made in the linker region. D_1 (green) is followed by the linker region, D_2 (purple) and D_3 (orange) are anchored to the cell –surface through the GPI-anchor found in D_3. "This research was originally published in Journal Biological Chemistry. Evelyn C. Nieves and Naveen Manchanda. A cleavage-resistant urokinase plasminogen activator receptor exhibits dysregulated cell-surface clearance. J Biol Chem. 2010 April 23; 285(17): 12595–12603. © the American Society for Biochemistry and Molecular Biology."

cDNA Sequence

```
NCBI u-PAR    GCCGGGCTGTCACCTATTCCCGAAGCCGTTACCTCGAATGCATTTCCTGTGGCTCATCAG 360
R83A/R89A     GCGCAGCTGTCACCTATTCCGCAAGCCGTTACCTCGAATGCATTTCCTGTGGCTCATCAG 360
R83E/R89E     GCGAGGCTGTCACCTATTCCGAGAGCCGTTACCTCGAATGCATTTCCTGTGGCTCATCAG 360
R83E/R89A     GCGAGGCTGTCACCTATTCCGCAAGCCGTTACCTCGAATGCATTTCCTGTGGCTCATCAG 360
R83A          GCGCAGCTGTCACCTATTCCCGAAGCCGTTACCTCGAATGCATTTCCTGTGGCTCATCAG 360
R89A          GCCGGGCTGTCACCTATTCCGCAAGCCGTTACCTCGAATGCATTTCCTGTGGCTCATCAG 360
Wt u-PAR      GCCGGGCTGTCACCTATTCCCGAAGCCGTTACCTCGAATGCATTTCCTGTGGCTCATCAG 360
              **   ***************   ************************************
```

Protein Sequence

```
NCBI u-PAR    ELVEKSCTHSEKTNRTLSYRTGLKITSLTEVVCGLDLCNQGNSGRAVTYSRSRYLECISC 120
R83A/R89A     ELVEKSCTHSEKTNRTLSYRTGLKITSLTEVVCGLDLCNQGNSGAAVTYSASRYLECISC 120
R83E/R89E     ELVEKSCTHSEKTNRTLSYRTGLKITSLTEVVCGLDLCNQGNSGEAVTYSESRYLECISC 120
R83E/R89A     ELVEKSCTHSEKTNRTLSYRTGLKITSLTEVVCGLDLCNQGNSGEAVTYSASRYLECISC 120
R83A          ELVEKSCTHSEKTNRTLSYRTGLKITSLTEVVCGLDLCNQGNSGAAVTYSRSRYLECISC 120
R89A          ELVEKSCTHSEKTNRTLSYRTGLKITSLTEVVCGLDLCNQGNSGRAVTYSASRYLECISC 120
Wt u-PAR      ELVEKSCTHSEKTNRTLSYRTGLKITSLTEVVCGLDLCNQGNSGRAVTYSRSRYLECISC 120
              ********************************************* ***** *********
```

Figure 3.2. DNA and protein sequence alignment. Top image, DNA sequence aligment using NCBI sequence for human wt u-PAR shows the presence of mutations made to the Arg codon in either position 83, position 89, or both. The region where mutations are found are underlined. Bottom image, the protein sequence of the u-PAR variants are shown here in bold and underlined to show the mutations in position 83 or 89 or both,

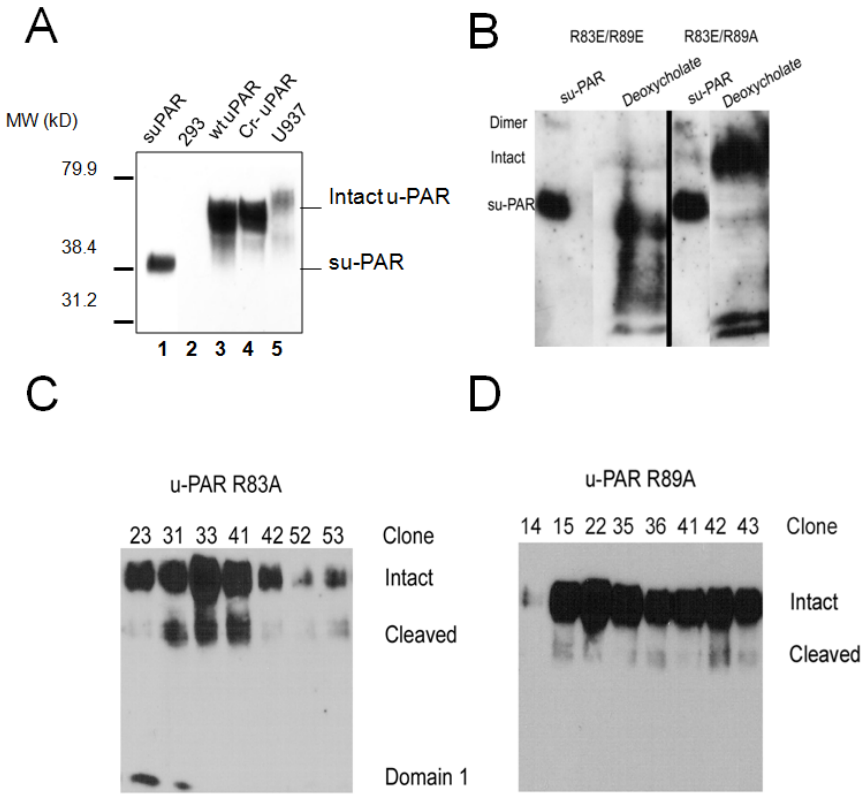

Figure 3.3. Expression of different u-PAR variants. **A**) Su-PAR (125 ng) (1), wt 293 cells (2), 293 wt u-PAR cells (3), 293 cr-uPAR cells (4) and 3-day PMA stimulated U937 cells (5) were immunoblotted using polyclonal α-human u-PAR to detect u-PAR in 5 µgs total cell lysate. **B**) Su-PAR (250 ng; left and right panels) was used as a control with cell lysates of u-PAR $R^{83}E/R^{89}E$ (left panel) and u-PAR $R^{83}E/R^{89}A$ (right panel) and detected using polyclonal α-human u-PAR. Expression levels of selected clones for the single point mutations $R^{83}A$ (**C**) and $R^{89}A$ (**D**) were detected using polyclonal α-human u-PAR.

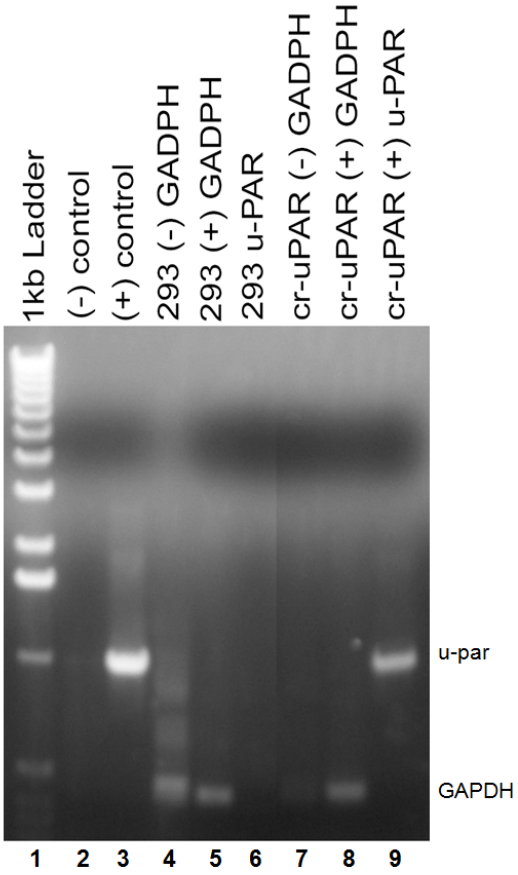

Figure 3.4. u-PAR mRNA detection in 293 cr-uPAR but not in 293 cells. First strand cDNA was amplified and ran on an agarose gel. Lane 1 shows the 1Kb ladder. No u-PAR cDNA (lane 2) was used as the negative control, whereas the plasmid containing the u-par gene was our positive control (lane 3). 293 cells cDNA was amplified in the absence (lane 4) of primers, presence of GADPH (lane 5) primers and in the presence of u-PAR primers (lane 6). 293 cells expressing cr-uPAR was amplified in the absence (lane 7) of primers, presence of GADPH (lane 8) primers and in the presence of u-PAR primers (lane 9).

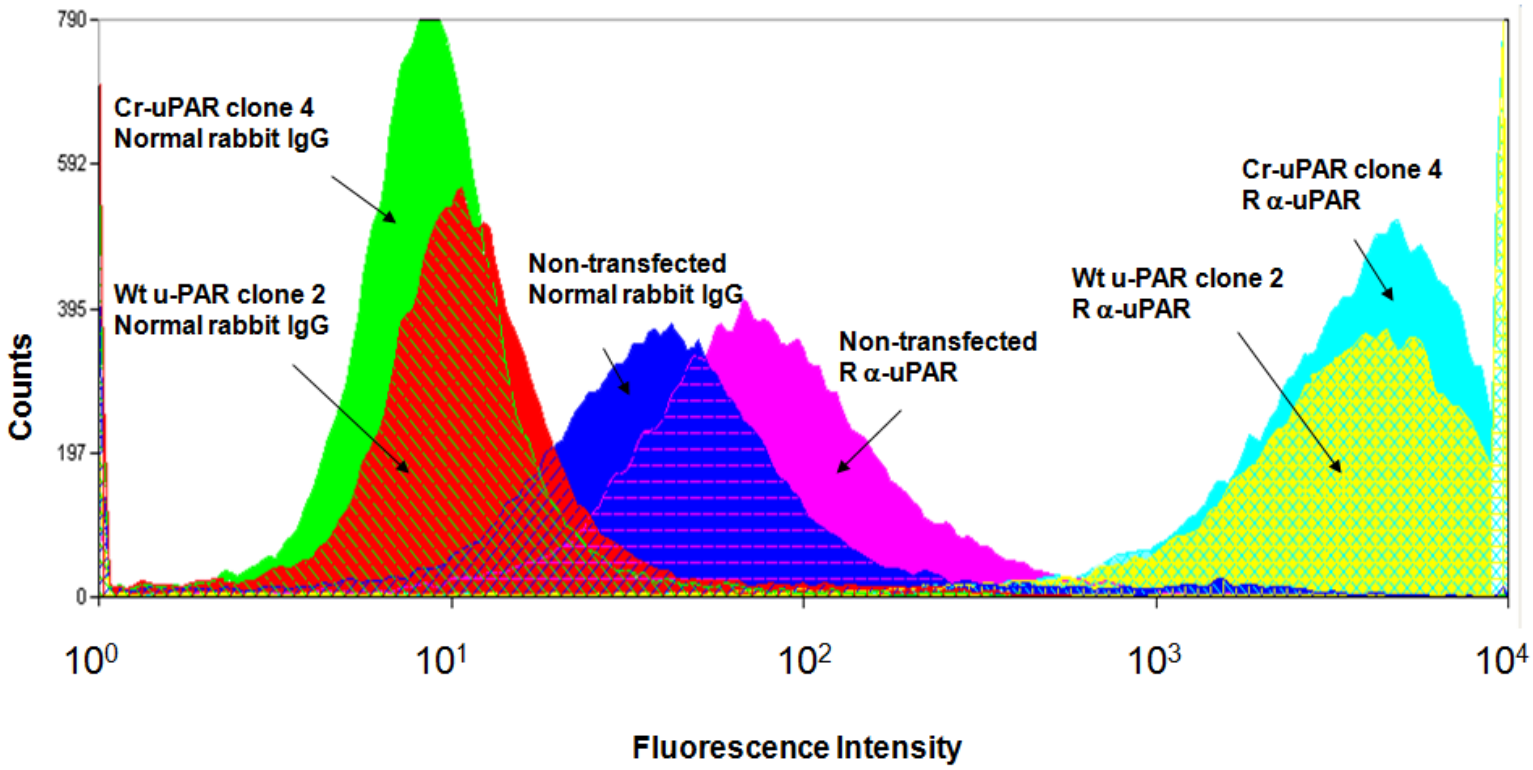

Figure 3.5. Detection of u-PAR by flow cytometry. Resuspended 293 (blue), 293 wt u-PAR (red) and 293 cr-uPAR (green) cells were incubated with normal rabbit IgG followed by goat α-rabbit Alexa 488. Polyclonal α-human-uPAR was used for u-PAR detection on 293 (magenta), 293 wt u-PAR (yellow) and 293 cr-uPAR (aqua) cells followed by the secondary goat α-rabbit Alexa 488.

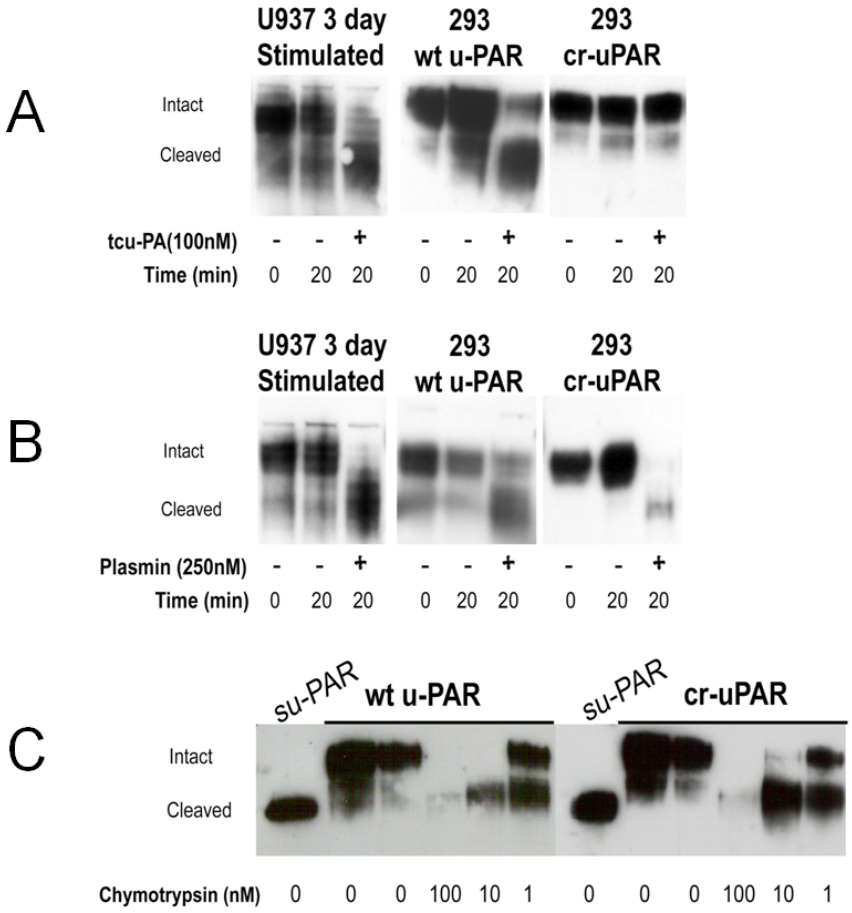

Figure 3.6. Cleavage profiles of u-PAR expressing cells. Receptor-bearing cells were exposed to tcu-PA (**A**), plasmin (**B**) or chymostrypsin (**C**). PMA-stimulated U937 (*left panel*), wt u-PAR (*middle panel*) and cr-uPAR (*right panel*) cells are shown in the absence of protease at 0 h, in the absence of protease at 20 h, and in the presence of tcuPA **(A)** or plasmin **(B)** for 20 h. **C**) Wt u-PAR (*left panel*) and cr-uPAR (*right panel*) expressing cells were subjected to cleavage by chymotrypsin. Lane 1 shows our control sample su-PAR. Cleavage was performed in the absence of protease for 0 h (lane 2) and 30 min (lane 3), in the presence of chymotrypsin 100 nM (lane 4), 10 nM (lane 5) and 1 nM (lane 6). Cell lysates were obtained and 4 µgs of total cellular protein lysate was loaded onto 10% PAGE gels and analyzed by western blot using polyclonal α-human u-PAR. "This research was originally published in Journal Biological Chemistry. Evelyn C. Nieves and Naveen Manchanda. A cleavage-resistant urokinase plasminogen activator receptor exhibits dysregulated cell-surface clearance. J Biol Chem. 2010 April 23; 285(17): 12595–12603. © the American Society for Biochemistry and Molecular Biology."

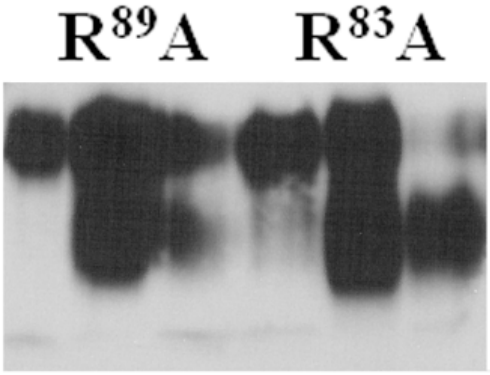

Tcu-PA (100 nM)	-	+	-	-	+	-
Chymotrypsin (10 nM)	-	-	+	-	-	+

Figure 3.7. Cleavage profiles for u-PAR expressing single point mutants. u-PAR $R^{89}A$ (*left panel*) and u-PAR $R^{83}A$ (*right panel*) expressing cells were exposed no protease (lane 1), 100 nM tcu-PA (lane 2) or 10 nM chymotrypsin (lane 3) for 1 h. 5 µg of total cellular

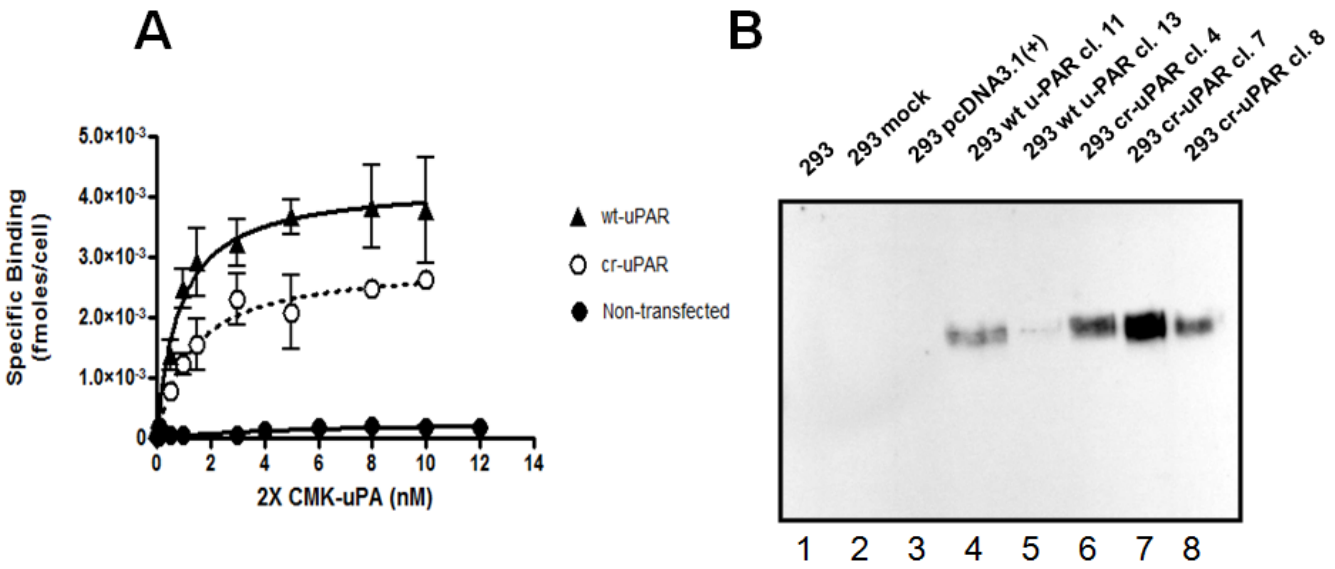

Figure 3.8. Competitive binding for u-PAR variants expressed in 293 cells. **A**) 293 cells either non-transfected (●), expressing wt u-PAR (▲) or cr-uPAR (O) were subjected to increasing concentration of ^{125}I-CMK-uPA. Graphs shown are representative of the mean and SEM of 4 individual replicates. **B**) 5 µg of cell lysate for 293 cells expressing different constructs of the plasmid, 293 (lane 1), 293 mock transfected (lane 2), 293 pcDNA3.1(+) (lane 3), 293 wt u-PAR clone 11 (lane 4), 293 wt u-PAR clone 13 (lane 5), 293 cr-uPAR clone 4 (lane 6), 293 cr-uPAR clone 7 (lane 7), 293 cr-uPAR clone 8 (lane 8) containing u-PAR were analyzed by immunoblotting using polyclonal α-human u-PAR.

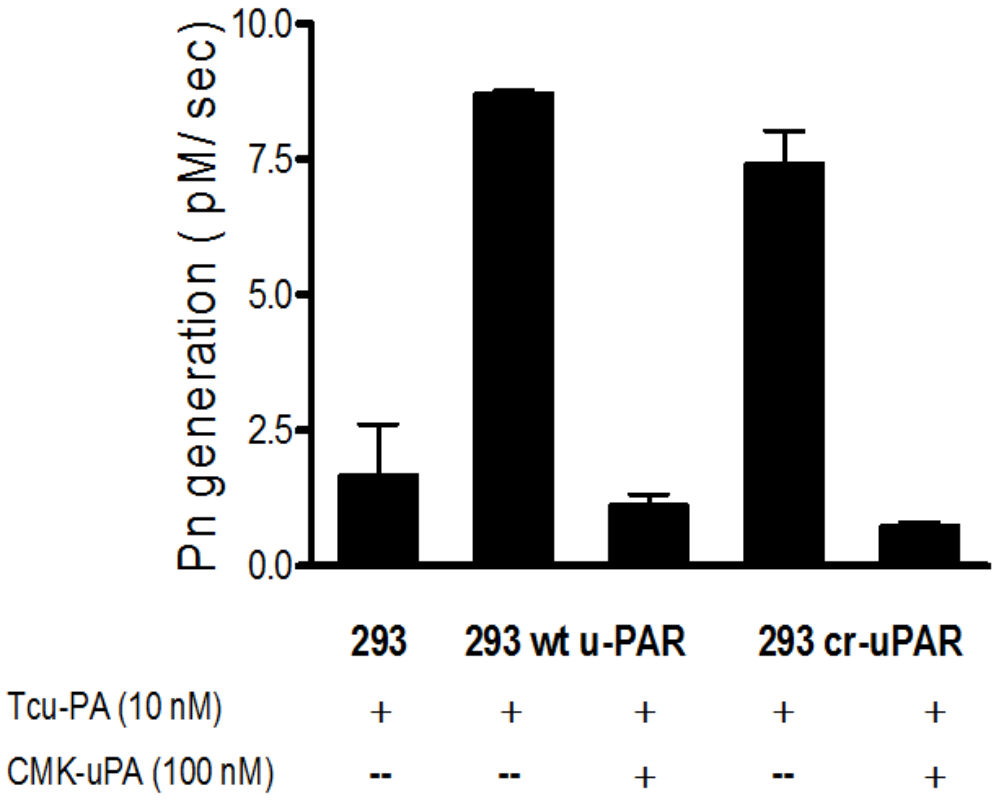

Figure 3.9. Both cell surface u-PAR variants bind specifically to u-PA and initiate Pg activation. Specific binding of tcu-PA to unoccupied u-PAR shows Pn generation by u-PAR bound tcu-PA. Cells were seeded O/N and incubated with tcu-PA for 30 min at 37°C. To block the unoccupied receptor, cells were incubated with 100 nM CMK-uPA in DMEM, 0.1% BSA for 30 min following an incubation with 10 nM tcu-PA for 30 min. Cells were washed to remove unbound proteins. Pn generation was initiated and quantified as described in materials and methods. Bars and error bars represent the mean and SD of 3 individual replicates. "This research was originally published in Journal Biological Chemistry. Evelyn C. Nieves and Naveen Manchanda. A cleavage-resistant urokinase plasminogen activator receptor exhibits dysregulated cell-surface clearance. J Biol Chem. 2010 April 23; 285(17): 12595–12603. © the American Society for Biochemistry and Molecular Biology."

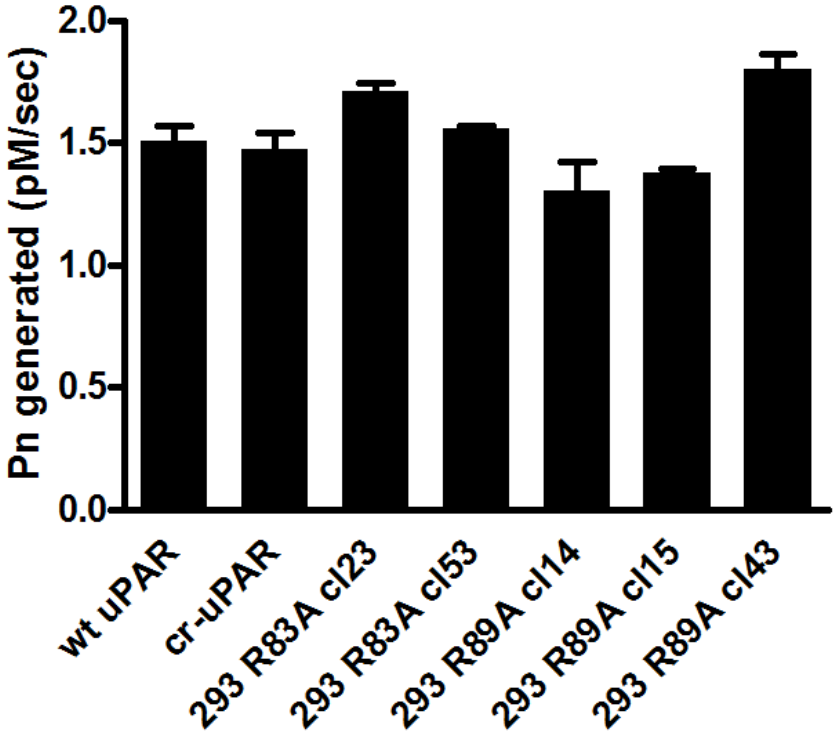

Figure 3.10. Cells expressing the single point u-PAR mutants can generate Pn. Binding of tcu-PA to unoccupied u-PAR shows Pn generation by u-PAR bound tcu-PA. Cells were seeded O/N and incubated with tcu-PA for 30 min at 37°C. Cells were washed to remove unbound proteins. Pn generation was initiated and quantified as described in materials and methods. Bars and error bars represent the mean and SD of 3 individual replicates.

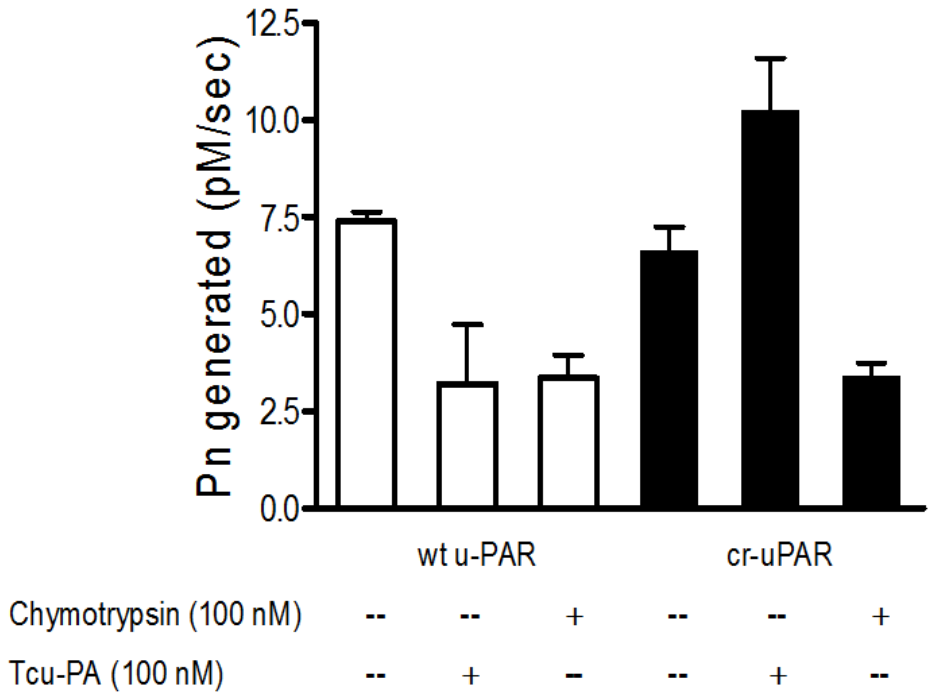

Figure 3.11. Cell surface u-PAR variants undergone receptor cleavage limits Pn generation. tcu-PA associated Pn generation was determined by cells expressing wt u-PAR (white bars) or cr-uPAR (black bars) after exposure with 10 nM chymotrypsin or 100 nM tcu-PA for 30 min at 37ºC. A secondary incubation with 10nM tcu-PA for 30 min at 37ºC was performed. Cells in the absence or presence of tcu-PA were used as control of basal levels of Pn generation. Pn generation was initiated and quantified as previously described. Bars and error bars represent the mean and SD of 3 individual replicates.

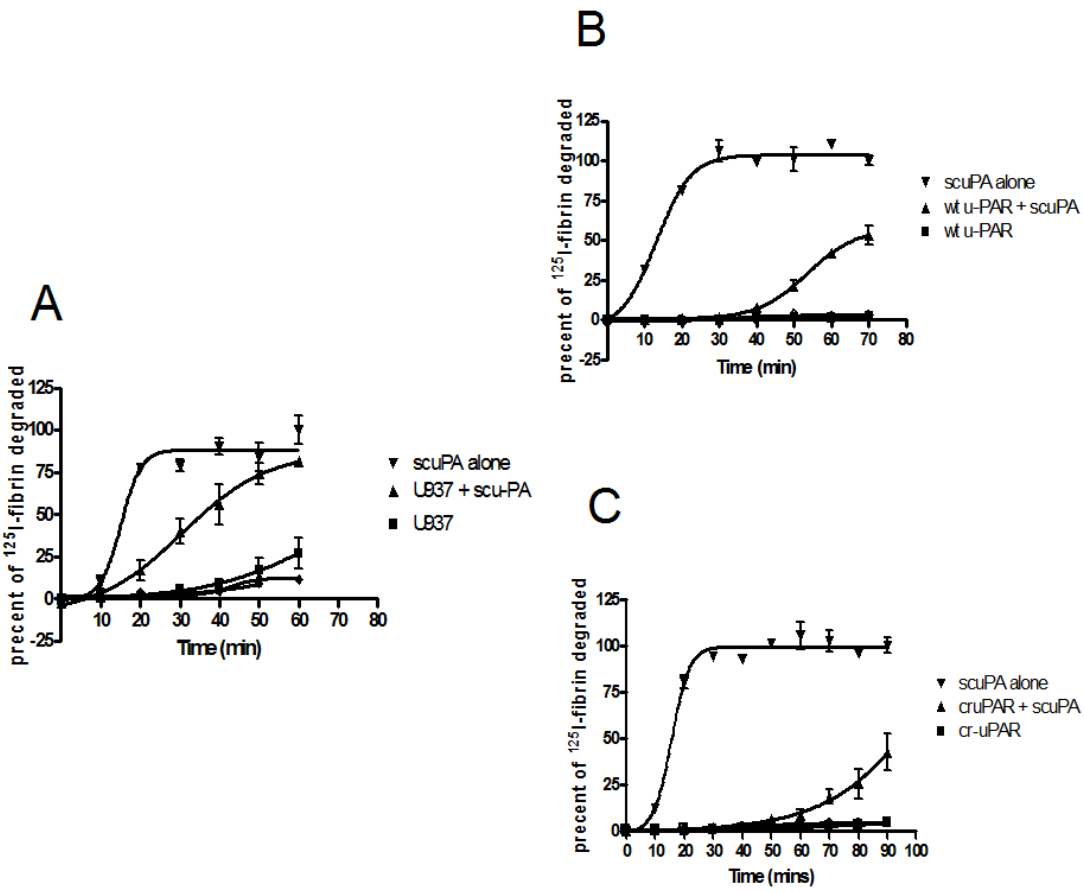

Figure 3.12. Generation of fibrin degradation fragments is deterred in cr-uPAR expressing cells. Cells expressing u-PAR variants are added to a pre-formed I-125 fibrin clot. A) 3-day PMA stimulated U937 in 0.1M Tris, B) 293 wt u-PAR cells in 1X Tris-EDTA, or C) 293 cr-uPAR cells in 1X Tris-EDTA were pre-incubated either alone (■) or with 1nM scu-PA (▲) for 30 mins prior to addition to the fibrin clot. As a control, 1 nM scu-PA (▼) was added to an individual well. All samples were incubated for 30 min at 37°C. The graphs represent the mean and SD of 3 individual replicates.

Table IV						
Binding of CMK-uPA to 293 cells						
Cell line	**293 wt u-PAR**			**293 cr-uPAR**		
	Clone 2	**Clone 11**	**Clone 13**	**Clone 4**	**Clone 7**	**Clone 8**
K_D (nM ±SEM)	1.3 ± 0.6	1.1 ± 0.4	1.1 ± 0.4	1.4 ± 0.4	1.5 ± 0.3	1.5 ± 0.2
Sites/cell (10^6 ±SEM)	2.0 ± 0.2	2.2 ± 0.6	0.68 ± 0.07	1.5 ± 0.1	3.8 ± 0.3	5.5 ± 0.2

CHAPTER 4. CR-UPAR IS IN A CONFORMATION THAT IS PREDOMINANTLY U-PA INDEPENDENT

4.1. Introduction:

The dissection of u-PAR activation mechanisms and their downstream effects is of great medical interest, since this receptor has been implicated in both physiological and pathophysiological processes, and has emerged as a potential therapeutic target in neoplasia. Emerging evidence suggests that conformation is an important aspect of u-PAR function. Indeed, u-PAR exists in at least three functionally distinct states: 1) full-length ligand-free (its latent or inactive state); 2) full-length with u-PA bound (its activated state); and 3) cleaved receptor (which no longer binds u-PA, but is active due to the proteolytically-exposed chemotactic peptide) (Ploug and Ellis 1994; Ploug, Ellis et al. 1994; Fazioli, Resnati et al. 1997; Huai, Mazar et al. 2006; Yuan and Huang 2007; Huai, Zhou et al. 2008). u-PAR crystal structures support conformational flexibility, with multiple receptor conformations depending on the ligand, such the antagonist ATF of u-PA, and the SMB domain of Vtn (Llinas, Le Du et al. 2005; Barinka, Parry et al. 2006; Huai, Mazar et al. 2006; Huai, Zhou et al. 2008). Functional studies of different receptor states has been complicated by the fact that some of the functions of u-PA-bound u-PAR and the cleaved receptor overlap (Resnati, Guttinger et al. 1996; Nguyen, Hussaini et al. 1998; Montuori, Carriero et al. 2002). Also, u-PAR is a substrate for its own cognate ligand, u-PA (Hoyer-Hansen, Ronne et al. 1992; Hoyer-Hansen, Ploug et al. 1997; Hoyer-Hansen, Pessara et al. 2001). Thus, the presentation of u-PA to u-PAR leads to activation of the receptor by two overlapping mechanisms that are difficult to separate.

u-PAR contains a unique linker region between D_1 and D_2 of its multi-domain (D_1-D_3) structure that is exposed in the presence of u-PA either by conformational change or cleavage of D_1 (Fazioli, Resnati et al. 1997; Huai, Mazar et al. 2006; Huai, Zhou et al. 2008). Bound tcu-PA cleaves D_1 of u-PAR at two sites (R^{83} and R^{89}), generating the cleaved form of u-PAR (D_2D_3) that is unable to bind u-PA (Hoyer-Hansen, Ronne et al. 1992), internalize u-PA-PAI-1 complexes, or efficiently bind Vtn and other matrix constituents (Montuori, Rossi et al. 1999). Cleavage of u-PAR is important in chemotaxis, cell migration and cell signaling, but the role of receptor cleavage in regulating several other cell-associated processes is not well understood (Fazioli, Resnati et al. 1997; Montuori, Rossi et al. 1999; Montuori, Carriero et al. 2002; Mazzieri, D'Alessio et al. 2006). This suggests that a ligand that strengthens the interaction between u-PAR and Vtn or integrins also has the potential to modulate the roles of u-PAR in chemotaxis, cell migration, and cell signaling.

In this section we demonstrate that 293 cr-uPAR cells exhibit normal promotion of cell-surface Pg activation. Clearance of u-PA-PAI-1 complexes, receptor recycling, and cell migration were enhanced in cr-uPAR expressing cells compared to cells expressing wt u-PAR. We also observed that cr-uPAR closely associates with LRP with higher affinity than wt u-PAR, regardless of whether u-PAR is unoccupied or bound to u-PA-PAI-1 complexes, resembling more the ligand-bound form than the unliganded form. Enhanced internalization of cr-uPAR might be related to an increase in pre-assembly of unoccupied u-PAR with LRP. We hypothesized that cr-uPAR retains some abilities associated with conformationally active u-PAR. Whether cr-uPAR confers advantages to cells (similar to heavily glycosylated cleavage-resistant u-PAR in cancer cells) awaits

further study (Ragno, Montuori et al. 1998; Montuori, Rossi et al. 1999; Montuori, Carriero et al. 2002).

4.2. Results:

4.2.1. Cell surface regulation of scu-PA and tcu-PA

PAI-1 plays a central role in inhibiting Pg activation by reversibly inhibiting scu-PA and irreversibly inhibiting tcu-PA, which is necessary for proper down-regulation of extracellular proteolysis. When we evaluated the ability of PAI-1 to access tcu-PA bound to cell-surface u-PAR, we found that cell-surface bound tcu-PA was efficiently inactivated by PAI-1 on both wt u-PAR cells and cr-uPAR cells (Fig. 4.2.1). Intriguingly, cr-uPAR cells had higher activity than wt u-PAR cells following treatment with PAI-1 (20% versus 5%, respectively). Cells expressing cr-uPAR may have mostly intact receptors on the cell surface, while cells expressing wt u-PAR may have more tcu-PA mediated cleavage. Since u-PA-PAI-1 complex formation is irreversible, we detected very little Pn generating activity from pre-formed complexes bound to the cell surface (Fig. 4.2.1 A). These data suggest that initiation and inhibition of Pg activation occur similarly on wt u-PAR cells and cr-uPAR cells.

Similar experiments using scu-PA rather than tcu-PA yielded unexpected results (Fig. 4.2.1 B). Because the scu-PA:PAI-1 interaction is reversible, we expected that Pn would be generated. Inhibition of scu-PA by PAI-1 with cells expressing wt u-PAR resulted in a 70% increase in Pn activity. Interestingly, with cells expressing cr-uPAR, there was only 25 - 30% activity. scu-PA:PAI-1 pre-complexes were then generated and allowed to bind to the u-PAR variants. For wt u-PAR we observed an 85% increase in proteolytic activity. On the other hand, cr-uPAR cells did not yield a significant change in activity.

Inhibition studies of u-PAR bound scu-PA or the pre-complexed scu-PA:PAI-1 yielded similar results for cr-uPAR. These results are consistent with the observations found in the fibrinolytic system (shown in chapter 3) and leads us to speculate a possible difference between scu-PA and tcu-PA.

4.2.2. Cells expressing cr-uPAR internalize u-PA-PAI-1 complexes more rapidly than those cells expressing wt u-PAR.

Internalization and clearance of u-PA-PAI-1 complexes are vital for the down-regulation of the Pg system. Inhibited u-PA bound to PAI-1 forms a hetero-trimeric complex with u-PAR that binds to the endocytic receptor, LRP. The resulting hetero-tetramer is internalized, u-PA-PAI-1 complexes are degraded, and LRP is recycled to the cell surface. In several cell types, levels of LRP expression are the limiting factor in the internalization and recycling rate of u-PAR (Li, Kuo et al. 1994; Nykjaer, Kjoller et al. 1994; Henic, Sixt et al. 2006). Because u-PAR is essential for the rapid endocytosis of u-PA-PAI-1 complexes, we examined the effect of the u-PAR mutations on this receptor function.

Upon pulse-labeling a pool of cell-surface receptors with biotin and addition of u-PA-PAI-1 complex, we detected u-PAR in the cytoplasmic fraction. Consistent with previous reports, cytoplasmic wt u-PAR increased in a gradual time-dependent manner to a maximum internalized amount at 13 min, followed by a gradual decline (Fig. 4.2.2 A) (Cortese, Sahores et al. 2008). In contrast, cr-uPAR bound to u-PA-PAI-1 complex was internalized with an initial peak that was detected at the first studied time point, followed by a secondary peak which resembles the endocytic profile of wt u-PAR, thus showing a shift in time frame for complex recycling (Fig. 4.2.2 B). RAP binding to LRP inhibits

endocytosis mediated by this cell-surface receptor (Griffith, Breitkreutz et al.). Figure 4.2.2 shows that RAP inhibits LRP-mediated endocytosis of u-PAR:u-PA-PAI-1 complexes to 10% of peak values seen in the absence of RAP. Thus, although a similar process may mediate the internalization of both types of receptors, cr-uPAR undergoes this process at a much faster rate compared to wt u-PAR. We evaluated the internalization of wt u-PAR and cr-uPAR in the absence of u-PA-PAI-1 complexes, to identify if the initial burst of cr-uPAR endocytosis was due to a mutant-specific response toward u-PA-PAI-1 exposure (Fig. 4.2.2 B). We found that cr-uPAR was rapidly internalized at 3 min in a manner similar to that seen in the presence of u-PA-PAI-1 complex (Fig. 4.2.2 B). A secondary internalization peak was seen at 33 min, consistent with a basal endocytosis cycle of about 30 minutes. While wt u-PAR internalization remained under 2% of total labeled receptor, internalization of cr-uPAR reached twice that level (Fig. 4.2.2 A). These data suggest that the initial rapid cr-uPAR internalization event can occur independently of the binding of u-PA-PAI-1 complexes.

To determine whether internalization of cr-uPAR is LRP-mediated, RAP was added to prevent LRP-mediated internalization. The initial burst of internalization was not observed for cr-uPAR internalization, and overall internalization was markedly inhibited. A similar findings was observed for wt u-PAR. These results suggest that endocytosis and clearance of the u-PA-PAI-1 complexes is primarily LRP-dependent. To rule out the possibility that biotinylation of u-PAR affected its internalization profile, a similar experiment was performed using biotinylated-PAI-$1_{14\text{-}1B}$ in complex with tcu-PA (Fig. 4.2.4). The results generated a similar endocytosis profile as those observed using biotinylated u-PAR. Both wt u-PAR and cr-uPAR cells exhibited similar peak

internalization (at 18 min), and an initial burst occurred with cr-uPAR (Figure 4.2.2 A). Furthermore, lower molecular weight biotin-positive species appeared in conjunction with the decrease in cytoplasmic biotinylated u-PA-PAI-1 complex, consistent with lysosomal degradation of the endocytosed complex (data not shown). The presence of RAP dramatically diminished u-PA-PAI-1 complex internalization, indicating involvement of LRP-mediated endocytosis.

4.2.3. cr-uPAR recycling is increased following internalization of u-PAR:u-PA-PAI-1 complexes.

u-PAR and LRP internalization is followed by recycling of these receptors to the cell surface and their spatial redistribution (Nykjaer, Conese et al. 1997). Having observed an initial rapid internalization of cr-uPAR, we determined whether the endocytosis of u-PA-PAI-1-bound cr-uPAR is followed by recycling/resurfacing of unliganded receptor. Receptor recycling was studied by saturating cell-surface u-PAR with u-PA-PAI-1 complexes, inducing internalization, and detecting resurfaced unoccupied u-PAR via binding of active tcu-PA in a Pg activation assay. Figure 4.2.5 shows that cells expressing cr-uPAR recycle the receptor faster than their wild-type receptor-expressing counterparts. Approximately half of internalized cr-uPAR had reappeared on the cell-surface 15 min after the induction of endocytosis, while internalized wt u-PAR required nearly twice the time (30 min) to reach a similar level of resurfacing. For the entire course of the experiments, synthesis of new receptor was prevented by the addition of CHX. Exposure of cells to RAP before addition of u-PA-PAI-1 complexes resulted in marked inhibition of receptor resurfacing, suggesting that LRP-mediated endocytosis is required for the appearance of unoccupied receptor on the cell surface and that

unoccupied receptor does not appear via simple dissociation of the initially formed u-PAR:u-PA-PAI-1 complex.

4.2.4. cr-uPAR binds LRP in the absence of u-PA-PAI-1 complex.

LRP associates with u-PAR bound u-PA-PAI-1 complexes (Andreasen, Sottrup-Jensen et al. 1994). This interaction is primarily between the u-PA-PAI-1 complex and LRP, though a direct u-PAR:LRP interaction may play a minor role (Czekay, Kuemmel et al. 2001). Since cr-uPAR has an altered LRP-mediated internalization profile which occurs even in the absence of u-PA-PAI-1 complex, we determined whether cr-uPAR and LRP are closely associated by co-immunoprecipitaion of u-PAR with a monoclonal α-LRP antibody, 11H4. In Figure 4.2.6 A and C, a trace amount of wt u-PAR was detected using 11H4 in the absence of u-PA-PAI-1 complex. In the presence of the complex, the amount of immunoprecipitated wt u-PAR was enhanced, an effect that was completely blocked by RAP (Fig. 4.2.6 A). In contrast, cr-uPAR alone co-immunoprecipitated with LRP, an association that was further enhanced by the addition of u-PA-PAI-1 complex (Fig. 4.2.6 B-D). Indeed, the amount of cr-uPAR precipitated with 11H4 in the absence of tcu-PAI-1 complex was comparable to that of wt u-PAR in the presence of the complex.

To disrupt the association of unliganded cr-uPAR and LRP, we selected molecules that bind specifically to u-PAR or LRP. The SMB domain of Vtn directly interacts with u-PAR in the linker region N-terminal to our mutated sites, while RAP prevents binding of several ligands to LRP. Figure 4.2.6 D shows that both SMB and RAP inhibited the co-immunoprecipitation of cr-uPAR by 11H4. Disruption of the cr-uPAR:LRP

interaction suggests that the receptors can directly interact or may be bridged by other unidentified molecules that specifically bind both receptors.

These studies were continued using peptides that target the linker region of u-PAR, blocking the interaction of the receptor with other binding partners. Peptides 7 and 25, were originally discovered using the epitopes found in u-PAR:ATF complexes. Peptide 7 is derived from the SMB region in Vtn, (Fong, Doyle et al. 2002) and directly binds to u-PAR in the linker region (Gardsvoll and Ploug 2007). Peptide 25 blocks the u-PAR-integrin β_1 interaction (Wei, Lukashev et al. 1996). A peptide derived from prothrombin (Pt peptide) was also used to demonstrate specificity of the peptides 7 and 25. In the absence of u-PA-PAI-1 complexes, peptides 7 and 25 caused a marked decrease in LRP:u-PAR interaction, while Pt peptide had no effect (Fig. 4.2.7) (Wei, Eble et al. 2001; Wei, Czekay et al. 2005). As expected, both peptides 7 and 25 partially disrupted the interaction between cr-uPAR with LRP in the presence of u-PA-PAI-1 complexes. These results indicate that cr-uPAR binding to LRP is a direct interaction, rather than merely a function of co-localization in discrete membrane domains such as clathrin-coated pits.

4.2.5. Chymotrypsin cleaves cr-uPAR at a different rate than wt u-PAR.

Previous studies have demonstrated that u-PA bound to u-PAR exposes the chemotactic epitope situated between residues 88 - 92 in the linker region (Llinas, Le Du et al. 2005; Barinka, Parry et al. 2006; Huai, Mazar et al. 2006; Huai, Zhou et al. 2008). X-ray crystallographic evidence suggests this u-PA-dependent conformational change in the receptor involves the rotation of Tyr^{87} away from the bulk solvent, thus decreasing its availability as the P1 residue for the chymotrypsin active site (Barinka, Parry et al. 2006; Huai, Zhou et al. 2008). Cells expressing wt u-PAR and cr-uPAR were exposed to

chymotrypsin in the presence or absence of the inhibited u-PA, CMK-uPA, to determine whether the linker region of cr-uPAR is conformationally altered compared to that of wt u-PAR (Fig. 4.2.8). Wt u-PAR alone was rapidly cleaved by 100 nM chymotrypsin, with most of the receptor converted to the D_2D_3 form within 1 min, and no detectable intact receptor remaining after approximately 5 min. The presence of CMK-uPA only slightly reduced the cleavage of wt u-PAR. In contrast, cr-uPAR cleavage by chymotrypsin was delayed, with intact receptor detectable until about 20 min into the reaction. CMK-uPA further delayed the cleavage of cr-uPAR by chymotrypsin, with roughly half of the receptor still being intact by the final time point (30 min). Thus, the addition of CMK-uPA to cr-uPAR expressing cells reduced chymotrypsin-associated receptor cleavage to a much greater extent than seen in similarly treated wt u-PAR expressing cells. Previous work demonstrated that u-PA binds with high affinity to both u-PAR (Table I), indicating that the differential protection of CMK-uPA against chymotrypsin is not a function of dissimilar u-PA-binding. These experiments suggest that there is a significant conformational difference between the linker regions of wt u-PAR and cr-uPAR that may correlate with different degrees of receptor behavior, such as receptor internalization and LRP-association.

4.3. Discussion:

Models for the function of u-PAR are complex and involve roles for the unoccupied receptor, u-PA-bound receptor, and u-PA-cleaved receptor. The exact consequences of each of these states may differ depending on the other receptors expressed on the same cell, the composition of the cellular environment, and the type of matrix in contact with the cell. Further confounding matters is the fact that the primary physiologic ligand of u-

PAR, u-PA, is also a potent source of cleaved receptor (Hoyer-Hansen, Ploug et al. 1997; Hoyer-Hansen, Pessara et al. 2001). In a simplified model, u-PA-binding is proposed to enhance the association of u-PAR with Vtn (Hoyer-Hansen, Behrendt et al. 1997) and integrins (Chapman and Wei 2001). While u-PA-dependent release of D_1 abolishes affinity for Vtn and integrins, and promotes binding to and signaling via G-protein coupled receptors such as FPRL-1 (Resnati, Pallavicini et al. 2002). These different interactions lead to changes in cellular migration, proliferation, and adhesion via simultaneous down-regulation of some signaling pathways (eg. those involving integrins) and upregulation of others (eg. those involving GPCRs) (Blasi and Carmeliet 2002). In a mixed population of receptors, however, it is difficult to delineate the specific contributions of u-PAR states.

Previous work attempted to address this issue using an uncleavable u-PAR variant, hcr-uPAR, which contained mutations of cleavage sites in the linker region for u-PA, plasmin, MMPs, and chymotrypsin (Liu, Aguirre Ghiso et al. 2002; Mazzieri, D'Alessio et al. 2006; Bernstein, Twining et al. 2007). While wt u-PAR exhibited u-PA-dependent ERK activation, hcr-uPAR did not, suggesting that cleaved u-PAR accesses alternate signaling pathways from intact u-PAR (Mazzieri, D'Alessio et al. 2006). Disruption of fibroblast to myofibroblast differentiation by hcr-uPAR further suggested that u-PAR cleavage is necessary for differentiation (Bernstein, Twining et al. 2007). However, since two of five residues in the chemotactic epitope (Arg^{89} and Arg^{91}) were altered in hcr-uPAR, including a residue essential to vitronectin-binding (Arg^{91}), it is unclear whether the functional differences observed between intact wt u-PAR and hcr-uPAR are solely related to cleavability (Madsen 2006; Gardsvoll 2007; Huai 2008).

cr-uPAR, is resistant to cleavage by u-PA but alters only one residue, Arg^{89}, in the chemotactic epitope and preserves the ability of the cells expressing the receptor to interact with a Vtn-rich matrix. This mutant receptor binds to u-PA and promotes Pg activation indistinguishably from wt u-PAR, implying that cr-uPAR is properly folded and oriented on the cell surface, allowing u-PA and Pg to interact. There also appears to be a close association between cr-uPAR and LRP. This result was unexpected given a tight interaction of these two receptors requires was thought to require the bridging effect of the u-PA-PAI-1 complex. Furthermore, the secondary profile of LRP-mediated internalization for cr-uPAR was the same as cells expressing wt u-PAR.

Moreover, unliganded cr-uPAR is constitutively endocytosed in an LRP-dependent manner, cr-uPAR and LRP can be co-precipitated from cell lysate, and this co-precipitation can be specifically blocked by RAP and SMB. These data may be explained by direct binding between cr-uPAR and LRP, by the two molecules indirectly co-associating within a larger cell-surface complex, or by the two receptors being co-localized in the same plasma membrane micro-domains. The data do not allow for discrimination between these possibilities, but the results suggest an intriguing implication: that cr-uPAR may represent a receptor variant that is constitutively active in the absence of ligand.

In several functional aspects, free cr-uPAR behaved similarly to liganded wt u-PAR. For instance, the peak amount of wt u-PAR endocytosed in the presence of u-PA-PAI-1 complex was similar to the peak amount of cr-uPAR internalized in the absence of the complex. Also, the amount of cr-uPAR that was precipitated with an α-LRP antibody

without u-PA-PAI-1 complex was identical to the amount of wt u-PAR captured in the presence of complex.

Note that while contaminant bovine-derived u-PA (from the serum) may have been present, binding of u-PA to human u-PAR is species-specific, so bovine-derive u-PA was unlikely to influence the results. In particular, regions known to mediate this specificity do not involve the residues mutated in cr-uPAR, and a residue in human u-PA, Trp^{30}, critical to this specificity is not conserved in bovine u-PA (Huai, Mazar et al. 2006). Thus, it is highly probable that, in the absence of added exogenous human u-PA, cr-uPAR was unoccupied.

The mechanism of this activation may involve local changes in the conformation of the linker region and chemotactic epitope, as evidenced by the differential susceptibility of wt u-PAR and cr-uPAR to partial proteolysis by chymotrypsin. This structural change may in turn affect the inter-domain relationships in the receptor, subtly altering its global conformation. Crystal structures of u-PAR in complex with various ligands including an antagonist peptide, the ATF of u-PA, and SMB, demonstrate just such differences in inter-domain distances and inter-domain loop conformations (Llinas, Le Du et al. 2005; Barinka, Parry et al. 2006; Huai, Mazar et al. 2006; Huai, Zhou et al. 2008). Although more biophysical characterizations are needed to ascertain whether unliganded cr-uPAR is conformationally similar to u-PA-bound wt u-PAR, it is clear that cr-uPAR is a functionally activated receptor in the absence of ligand-binding. The questions of whether or not other aspects of receptor function are upregulated in cr-uPAR, and the possible impact of this putative activation on cellular behavior, await further study.

The precise role of u-PAR cleavage in cancer biology remains elusive. Soluble and cell-surface cleaved u-PAR are promising markers in the early detection, prognosis, and monitoring of response to treatment of cancers of the prostate, ovary, breast, and bone marrow (for a review, see (Rasch, Lund et al. 2008). Since cleaved u-PAR can induce u-PA independent cell migration via GPCRs, receptor cleavage may promote metastasis (Montuori, Carriero et al. 2002). However, in at least the aggressive cancer, anaplastic thyroid carcinoma, u-PAR cleavage is prevented by over-glycosylation (Ragno, Montuori et al. 1998). Less aggressive forms of thyroid carcinoma, as well as benign thyroid adenoma, express cleavable receptor. Thus perhaps in thyroid cancers, u-PAR cleavage down-regulates invasiveness (Ragno, Montuori et al. 1998). Cr-uPAR may consequently represent an important tool in the dissection of the roles of u-PAR in cancer. Further investigation into the constitutive activity of this mutant may shed light on the ligand-induced conformational activation of the intact wild-type receptor.

4.4. Figures and Tables:

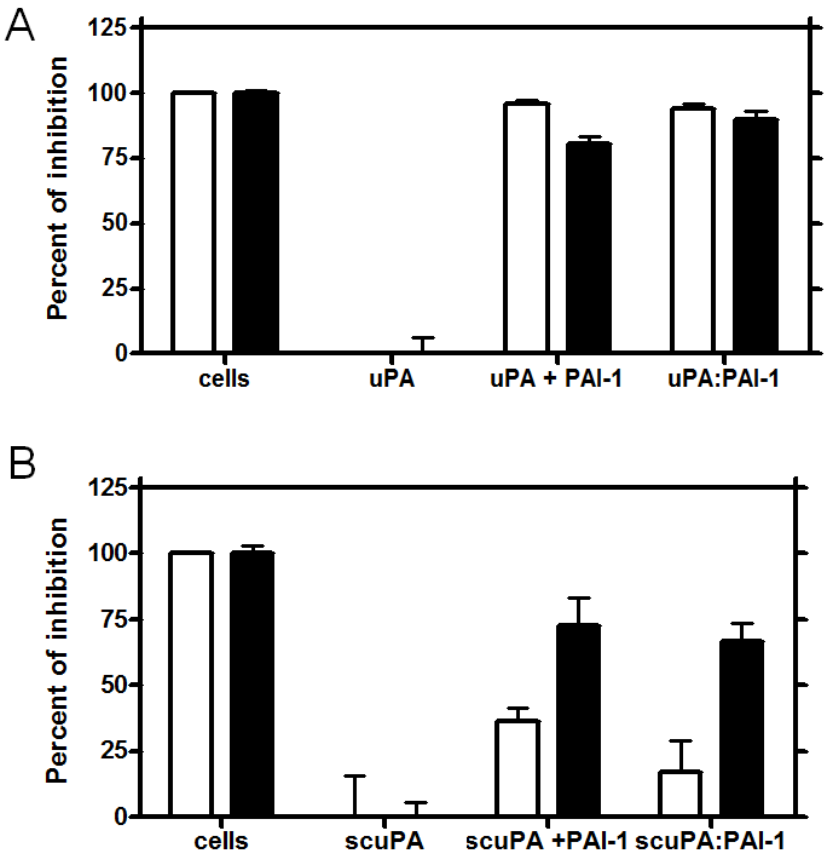

Figure 4.1. u-PA inhibition by PAI-1 is unaffected by the presence of cr-uPAR. $5x10^4$ cells/ well were seeded O/N, washed and incubated with proteins as follows. Wt u-PAR (white bars) and cr-uPAR (black bars) expressing cells were treated several ways. **A)** Cells were incubated with 10 nM tcu-PA alone for 30 min, followed by Pn generation which was standardized to 0%. Cell bound tcu-PA was inhibited by the addition of 20 nM PAI-1 for 30 min. Additionally, pre-complexed 10 nM u-PA-PAI-1 was bound to cells for 30 min. **B)** Cells were also treated with 10 nM scu-PA alone and were standardized to 0%. The cell bound tcu-PA was inhibited by the addition of 20 nM PAI-1 or by pre-complexed 10 nM u-PA-PAI-1 which were bound to cells for 30 min. Pn generation was analyzed as mentioned in the materials and methods. Bars and error bars represent the mean and SD of 3 individual replicates.

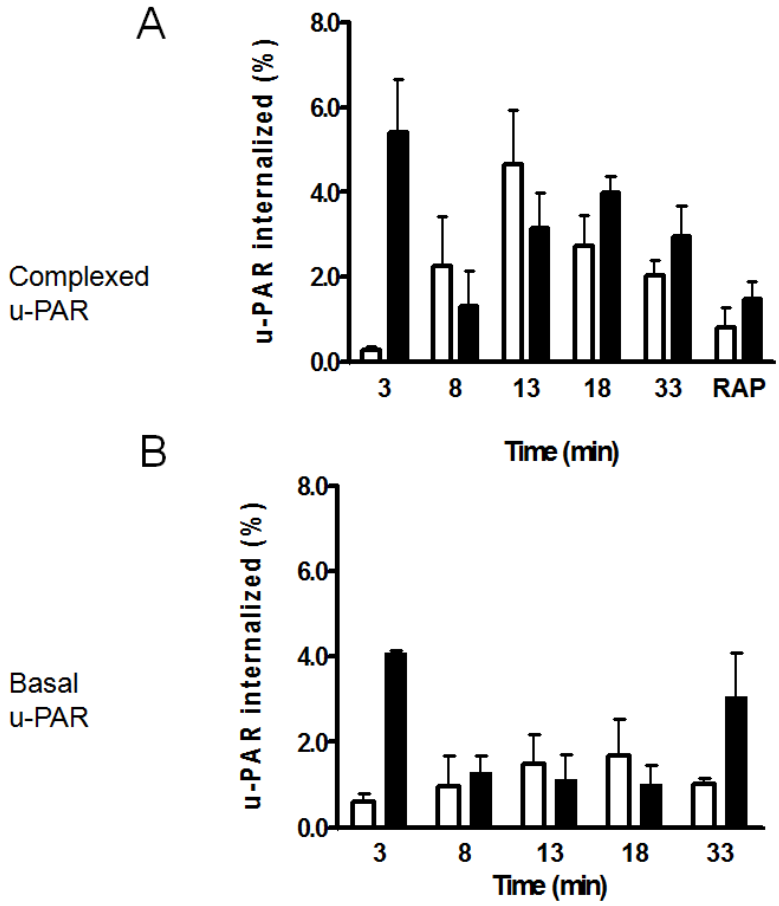

Figure 4.2. Internalization and receptor resurfacing is dramatically faster in the presence of cr-uPAR. $1.5x10^5$ cells are harvested 18 h prior to labeling. Wt u-PAR (white bars) and cr-uPAR (black bars) cells briefly biotinylated with 200μM NHS-LC-S-S-biotin where then incubated with either **A)** 10 nM of complex or **B)** buffer alone at 4°C. Cells were then exposed to 37ºC to initiate internalization. Each time point is attributed to the time cells were at 37ºC post reduction using DTT. All biotinylated u-PAR samples were exposed to immobilized strepavidin, elution and subjected to immunoblotting. In our control reaction, 500nM of RAP was added to one well every time a new incubation occurred. Total u-PAR was normalized by extracting 20 μl of total cell lysate and subjected to detection by immunoblotting. Analysis was preformed by taking the ratio of amount reduced/ total u-PAR. Symbols and error bars represent the mean and SEM of minimum 3 independent replicates.

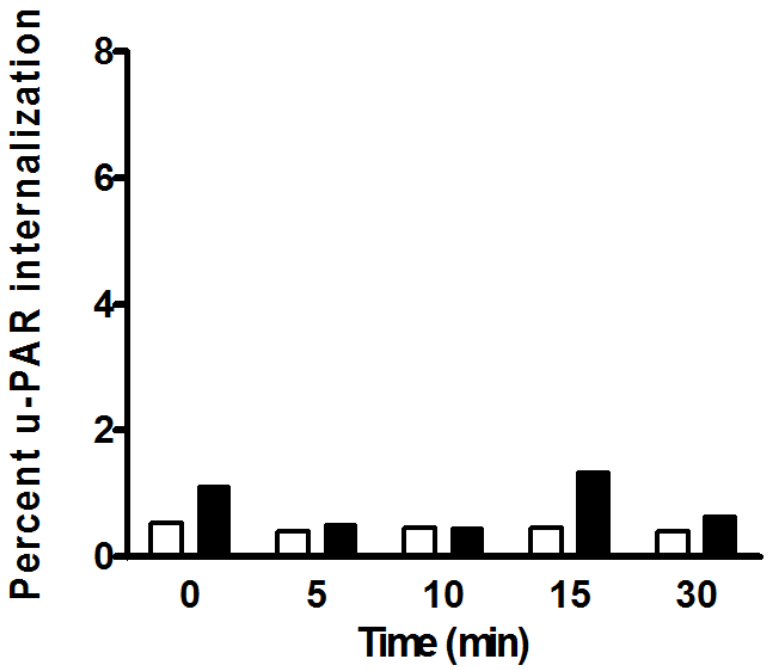

Figure 4.3. Presence of RAP prevents internalization of tcu-PA-PAI-1 bound to u-PAR. $1.5x10^5$ cells are harvested 18 h prior to labeling. Wt u-PAR (white bars) and cr-uPAR (black bars) cells briefly biotinylated with 200 μM NHS-LC-S-S-biotin where then incubated with 500 nM of RAP and incubated at 4°C. Cells were then exposed to 37°C to initiate internalization. Each time point is attributed to the time cells were at 37ºC post reduction using DTT. All biotinylated u-PAR samples were exposed to immobilized strepavidin, elution and subjected to immunoblotting. Total u-PAR was normalized by extracting 20 μl of total cell lysate and subjected to detection by immunoblotting. Analysis was preformed by taking the ratio of amount reduced/ total u-PAR. Bars represent 3 independent experiments.

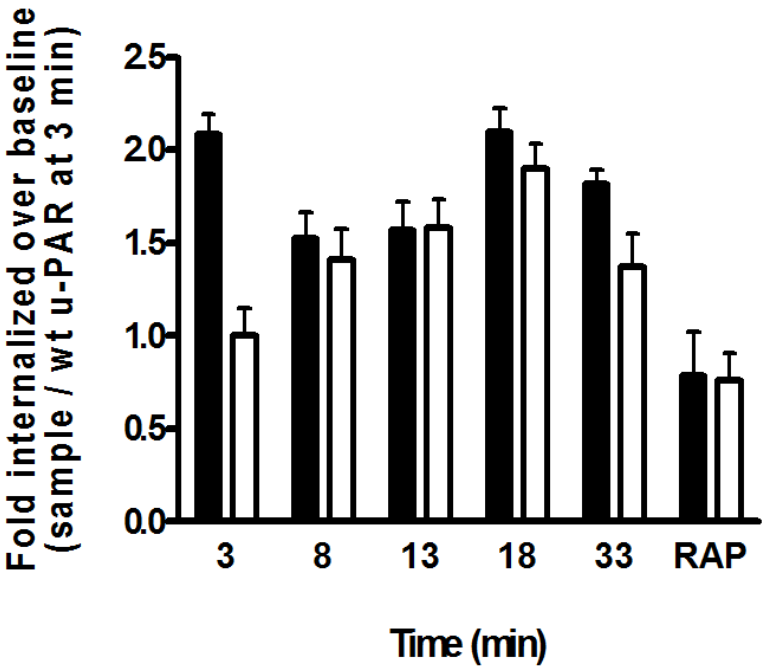

Figure 4.4. Addition of biotinylated complex promotes internalization of u-PAR. 293 wt u-PAR (white bars) and cr-uPAR (black bars) were incubated with 10 nM biotinylated-PAI-$I_{14\text{-}1B}$:u-PA complex for 30 min at 4°C. Cells were exposed to 37°C to initiate internalization. Each time point is attributed to the time cells were at 37ºC post acid wash to remove cell-surface bound biotinlyated-PAI-1:u-PA complex. Analysis was performed by using wt u-PAR at 3 min as our baseline. As a control, 500 nM RAP was incubated with u-PA-PAI-1 with continuous addition of RAP following incubation for 30 min at 37ºC. Symbols and error bars represent the mean and SEM of 5 independent replicates. .

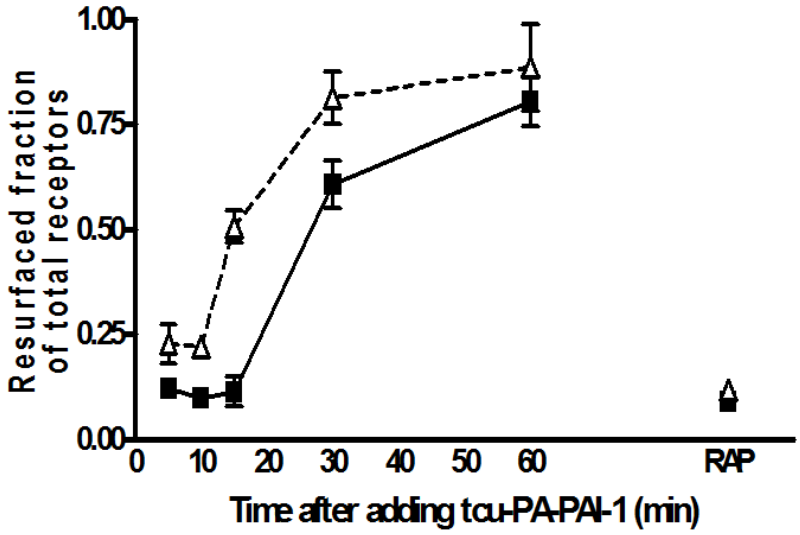

Figure 4.5. Unoccupied cr-uPAR resurfaces more rapidly. Wt u-PAR (■) and cr-uPAR (Δ) expressing cells were incubated with pre-assembled u-PA-PAI-1 complexes for 30 min at 4ºC. Unbound complex was washed off and the cells were incubated at 37ºC for different times. 10nM tcu-PA was then added and incubated for an additional 30 min. Pn generation was detected as previously described. Samples were analyzed by taking the slope of newly unoccupied u-PAR at each time point /slope of total available u-PAR. As a control, 500 nM RAP was incubated with u-PA-PAI-1 with continuous addition of RAP following incubation for 30 min at 37ºC. Symbols and error bars represent the mean and SEM of 4 independent replicates.

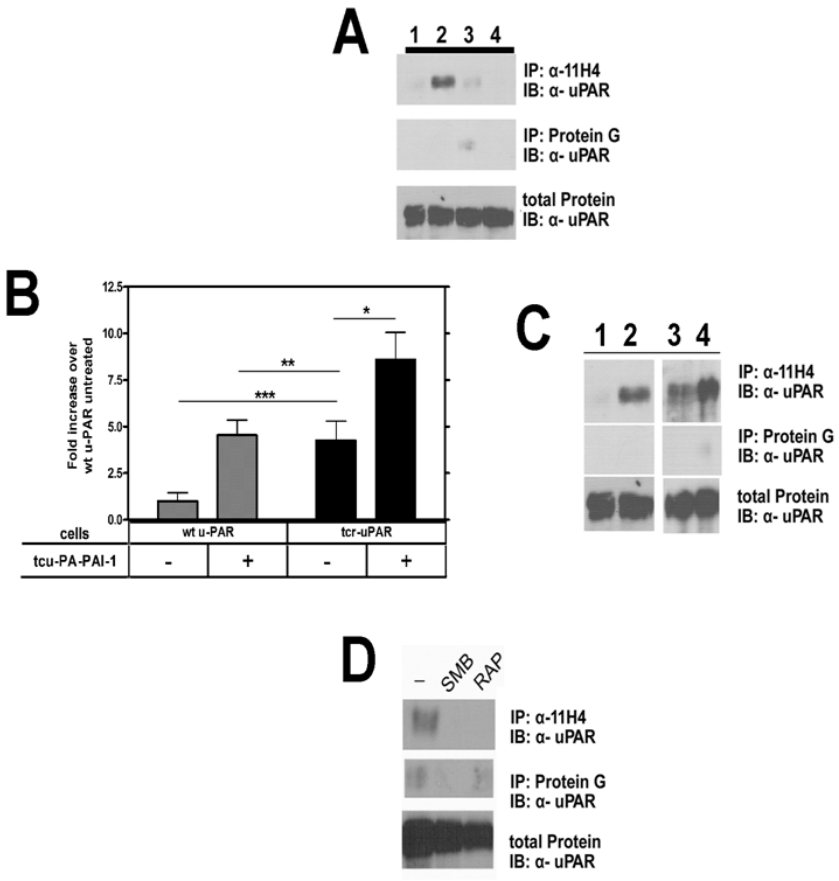

Figure 4.6. cr-uPAR co-immunoprecipitates with LRP in the absence of u-PA-PAI-1 complexes. Treated cells were lysed with PBS +0.1% triton-X 100 following an incubation for 18 h at 4°C with 20 μl/ml of immobilized Protein G in combination with 2.8 μg of mAb 11H4 (top blot), alone (middle blot) or no treatment (bottom blot). Immunoprecipitates were eluted subjected to PAGE and immunoblotted using polyclonal α-u-PAR. **A)** Wt u-PAR expressing cells were incubated at 4°C in the absence (lane 1) or presence (lane 2) of 10nM u-PA-PAI-1 complex, or in the presence or absence of 500 nM RAP (lane 3 and 4, respectively) for 30 min. **B)** wt u-PAR (lanes 1 and 2) and cr-uPAR (lanes 3 and 4) were incubated at 4°C in the absence or presence of 10 nM u-PA-PAI-1 complexes, respectively. Blots were imaged and analyzed using the Kodak 1D system and normalized to lane 1. Bars and error bars represent the mean and SD of 3 individual replicates. (t test; *, $P < 0.001$; **, $P<0.05$; n.s.: not significant). **C)** cr-uPAR expressing cells were then treated with 10 μM peptide 7 (lane 1), 10 μM peptide 25 (lane 2), 0.5 μM RAP (lane 3), 10 μM prothrombin peptide (lane 4) or *2.5* μM SMB (lane 5). .

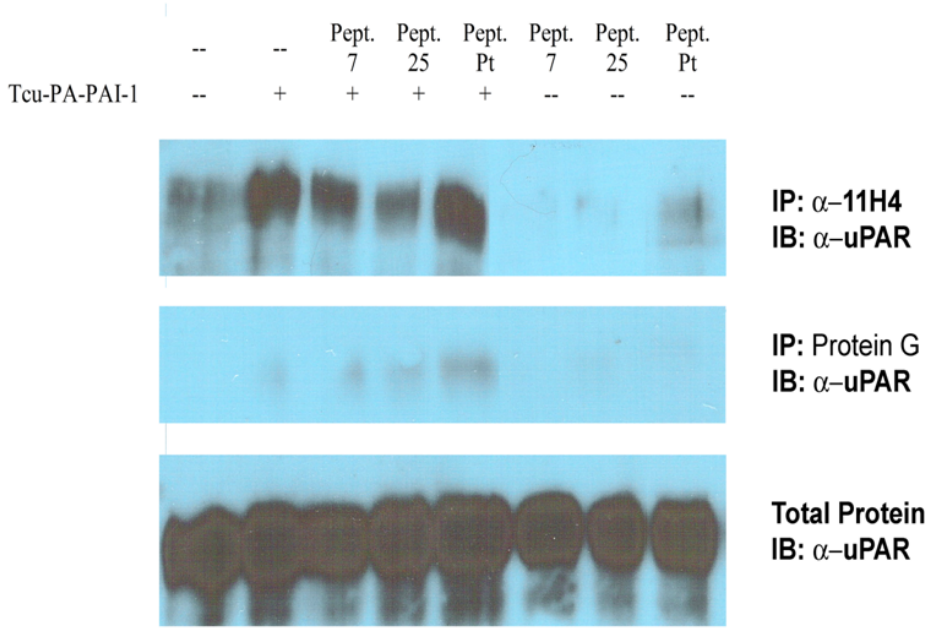

Figure 4.7. LRP interaction by cr-uPAR is not significantly disrupted by addition of complex. Cr-uPAR expressing were incubated at 4°C in the absence, in the presence of u-PA-PAI-1 complex or treated with either 4 μM peptide 7, 4 μM peptide 25 or 4 μM Pt peptide for 30 min. Cell lysates were subjected to analysis as previously described.

A

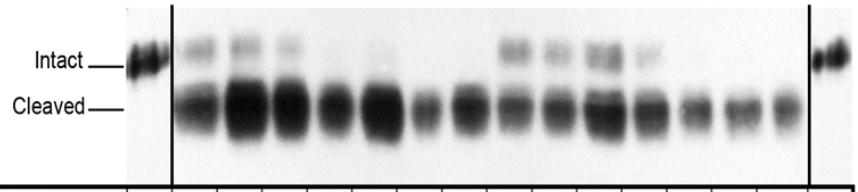

Time (min)	0	1	2.5	5	7.5	10	20	30	1	2.5	5	7.5	10	20	30	30
100 nM CMK-uPA	-	-	-	-	-	-	-	-	+	+	+	+	+	+	+	-
100 nM Chymotrypsin	+	+	+	+	+	+	+	+	+	+	+	+	+	+	+	-

B

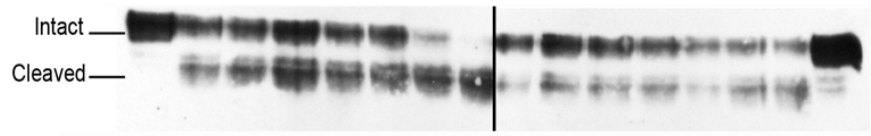

Time (min)	0	1	2.5	5	7.5	10	20	30	1	2.5	5	7.5	10	20	30	30
100 nM CMK-uPA	-	-	-	-	-	-	-	-	+	+	+	+	+	+	+	-
100 nM Chymotrypsin	+	+	+	+	+	+	+	+	+	+	+	+	+	+	+	-

4.8. Impaired cleavage of cr-uPAR by chymotrypsin as compared to wt u-PAR. Cell suspension ($2.5x10^6$ cells/ml) of **A**) wt u-PAR and **B**) cr-uPAR expressing cells were incubated with buffer (left half) or 100nM CMK-uPA (right half) for 30 min at 37°C in DMEM, 0.1%BSA, 100 µg/ml CHX buffer. Cleavage was initiated by addition of chymotrypsin (100 nM) at 37ºC for set times. Cells were then washed and lysed using RIPA buffer. 10 µgs of total cellular protein lysate was loaded into 10% PAGE gels and analyzed by western blot using polyclonal α-u-PAR. Blots were imaged using Kodak 1D system. Blots represent 4 independent replicates. "This research was originally published in Journal Biological Chemistry. Evelyn C. Nieves and Naveen Manchanda. A cleavage-resistant urokinase plasminogen activator receptor exhibits dysregulated cell-surface clearance. J Biol Chem. 2010 April 23; 285(17): 12595–12603. © the American Society for Biochemistry and Molecular Biology."

CHAPTER 5. EFFECTS OF CR-UPAR ON CELL MORPHOLOGY AND BIOLOGY

5.1. Introduction

The expression of u-PA and u-PAR on cancer cells modulate adhesion and migration, which in turn can determine metastatic potential, *in vitro* studies, tumor progression and patient survival, *in vivo* studies. There is increasing evidence linking over-expression of u-PA and u-PAR and several cancer cell lines (Plesner, Ralfkiaer et al. 1994; Shetty and Idell 1998; Mustjoki, Alitalo et al. 1999). The expression of cell surface proteins changes how a cell interact with its environment, promoting an increase in cellular adhesion, migration and cytoskeleton rearrangement. The binding of u-PA to u-PAR induces a conformational change in u-PAR which activates the receptor however, u-PA binding is dependent on the presence of an intact receptor with a significant decrease in affinity when u-PAR is converted to the cleaved form. The formation of cleaved u-PAR is hypothesized to be accompanied with exposure of the chemotactic epitope. Accordingly, the binding of u-PA to u-PAR should promote re-distribution of active u-PA to the leading edge of migrating cells promoting proteolysis (Estreicher, Muhlhauser et al. 1990). In contrast, u-PA cleavage of cell surface u-PAR can block integrin-dependent signaling, altering cytoskeleton rearrangement by reducing signals to actin (Margheri, Manetti et al. 2006).

Recently, u-PAR studies have focused on protein interactions, which are dependent on the conformation of u-PAR. u-PAR interacts with many cell surface proteins including Vtn, integrins, GPCR and EGFR, with many of these interactions requiring an intact form of u-PAR. Currently the interactions of u-PAR with the aforementioned

proteins are hypothesized to promote cellular changes via a multiprotein signaling-receptor complex (MSRC). The preferential interaction of u-PAR with Vtn and other proteins on the extracellular matrix induces cellular adhesion to Vtn. Vtn can activate Rac-1, a small GTPase, which can then regulate the downstream pathway involved in actin polymerization (Wei, Lukashev et al. 1996; Kjoller and Hall 2001; Ma, Thomas et al. 2002). Additionally, 293 cells expressing the intact form of u-PAR on a cell surface directs the interaction from a primarily fibronectin base to a Vtn based attachment (Waltz and Chapman 1994; Waltz, Natkin et al. 1997). This effect is thought to be u-PAR:integrin mediated, since in the absence of u-PAR the cells adhere via a integrin-fibronectin interaction. Our studies demonstrate the dramatic difference in cell morphology between cells that express the inactive receptor (wt u-PAR) and a constitutively active receptor (cr-uPAR). Previously, these enhanced morphology changes were attributed to the binding of u-PA to u-PAR. A pronounced morphologic change was seen in 293 cr-uPAR cells, consistent with a uPA-bound form of u-PAR. However, we do not see a significant difference in Vtn adhesion between the two u-PAR variants.

5.2. Results:

5.2.1. Expression of u-PAR alters the cells by elongating their processes.

The expression of u-PAR is known to influence changes in morphology. When u-PAR is expressed on the cell surface it induces polarization that leads to process elongation. We found that cells expressing cr-uPAR had changes in cell morphology once the cells were stably transfected. The visual difference observed between the 293

non-transfected cells and u-PAR expressing cells led us to look at basal changes in the cell morphology. 293 cells which either were not transfected or have only the blank plasmid, pcDNA3.1(+), transfected had no change from previously reported morphology (figure 5.2.1). The expression of wt u-PAR on the cell surface in all clones selected led to a dramatic change in flattening of the cells, conversion to an elongated form, reduction of the cell body, an extensive formation of lamellipodia and F-actin cytoskeleton rearrangement, also observed by several other researchers. In addition, since the u-PA:u-PAR interaction is species-specific, the presence of FBS which contains bovine u-PA should not affect the study. When cr-uPAR is expressed on the cell surface, we observed a more prominent processes elongation than that of wt u-PAR. Not surprisingly, processes elongation scored by three unbiased independent researchers led to unequivocal similar assignments of processes. The observed effect here was also clone independent (figure 5.2.1 bottom left panel). However, at least for wt u-PAR, the observed effects were expression level dependent since clone 11 expresses twice the amount of clone 4 yet had prominent elongated processes similar to that of cr-uPAR. On the other hand, expression of cr-uPAR did not have a significant impact on processes elongation. The cell-cell contacts between the cr-uPAR cells had changed in comparison to both 293 cells and 293 wt u-PAR cells with a larger population of cells localizes in the same region, making contact along the protrusions. Furthermore, some cells had both lamellipodia and filopodia. As mentioned in Chapter 3, we used similar expression levels for both u-PAR variants in an effort to prevent the over-expression of u-PAR. We tested whether the cell morphology for the u-PAR variants could be reverted to that of 293 non-transfected cells by treating the cells with a D-mannosamine (Fig. 5.2.2). D-mannosamine blocks the

generation of a GPI-tail and prevents all GPI-anchored proteins from being transported to the cell surface. Both u-PAR expressing cells reverted the morphology of 293 non-transfected cells, while treatment of 293 non-transfected cells with D-mannosamine caused no morphological changes. Neither integrins nor LRP are affected by this treatment since, these are transmembrane proteins that lack any GPI modifications. This shows that u-PAR expression is potentially responsible for the changes observed.

5.2.2. Localization of u-PAR to focal adhesion points.

We next determined the distribution of u-PAR on the cell surface, since investigators have reported the receptor spreading evenly along the cell surface. We noted in the previous section that 293 cr-uPAR cells have longer processes, compared to 293 wt u-PAR cells. Fluorescently tagged CMK-uPA was used to identify how the over-expressed receptor is distributed. Fluorescently tagged u-PA was distributed along the cell surface extending to the processes elongations. u-PA also localized to the cell-cell attachments and focal adhesion sites (Fig. 5.2.3 and 5.2.4). u-PAR is near the same sites as the actin filaments, identified by the addition of rhodamine-labeled phalloidin, which directly binds F-actin. We detected no CMK-uPA localization on the cell surface of untransfected 293 cells.

293 expressing u-PAR, but not 293 non-transfected, cells had protrusions extending from the cell body, accompanied by the formation of lamellipodia. As demonstrated by Madsen, our transfected 293 u-PAR cells formed lamellipodia. In addition, there was an increase in the protrusion length of the 293 cr-uPAR that correlated with a narrower cell body, resembling highly mobile cells. Indeed, cr-uPAR cells had a small amount of

filopodia. These studies suggest that 293 cr-uPAR expressing cells resemble more activated u-PAR, rather than the latent counterpart.

5.2.3. u-PAR variants promote enhanced adhesiveness and delay cellular dissociation on a Vtn based matrix.

Since u-PAR directly interacts with Vtn, we determined whether cr-uPAR has an altered affinity toward Vtn. When either wt u-PAR or cr-uPAR were expressed on the cell surface, followed by harvesting of cells onto Vtn coated plates, we saw a similar increase in adhesion for both receptors, as previously noted for u-PAR (Fig. 5.2.5 A). This effect is not entirely surprising, since the cells were non-enzymatically dissociated and had the u-PAR variants on the cell surface. However, this method cannot discern between latent u-PAR and the u-PA bound active form. When the same experiment was performed using FCS we detected the same increase in adhesion as with Vtn. Thus our cr-uPAR expressing cells have an increased affinity toward Vtn, promoting adhesion, since FCS also contains other matrix proteins which can be utilized by 293 cells to adhere, i.e. integrin-mediated fibronectin adhesion.

We determined whether cell anchorage was altered when cells expressed u-PAR, since cell surface expression of u-PAR can shift the binding from integrin-based binding to Vtn-based binding. A buffering system that does not have proteases present but mainly EDTA allows us to distinguish binding that is primarily integrin dependent versus Vtn dependent matrices. The expression of u-PAR on the cell surface made the cells less amenable to dissociation (Fig. 5.2.5 B). However, cells not expressing u-PAR on the cell surface were prone to faster dissociation. This is mainly attributed to integrins being

unable to associate with a fibronectin matrix, since they are calcium-dependent. These dissociation studies confirm an increase in adhesion that is Vtn dependent. A key point is cells overexpress the receptor, mimicking the events found in cancer cells. We suggest that over-expression of cr-uPAR may overcome the need for u-PA dependent activation of the receptor.

5.3. Discussion

Expression of u-PAR induces morphologic changes and enhanced adhesion in cells, as previously reported. The interaction of u-PAR with Vtn directly affects the adhesion characteristics of cells, at least in our system. Strong adhesion to a cell matrix, such as Vtn, can promote cell growth and cell differentiation, a trait that cancer cells assume after they have migrated to a new environment. Integrins are another set of molecules that interacts with u-PAR, although recently there have been some conflicting studies which question if this interaction is direct or indirect via lateral interplay. The ability of u-PAR to modulate cell morphology by binding to integrins and activating downstream cell signaling events causing morphological changes was recently investigated by two independent research groups (Madsen, Ferraris et al. 2007; Hillig, Engelholm et al. 2008). There is a conflict regarding the necessity of Vtn for cytoskeleton rearrangement. Madsen et al., 2007, suggested that the u-PAR:Vtn interaction is necessary for changes in morphology, but the studies imply that a lateral interaction between u-PAR and integrins is unnecessary. Mutations in the RGD portion of Vtn were essential for morphologic effects, which were absent in the Vtn_{RAD} mutant. However, the RGD integrin binding site is lateral to the SMB domain in Vtn and is separate from the u-PAR binding region

(Madsen, Ferraris et al. 2007). Hillig *et al*., (2008) on the other hand, reported that although cytoskeletal re-arrangement and adhesion was pronounced when u-PAR was expressed on the cell surface, their Vtn defective u-PAR mutant, (u-PAR_{W32A}), was incapable of producing the same effect (Hillig, Engelholm et al. 2008). However, cytoskeletal rearrangement was found to not be fully dependent on Vtn-adhesion. They found that u-PAR_{W32A} generated morphological changes independent of Vtn binding in the presence of scu-PA. A secondary protein, such as integrin, may mediate the observed u-PAR-dependent morphological changes. scu-PA can restore cell adhesion and morphology, except when either residues W^{32} and R^{91} are mutated (Ploug 2003; Madsen and Sidenius 2008). Although both studies have conflicting conclusions, they identify u-PAR as a mediator of morphologic changes and the importance of u-PAR for Vtn adhesion, a trait that resonates with our results. A dramatic difference was seen due to expression of u-PAR. Expression of active u-PAR in the form of cr-uPAR may present a new challenge to a cell, since it does not appear to require the presence of u-PA. Although our studies were preformed mainly in the absence of exogenous u-PA these studies strongly supports the hypothesis that cr-uPAR is in a state that resembles the active conformation which affects process elongation, similar to the effect of bound u-PA. Our studies show that wt u-PAR and cr-uPAR have similar Vtn adhesion, potentially due to excess receptor expression. Because of the small difference in Vtn adhesion and the small increase in initial internalization reported in the previous chapter, there may be a small population of u-PAR that interacts with LRP, not Vtn. In addition, the most probable binding site for Vtn and LRP is the opposite site of the u-PA cavity. Thus, the availability of the receptor is limited to which molecule it is interacting with.

Efforts to distinguish between intact u-PAR and cleaved u-PAR were performed by using either inactive u-PA or the ATF of u-PA that is devoid of its proteolytic domain. Binding of u-PA was found to be sufficient for a morphological effect, but cleaved u-PAR generated a stronger effect. Studies performed with a synthetic peptide mimicking u-PA do not entirely recover the u-PAR mutant conformational change, suggesting that there is a minimal conformational change necessary to induce the same conformation as a u-PA bound u-PAR. Thus, we hypothesize that the activation of u-PAR can support cell signaling sufficient to induce morphology changes and cytoskeletal rearrangement. We also suggest that there is a small population of receptors in a similar conformation that can promote the events in the absence of any external stimulus, since most of our studies are based on basal studies and do not include human u-PA. We speculate that the observed morphological and adhesion changes may be due to cell signaling which is unregulated by cr-uPAR.

5.4. Figures and Tables

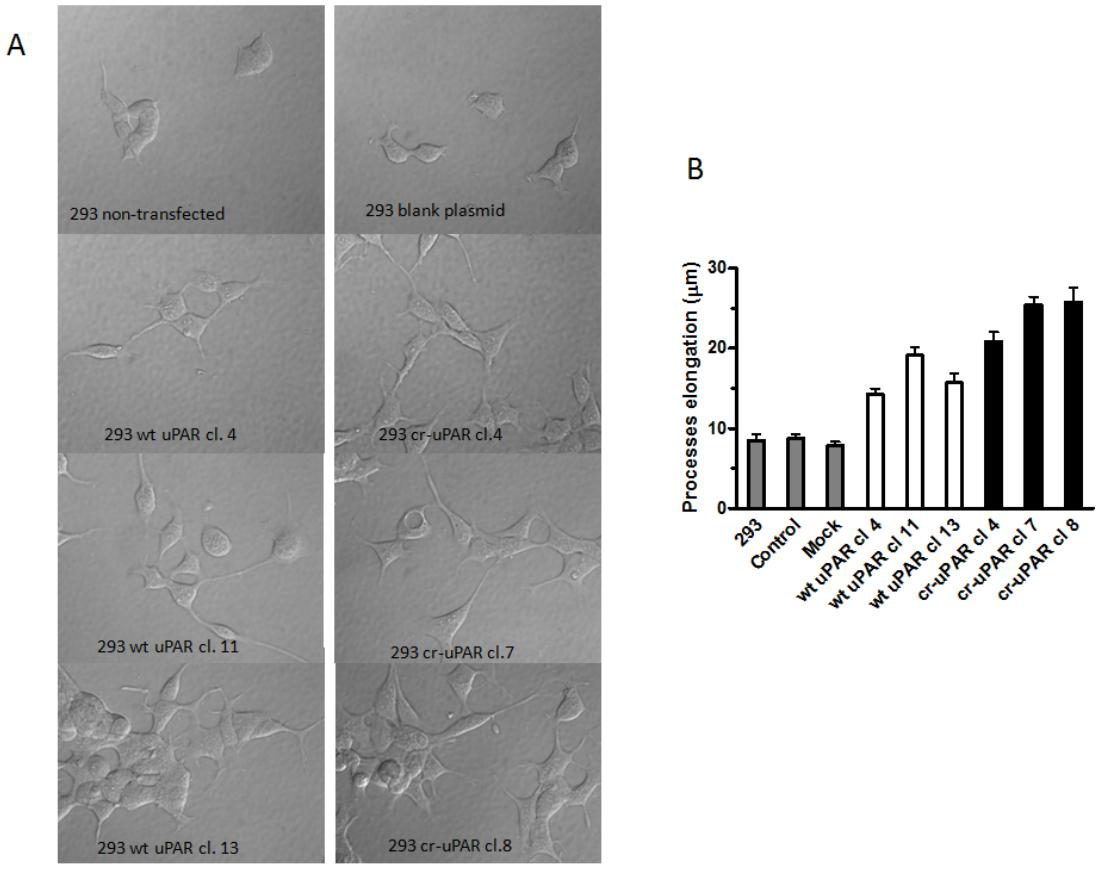

Figure 5.1. Expression of u-PAR alters the 293 cell morphology. A) Images of different 293 transfected, adherent, unfixed and non-permeabilized cells after a 3 day incubation under normal conditions. Image was taken at 20X magnification using a DIC microscope. B) Quantitative analysis of blind scores measuring processes elongation for 293 (grey), 293 wt u-PAR (white) and 293 cr-uPAR (black). Data shown is the mean ± SEM of 3 independent scoring.

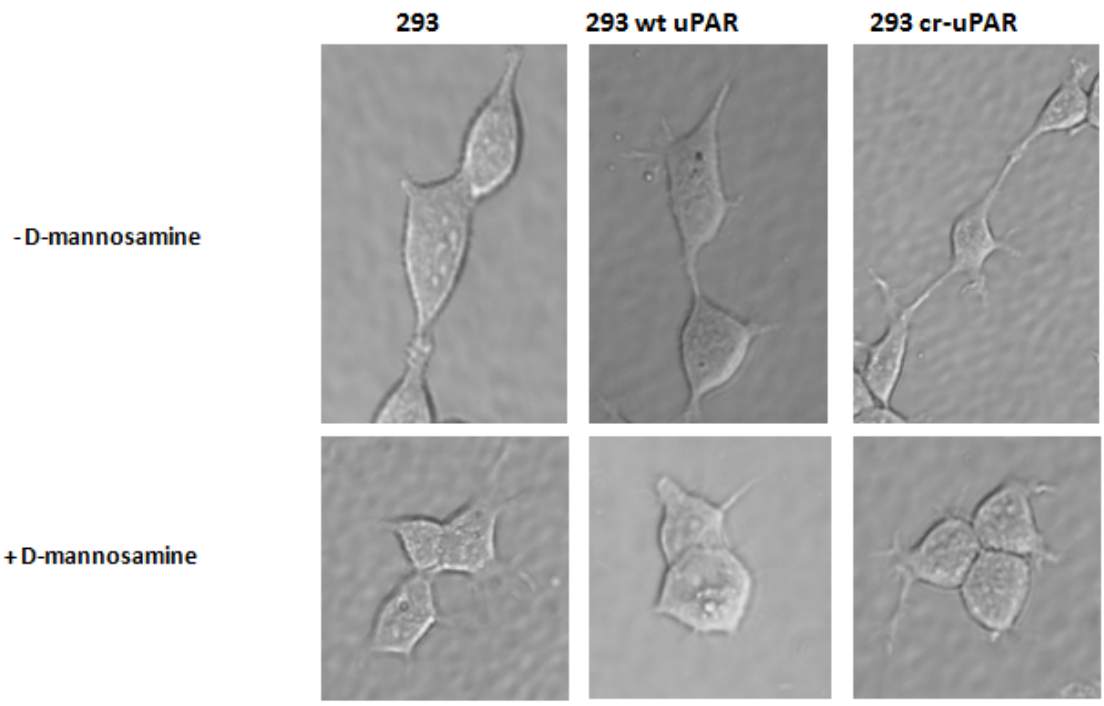

Fig 5.2. Removal of GPI-anchored receptors shows reversal of cell morphology changes. 293, wt u-PAR and cr-uPAR were incubated for 18 h after the addition of 10 µg/ml D-mannosamine. Cell analysis was performed as described in the material and Method. Images are representative of 3 individual experiments.

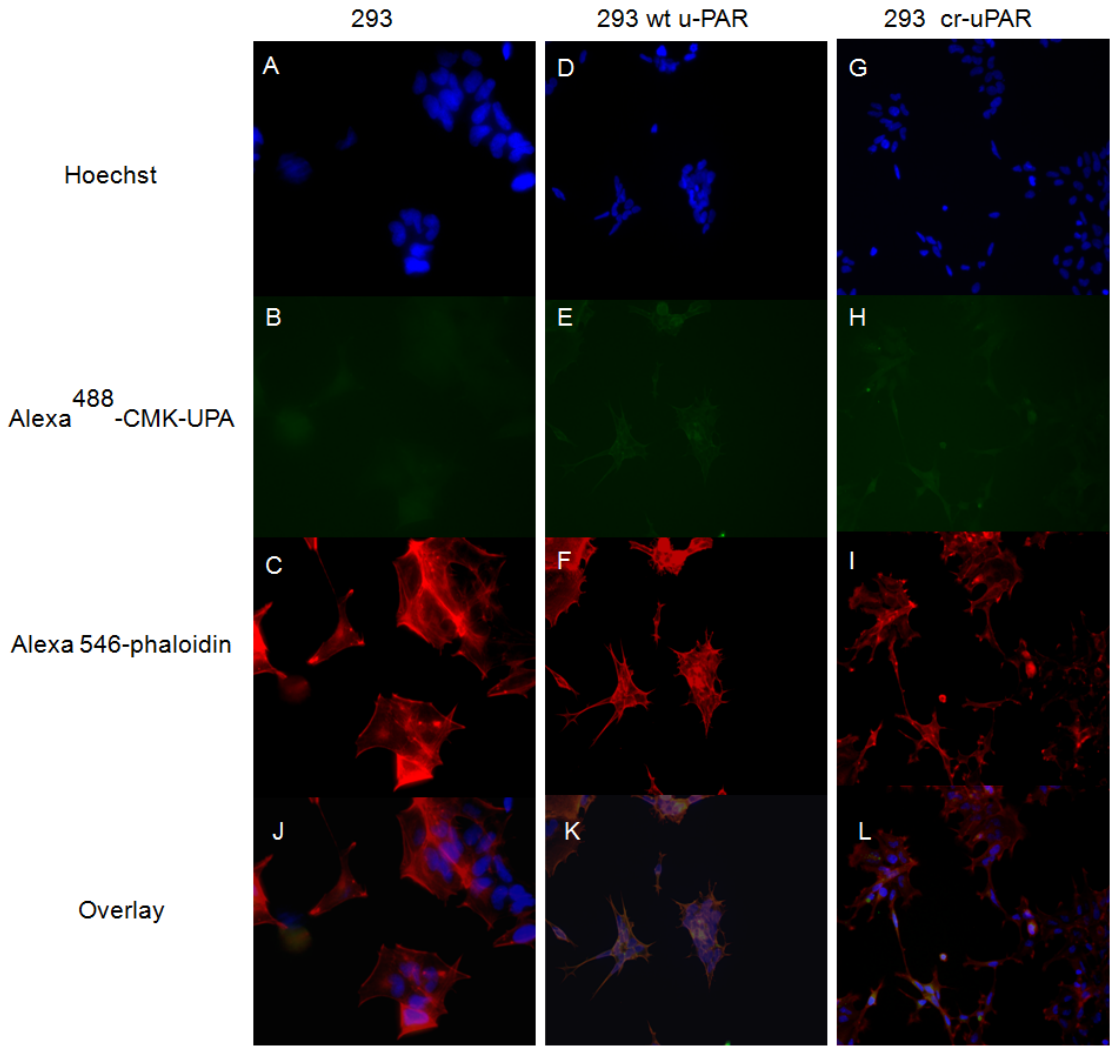

Fig 5.3. Distribution and cell-surface localization of u-PAR on 293 cells. 293 (A-C, J), 293 wt u-PAR (B-F, K) and 293 cr-uPAR (G-I, L) cells were permeabilized and stained with Hoechst (top panel), Alexa488-CMK-uPA (second panel), or Alexa546-phalloidin (third panel). An overlay (bottom panel) shows the distribution and localization of u-PAR.

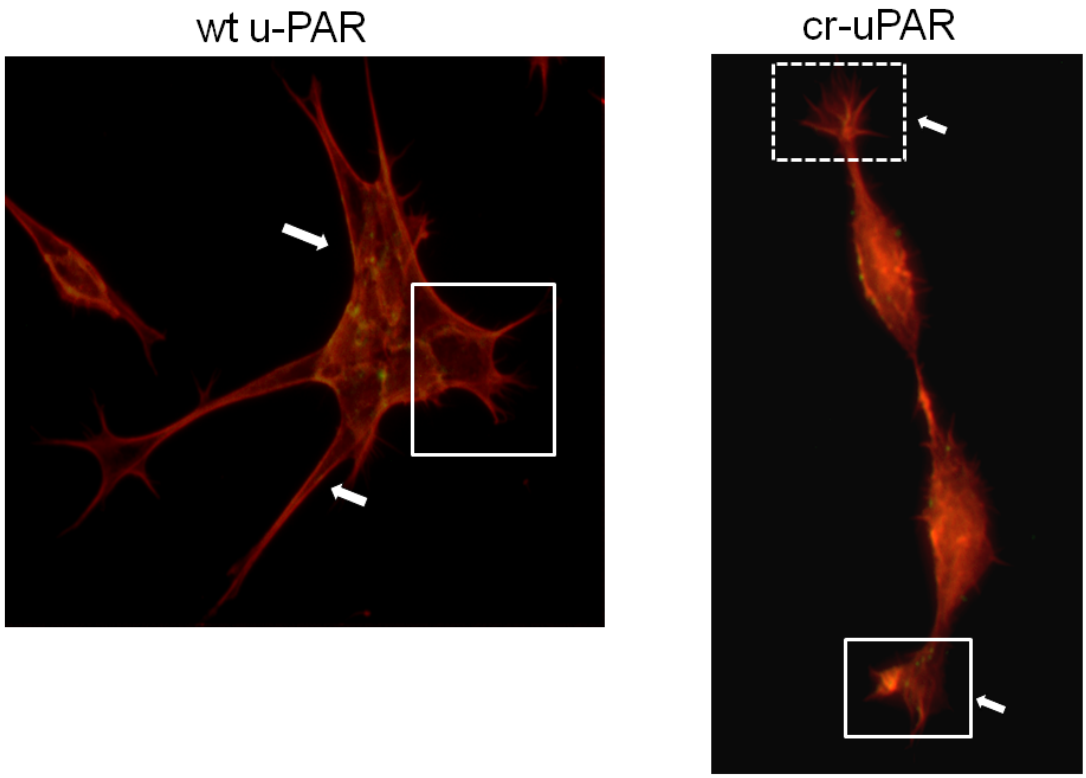

Fig 5.4. Expression of u-PAR variant on 293 cells leads to changes in processes. 293 wt u-PAR (left) and 293 cr-uPAR (right) cells were permeabilized, stained with Alexa^{488}-CMK-uPA (second panel), or Alexa^{546}-phalloidin (third panel) then overlaid. The arrows point to regions with Alexa^{488}-CMK-uPA bound u-PAR. The solid white boxes show lamellipodia formation while the dashed white box shows formation of filopodia.

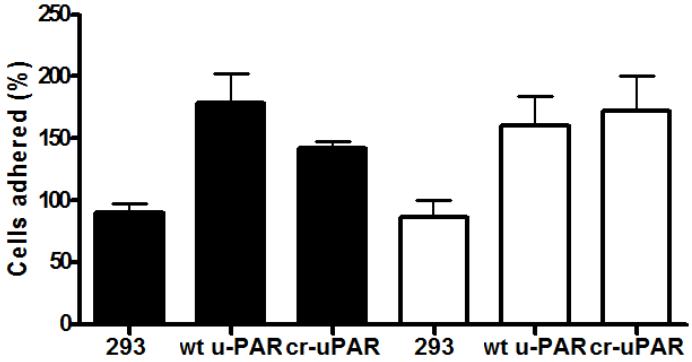

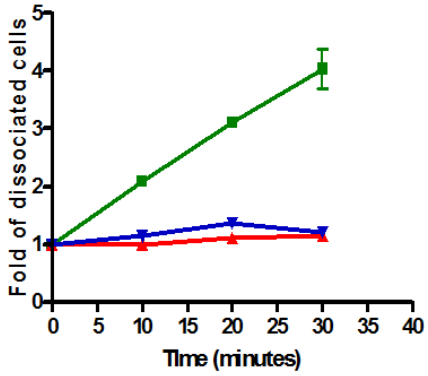

Fig 5.5. Expression of u-PAR leads to changes in adhesion and dissociation in 293 cells. A) Adhesion of 1 x 10^5 cells was performed by incubation of dissociated cells on pre-coated wells with Vtn (black bars) or FCS (white bars) and incubated for 1h under normal growth conditions. Detection of adherent cells and analysis were performed as described in materials and methods. **B**) A cell dissociation time course was performed for 293 (■), 293 wt u-PAR (▲) and 293 cr-uPAR (▼) by non-enzymatic means. Cells were analyzed as described in experimental procedures. Data is representative of the mean ± SD of 3 individual experiments.

Table V

Elongation of cellular processes

Clones were harvested and analyzed as described in experimental procedures. Data represented by the mean (μm) ± SD of 3 individual scoring

Cell line	293			293 wt uPAR			293 cr-uPAR		
Clones	**Non-transfected**	**Blank plasmid**	**mock**	**4**	**11**	**13**	**4**	**7**	**8**
Processes (μm)	8.51 ± 2.32	8.75 ±1.49	7.86 ±1.34	14.23 ±3.60	19.14 ±2.61	15.71 ±3.15	21.40 ±4.44	25.40 ±2.30	25.75 ±3.59

CHAPTER 6. CELLULAR RESPONSES CHANGE DRAMATICALLY WHEN CR-UPAR IS EXPRESSED.

6.1. Introduction:

The function of the u-PA/u-PAR system was originally thought to be limited to localizing the Pg activation cascade and promoting pericellular proteolysis. More recently expression of u-PAR has been attributed to cancer progression and metastasis in mice that is u-PA-independent (Jo, Takimoto et al. 2009). Additionally, in thyroid carcinoma an increasing degree of metastasis follows a parallel pattern of u-PAR cleavage resistance.

Like many other GPI-anchored proteins, u-PAR can participate in cell signaling events which can affect multiple cellular events (Barker, Pallero et al. 2004). Although u-PAR is not a transmembrane protein, it interacts with many transmembrane proteins, i.e. integrins, GPCR, FPRL1, and LRP. These interactions activate many cellular signaling pathways, which include ERK/MAPK, focal adhesion kinase (FAK), JAK/ STAT, Rac-1, Src, and tyrosine- and serine-protein kinases (D'Alessio and Blasi 2009). Not all functions affected by cell-signaling events are u-PA dependent. Indeed, u-PAR expression can induce cellular adhesion that is mediated exclusively by Vtn, since over-expression of u-PAR can make the Vtn effect u-PA-independent. In addition, u-PAR can interact with integrins to regulate their activation or deactivation. Both of these effects are nullified when the D_1 of u-PAR is removed. In migrating cells, u-PAR has been detected at the leading edge, an area of lamellipodia formation. Furthermore, cell migration via u-PAR is usually enhanced through conformational changes induced by u-PA, which leads to exposure of the chemotactic epitope either by u-PAR activation or the

cleavage of D_1. The presence of u-PA also leads to increased cell proliferation via activation of the ERK/MAPK pathway. To our knowledge ligand-induced activation is sufficient for these events to occur, but it still remains unclear whether conversion to the fully active cleaved form is necessary for the events to persist or if cleavage is just a key regulatory point that diverges from Vtn and integrin-induced events.

Studies performed on u-PAR knockout mice indicated that homozygotes reached adulthood and reproduced normally (Bugge, Suh et al. 1995). However, the lack of u-PAR caused dramatic changes in several cell signaling pathways, which in turn affected cell proliferation, adhesion, migration, and differentiation. When u-PA and u-PAR expression were knocked down via hairpin RNA (hpRNA), there was a decrease in phosphorylation of ERK1/2, JNK, p38, FAK and PI(3)K, all major players in proliferation and survival (Gondi, Kandhukuri et al. 2007). u-PAR and integrin α5β1 activate ERK via EGRF, in a FAK-dependent manner, promoting cancer cell growth (Aguirre-Ghiso, Liu et al. 2001). Studies using a scid mouse model demonstrated that expression of u-PAR leads to metastasis that is independent of u-PA (Jo, Takimoto et al. 2009).

In this chapter, we show that the inability to cleave cr-uPAR results in the inability of u-PAR to regulate its multiple interactions, heightening most of the biological functions studied. However, cr-uPAR did not diverge from the pathways normally used by wt u-PAR. We hypothesize that expression of cr-uPAR in a conformation similar to the u-PA bound u-PAR leads to changes in the phenotype of 293 cr-uPAR cells, which resemble the well defined characteristics of a cancer cell. Thus, the modulation of u-PAR activity may play a role in both physiological and pathophysiological events.

6.2. Results:

6.2.1. cr-uPAR expression accelerates cellular proliferation independent of u-PA.

Since u-PAR is over-expressed in tumor cells and can modulate tumor growth, we speculated that u-PAR can regulate tumor proliferation and tumor progression. Cells expressing u-PAR have cell morphological changes and enhanced Vtn adhesive properties (Chapter 5). Also, after stable transfection 293 cr-uPAR cells appeared to reach confluency much faster than 293 non-transfected cells and 293 wt u-PAR cells. Thus, we determined whether the presence of cr-uPAR alters cell growth to the extent previously observed when u-PA stimulated u-PAR.

Figure 6.2.1 shows that 293 wt u-PAR cells exhibited the same doubling time as non-transfected, mock, or plasmid-only transfected 293 cells , ~39 h (Table VI). In contrast, 293 cr-uPAR cells showed a 1.5-fold faster doubling time at ~25 h. This trend was independent of receptor expression level as shown via monitoring of different clones of wt u-PAR or cr-uPAR expressing cells (Table VI). u-PAR induces cell proliferation in part by activating the ERK pathway, which can be interrupted by using the MEK inhibitor, PD98059. Proliferation of 293 cells was nearly completely abolished by the addition of PD98059 (Fig. 6.2.2 A). On the other hand the presence of PD98059 only suppressed approximately 50% of cell growth of wt u-PAR or cr-uPAR expressing cells. Since over-expression of u-PAR can stimulate the JNK pathway as well, we similarly studied its contribution to u-PAR-dependent proliferation using the JNKII inhibitor, JNKi. JNKi was able to significantly suppress the proliferation of non-transfected 293

cells. The addition of JNKi modestly decreased the proliferation of wt u-PAR cells (18%), while strongly affecting cr-uPAR cells (52%). Treating cells with PD98059 and JNKi jointly suppressed cell proliferation of 293 wt u-PAR and 293 cr-uPAR cells in a manner that resembled the additive effects of either treatment alone. The presence of u-PA induced the proliferation of cells expressing u-PAR (Fig. 6.2.2 B). Addition of u-PA had no effect on 293 cells since they do not express u-PAR. Addition of PD98059 or JNKi suppressed the proliferation of wt u-PAR cells in the presence of u-PA to nearly 50%, when compared to its absence. Cell proliferation of 293 cr-uPAR cells in the presence of PD98059 or JNKi and u-PA had similar effects as in the presence of serum. These results suggest that unliganded wt u-PAR predominantly stimulates cellular proliferation via the ERK pathway, while binding to u-PA also activates the JNK pathway. 293 cr-uPAR cells utilize both ERK and JNK pathways to promote proliferation even in the absence of u-PA, indicating that the free mutant receptor is stimulating cell proliferation in a similar manner as u-PA-bound receptor

6.2.2. The presence of cell-surface cr-uPAR enhances basal activation of ERK similar to active wt u-PAR.

u-PAR expression on 293 cells upregulates basal ERK activation. Serum stimulation of 293 cells enhances ERK activation (Fig. 6.2.3 A and B). 293 non-transfected cells had undetectable ERK phosphorylation with an 8-fold increase when serum stimulated. The addition of PD98059 to serum-stimulated 293 cells reduced ERK phosphorylation to basal levels. Unstimulated 293 wt u-PAR cells had a 4-fold increase in basal ERK phosphorylation while the addition of serum caused a 2.8-fold increase in ERK

phosphorylation over baseline. Basal levels of ERK phosphorylation in 293 cr-uPAR cells was 4-fold higher than the basal levels observed in 293 wt u-PAR cells, which corresponded to the changes seen in cell proliferation. The binding of the ATF to cells expressing uPAR led to a 5.5-fold increase in ERK phosphorylation of 293 cr-uPAR cells, compared to 293 wt u-PAR basal ERK phosphorylation (Fig. 6.2.3 C and D). The addition of PD98059 in the presence or absence of JNKi led to significant, but incomplete, attenuation of ERK activation only in 293 cr-uPAR cells. Exposure of cells with the JNKi and PD98059 did not significantly reduced ERK signaling.

6.2.3. Both wt u-PAR and cr-uPAR cell variants use additional signaling pathways.

In cancer, over-expression of uPAR induces JNK activation (Aguirre-Ghiso; 1999), raising the question whether the altered biological changes observed in 293 cr-uPAR cells are due to the induction of an alternate signaling pathway. Thus, wt u-PAR and cr-uPAR cells were tested for changes in JNK phosphorylation (Fig. 6.2.3 E and F). There was an increase in basal JNK phosphorylation in cr-uPAR expressing cells that was not detected in 293 wt u-PAR cells. However, 293 wt u-PAR cells stimulated with serum had a slight increase in JNK phosphorylation. These results are in agreement with the observed changes in cr-uPAR dependent proliferation. In 293 wt u-PAR cells, the addition of ATF had no effect on JNK phosphorylation. Interestingly, when cells were exposed to the JNKi in the presence of uPA and/or PD98059, JNK activation was not completely inhibited, suggesting that there may be cross-talk between pathways. These studies also

suggest that cr-uPAR can use a secondary pathway to enhance downstream cell signaling events and further promote proliferation.

6.2.4. Decreased apoptosis contributes to the enhanced cell number seen in 293 cr-uPAR cell cultures.

To determine if the enhanced proliferation observed in 293 cr-uPAR cells was based on an increased proliferation rate or a decrease in apoptosis, we quantified the number of apoptotic non-transfected, wt u-PAR and cr-uPAR cells after normal growth. Cells were Hoechst stained and visually scored for chromatin condensation as a sign of apoptotic change (Fig. 6.2.4 A-D). In 293 cell cultures and cultures of cells expressing wt u-PAR the Hoechst intensity per cell was similar, and thus the number of cells undergoing apoptosis is similar (Fig. 6.2.4 B). In contrast, 293 cr-uPAR cells had a decrease in Hoechst intensity, which suggests that the mutant receptor protects against induced apoptosis (Fig. 6.2.4 C). To determine if this effect was reproducible when apoptosis was induced, we stained the cells with PE-Annexin V in the presence or absence of TNF-α and CHX (Fig. 6.2.4 E). We observed no difference in apoptosis under normal conditions. However, in the presence of TNF-α there was an increase in apoptosis for the non-transfected cells. There was a moderate protection when wt u-PAR was expressed. Protection against apoptosis was more pronounced when cr-uPAR was expressed. Thus these studies suggest the enhanced proliferation of cr-uPAR cells results from a combination of increased cellular division and decreased cell death. This led us to study overall cell death induced by serum starvation, with CO_2 depravation, or serum starvation and the addition of TNF-α (Fig. 6.2.5 A). We observed that 293 cr-uPAR cells were less

affected than 293 non-transfected cells and 293 wt u-PAR cells. A 30% rate of cell death compared was seen for cr-uPAR cells undergoing serum starvation relative to 60 and 70% cell death for 293 non-transfected and wt u-PAR cells, respectively. Thus, cr-uPAR expression can enhance cell survival.

An additional study was performed to determine whether increased apoptosis contributes to the increase in cell numbers seen in cr-uPAR cell cultures. The first study sought to identify changes in proteins associated with apoptosis under basal conditions. Basal levels of activated caspase 3/7 were indistinguishable between the three cell lines (Fig. 6.2.5 B). However, 293 cells treated with TNF-α had 3-fold higher caspase activity, than wt u-PAR or cr-uPAR expressing cells. Interestingly, there was a pronounced decrease in caspase activity in cr-uPAR cells relative to wt u-PAR cells. These results suggest that the effects observed in proliferation are not an immediate result of resistance to apoptosis, since there is no basal difference in cell death between the cells, a trait also observed in the highly metastatic ARO cells (Int. J. Cancer 81:956-962, 1999). The observed increase in apoptosis in the presence of u-PA in cr-uPAR cells and the lack of significant difference in the presence of PD98059 suggests that cr-uPAR may use other pathways to control these events.

6.2.5. Expression of cr-uPAR promotes migration paralleling the effects of activated wt u-PAR.

We hypothesized that cr-uPAR induces enhanced migration similar to the u-PA-bound active form of u-PAR. Using serum as a stimulus, we observed that non-transfected 293 cells were unaffected by the presence of either Vtn based matrix (Fig.

6.2.6) or serum based matrix (Fig. 6.2.7). 293 cells expressing wt u-PAR or cr-uPAR had slightly reduced migration in the absence of stimulus compared to untransfected cells, which might be due to increased cellular adhesion secondary to u-PAR expression (Wei, Waltz et al. 1994). On exposure to serum, cells expressing wt u-PAR had an approximate 200% increase in migration compared to normal controls, while cells expressing cr-uPAR had an approximate 300% increase in migration compared to controls. Stimulation with tcu-PA increases migration of cells expressing wt u-PAR. Thus, we asked whether wt u-PAR cells that had been stimulated with a low dose of tcu-PA increased migration to the levels seen for cr-uPAR cells (Fig. 6.2.6). Stimulation of wt u-PAR with tcu-PA caused an approximate 400% increase in migration. However, when cr-uPAR cells were stimulated, we observed no significant change in migration when compared to the basal migration. This was not due to random chemotaxis as cell expressing either u-PAR variants had little directed migration in the absence of serum (Figure 6.2.8).

6.2.6. Migration via the GPCR pathway is unaffected by the presence of cr-uPAR.

Expression of unoccupied uPAR leads to limited cell migration, since the cryptic chemotactic epitope needed for migration is unavailable to interact with pro-migratory receptors, most notably GPCRs (Mazzieri, D'Alessio et al. 2006). We previously found that cells expressing cr-uPAR exhibited an enhanced basal tendency to migrate as compared to wt u-PAR cells. u-PA further stimulated the migration of wt u-PAR cells but not of cr-uPAR cells, suggesting that cr-uPAR expression promoted cell migration in a ligand-independent manner. To determine whether cr-uPAR also utilized GPCR signaling to induce cell migration, we monitored the effect of the GPCR pathway

inhibitor, pertussis toxin (PTX) on the migration of wt u-PAR and cr-uPAR cells (Fig. 6.2.9). In the absence of PTX, 10% FCS as a general chemoattractant induced a two-fold increase in migration in wt u-PAR cells over their basal migration rate without serum. As previously reported, the FCS-stimulated migration rate of cr-uPAR cells is approximately another two-fold higher than that of wt u-PAR cells (Nieves and Manchanda 2010). Binding of u-PA induces a similar two-fold enhancement of wt u-PAR cell migration. However, u-PA has no additional stimulatory effect on cr-uPAR cell migration. Pre-incubation of either wt u-PAR or cr-uPAR cells with PTX abolishes serum-dependent migration regardless of the presence of the u-PA stimulant. These results suggest that 293 cr-uPAR cells use the GPCR pathway to induce migration, similar to 293 wt u-PAR cells. Furthermore they indicate that while unliganded cr-uPAR promotes cellular migration similar to ligand-activated wt u-PAR, both receptors utilize GPCR pathways to regulate the process.

6.3. Discussion:

In thyroid cancer cells resistance to u-PAR cleavage correlates with cancer malignancy. ARO, anaplastic thyroid cancer cells, also have abundant levels of u-PAR but are resistant to cleavage by tcu-PA. WRO, a follicular thyroid carcinoma, have less cleavage resistance than their ARO counterpart and decreased malignancy (Ragno, Montuori et al. 1998).

Expression levels of both u-PA and u-PAR correlates to patient outcome, metastatic potential (*in vitro*), and tumor progression (Pyke, Kristensen et al. 1991; Plesner, Ralfkiaer et al. 1994; Carriero, Del Vecchio et al. 1997). The role of u-PAR in

malignancy is accentuated by the ability of PAI-1 to inhibit migration of tumor cells, implying u-PAR is a potential regulatory target of cancer malignancy. Indeed, u-PAR can induce tumor progression and metastasis in the absence of u-PA (Jo, Takimoto et al. 2009). In many cancers, the MAPK/ERK pathways are frequently hyper-expressed and over-active (Sivaraman, Wang et al. 1997). The increase in ERK phosphorylation seen in cr-uPAR cells is most likely mediated by the presence of an active receptor, which in turn can activate downstream genes responsible for driving the cells into S-phase. Our studies here are focused on determining the differences between the basal effects from the u-PAR variants rather than pinpointing which pathway is responsible for these cellular changes. Mazzieri et al., reported that a highly mutated receptor with a total of 5 residues altered in the linker region alone produced a u-PAR that is resistant to cleavage by tcu-PA, Pn, chymotrypsin and MMPs. They observed a change in protein interaction which lead the receptor to interact prominently with EGFR and integrin $\alpha_5\beta_1$ but is unable to interact with FPRL-1. However, in our system we show that cr-uPAR can interact with Vn, unlike the hcr-uPAR mutant. Madsen et al, showed that switching key residues in u-PAR can lead to disruption of Vtn interaction, residues W^{32} and R^{91}, and decrease both adhesion and changes in cell morphology. Although, our mutant has two sites mutated in the linker region between D_1 and D_2, we show that most of the normal interactions are maintained, since there is no loss of wild-type features.

The lack of regulation of u-PAR activation, cleavage and protein interactions promotes enhanced cellular functions that resemble characteristics of a cancer cell. The ability of cr-uPAR expressing cells to proliferate faster in the absence of u-PA is only one example of this dysregulation. Indeed, cr-uPAR cells promote cell proliferation in the

presence of PD98059, a MEK inhibitor. Yet the addition of a JNK inhibitor in tandem with PD98059 is capable of preventing cell growth. This suggests that more than one pathway is activated by the presence of cr-uPAR. This effect is reproduced in cell migration, a mechanism that also utilizes cell signaling events to mediate the function (Fig. 6.2.6). We observed that in the absence of u-PA there is significant stimulation of directed migration. However, cr-uPAR uses the same pathway as wt u-PAR, since the GPCR uncoupler, PTX, prevents any cell migration (Fig. 6.2.14). Unlike the observations made with hcr-uPAR, our cr-uPAR did not diverge from utilizing wt u-PAR pathways. These results also suggest that u-PAR adapts to its environment, adding to the complicated knowledge we have of this system. The cr-uPAR receptor seems in a structural change that resembles that of the active receptor. This change leads to a hyper-active state, a lack of regulation by u-PA and the system, not to mention instead of separating each individual component has brought together both the ability to constitutively maintain functions associated with Vtn and integrins, and those functions associated with the cleaved form of u-PAR. cr-uPAR behavior like the active receptor, most probably having the chemotactic epitope exposed, induces the capabilities which to date have only been observed to be u-PA dependent.

6.4. Figures and Tables:

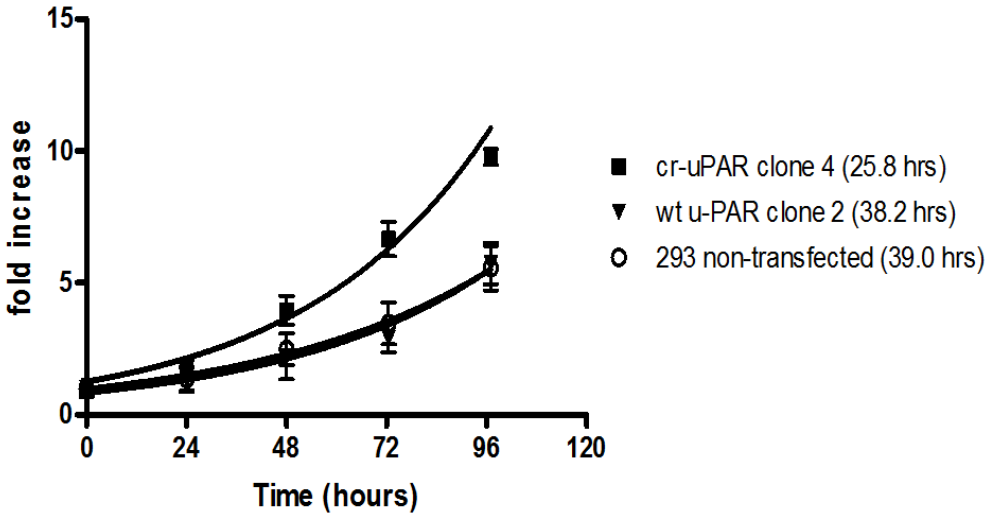

Fig 6.1. cr-uPAR expressing cells proliferate more rapidly than their untransfected counterparts. 293 untransfected (○), 293 wt u-PAR (▼) and 293 cr-uPAR (■) cells were harvested, incubated for the times indicated in media with or without G418, and analyzed as described in the Experimental Procedures. Data is representative of the mean ± SD of 8 replicates.

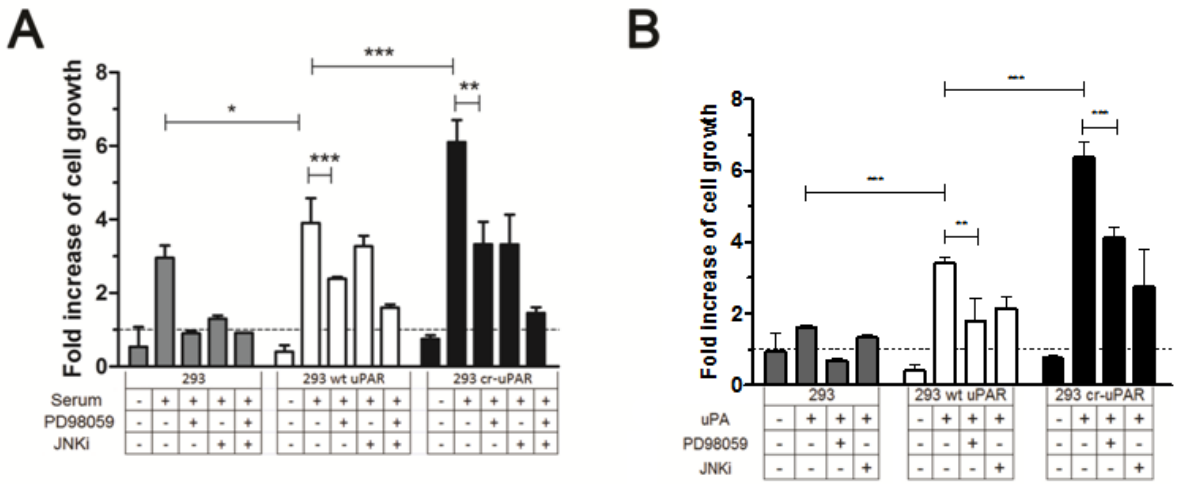

Fig 6.2. cr-uPAR cells proliferate similar to uPA-bound wt u-PAR cells, which are regulated by multiple pathways. A) Cells expressing 293 (grey bars), 293 wt u-PAR (white bars) and 293 cr-uPAR (black bars) were incubated in the absence or presence of serum, with 40 μM PD98059, 10 μM JNKII inhibitor (JNKi) or a combination of both inhibitors, or **B)** cells were harvested, incubated for 3 days in SF media, in the presence of 10 nM u-PA alone, with 10 nM u-PA and 40 μM PD98059 or with 10 nM u-PA and 50 μM JNKi. Data represents the mean ± SD of 3 individual experiments performed in triplicates. (student's t test: *, p=n.s.; **, p <0.01; ***, p<0.001).

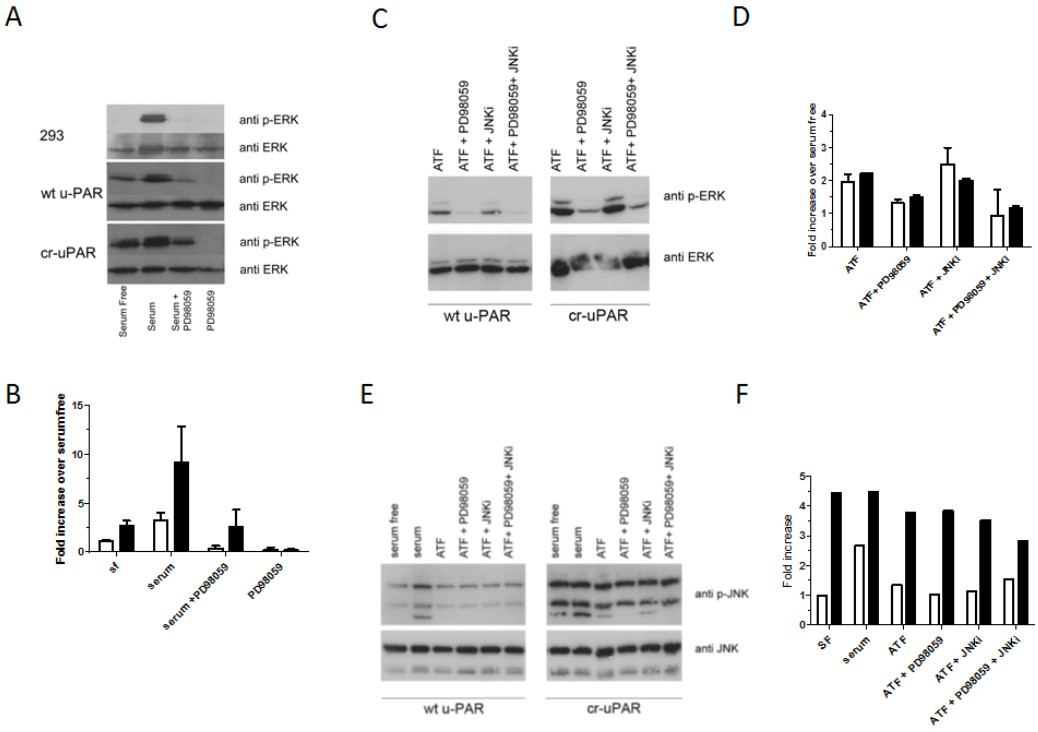

Fig 6.3. Expression of cr-uPAR induces hyper-activation of ERK. Adherent cells were harvested and grown to 80% confluency. Cells were stimulated with SF media, serum, 10 nM ATF, and a combination of 40 μm PD98059, 10 μM JNKII inhibitor, or all of the above. **A)** Cell lysates were subjected to immunoblotting using α-phospho ERK and α-ERK antibodies. **B)** Changes in ERK phosphorylation for wt u-PAR (white) and cr-uPAR (black) after stimulation with SF media, serum only, serum with 40 μm PD98059 or 40 μM PD98059 only was detected. **C)** Cell lysates were subjected to immunoblotting using α-phospho ERK and α-ERK antibodies. **D)** wt u-PAR (white) and cr-uPAR (black) were analyzed after stimulation with SF media for fold-increase in phosphorylated ERK (right). **E)** Blots of cell lysates were incubated with α-phospho JNK and α-JNK antibodies. **F)** wt u-PAR (white) and cr-uPAR (black) were analyzed after stimulation with SF media for fold-increase in phosphorylated JNK (right).

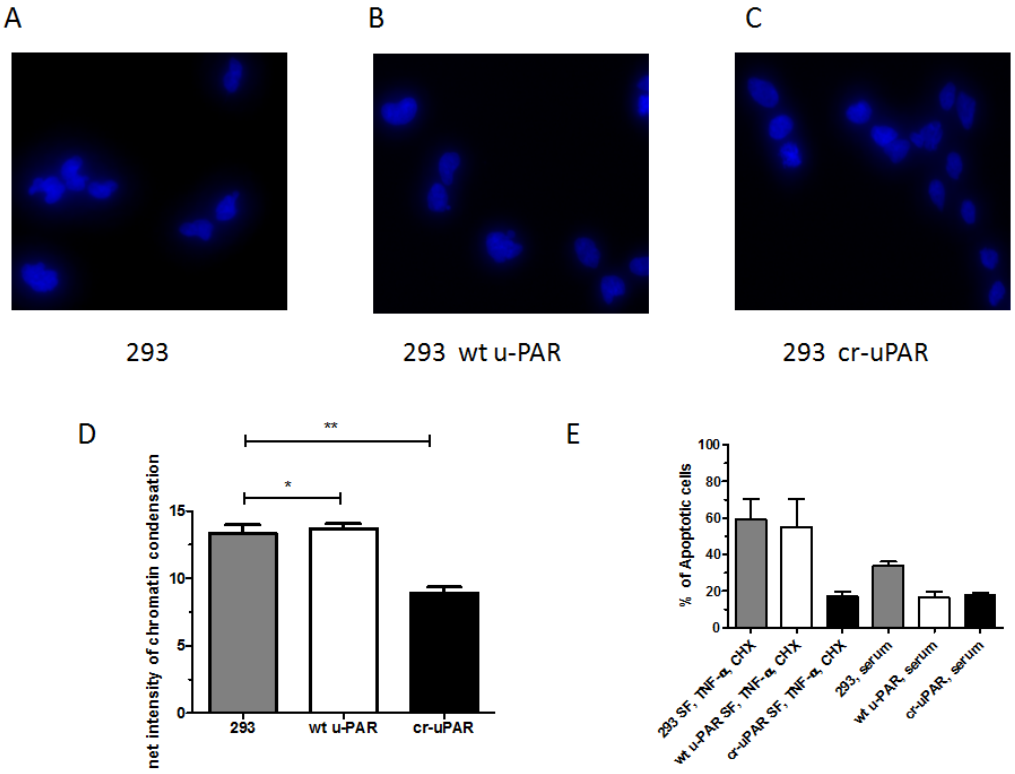

Fig 6.4. 293 cells expressing uPAR have reduced apoptosis. 293 (A), 293 wt u-PAR (B) and 293 cr-uPAR (C) cells were permeabilized and stained with Hoechst as described in the experimental procedures. The average nuclear Hoechst intensity was obtained by densitometry. The images represent 3 individual experiments (student's t test: *, p=n.s.; **, p <0.01). (D) 293 non-transfected (grey bars), wt u-PAR (white bars) and cr-uPAR (black bars). (E) 293, 293 wt u-PAR and 293 cr-uPAR cells were treated with DMEM and 10% FCS or DMEM with 10 nM TNF-a and 10 µg/mL CHX for 18 h and stained with PE-Annexin V. Data represents the mean ± SD of 2 individual experiments performed in quadruples.

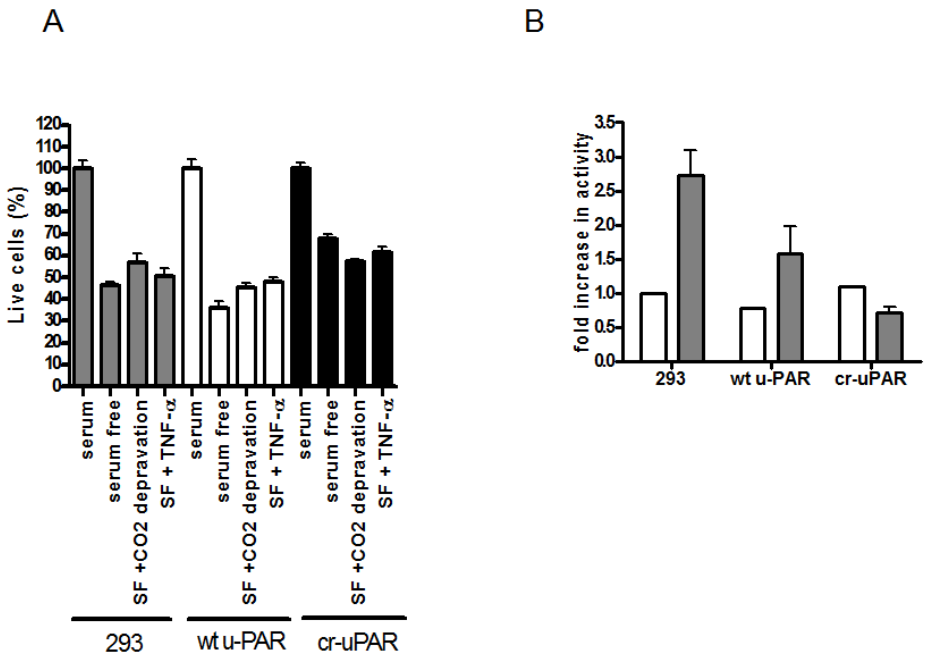

Fig 6.5. Expression of u-PAR diminishes induction of cell death. A) 2x 10^5 cells seeded and expressing no u-PAR (grey bars), wt u-PAR (white bars), or cr-uPAR (black bars) were subjected to serum, SF media, SF media and CO_2 deprived, or SF media and 10 nM TNF-α for 24 h at 37°C and followed our standard proliferation setup. **B)** Caspace 3/7 levels were detected in 293, wt u-PAR and cr-uPAR cells. SF media (white bars) or media containing 10 nM TNF-α (grey bars) were incubated for 4 h at 37°C and experiment was assayed for 16 h post-induction.

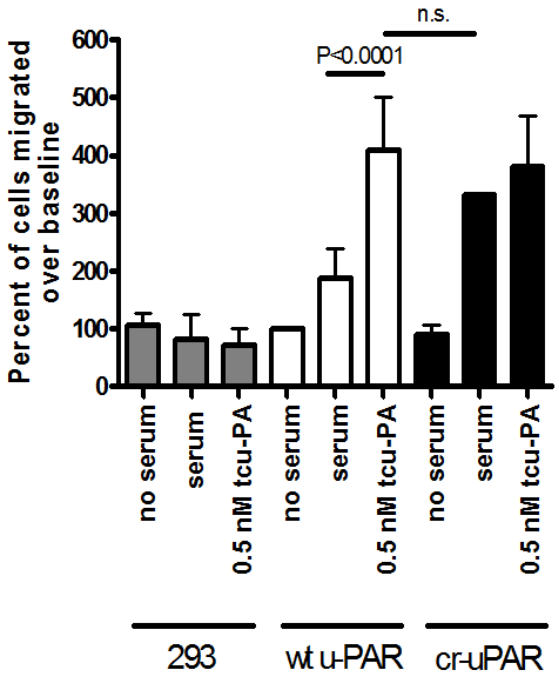

Fig 6.6. 293 cr-uPAR expressing cells promote u-PA-independent migration. 293 (grey bars), 293 wt u-PAR (white bars), and 293 cr-uPAR (black bars) expressing cells were serum starved and suspended in SF DMEM. Cells were either pre-treated with SF DMEM and allowed to migrate over Vtn-coated chambers with no serum gradient (*SF*), pre-treated with SF DMEM and allowed to migrate toward 10% FCS (*serum*), or pre-treated with 0.5 nM tcu-PA and allowed to migrate toward 10% FCS (*0.5 nM tcu-PA*) for 2 h at 37°C. Data represent the means and SD of at least 3 individual replicates and were analyzed using a Student's t-test.

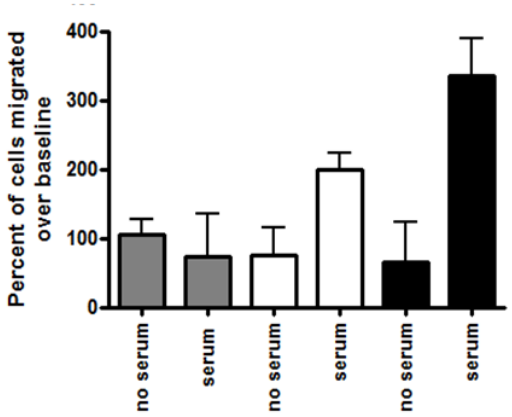

Fig 6.7. Migration of cr-uPAR on serum-coated membranes is similar to that of Vtn coated membranes. 293 (grey bars), 293 wt u-PAR (white bars), and 293 cr-uPAR (black bars) expressing cells were serum starved and suspended in SF DMEM. Cells were either pre-treated with SF DMEM and allowed to migrate over FCS-coated chambers with no serum gradient (*SF*) or pre-treated with serum-free DMEM and allowed to migrate toward 10% FCS (*serum*) for 2 h at 37°C. Data represent the means and SD of at least 8 individual replicates. "This research was originally published in Journal Biological Chemistry. Evelyn C. Nieves and Naveen Manchanda. A cleavage-resistant urokinase plasminogen activator receptor exhibits dysregulated cell-surface clearance. J Biol Chem. 2010 April 23; 285(17): 12595–12603. © the American Society for Biochemistry and Molecular Biology."

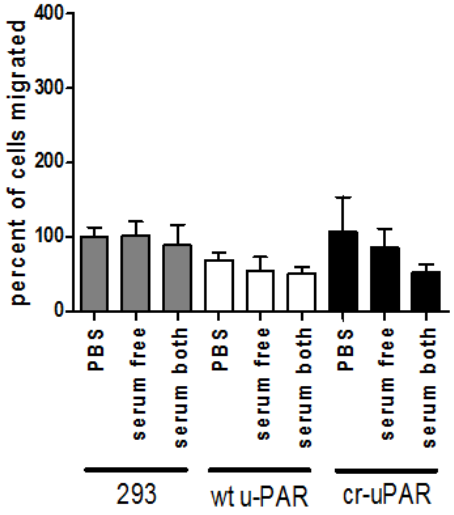

Fig 6.8. 293 cells show no random chemotaxis. 293 (grey bars), 293 wt u-PAR (white bars), and 293 cr-uPAR (black bars) expressing cells were serum starved and suspended in SF DMEM. Cells were either pre-treated with SF DMEM and allowed to migrate over FCS-coated chambers with PBS or SF, or pre-treated with SF DMEM and allowed to migrate with 10% FCS on both sides of the chamber for 2 h at 37°C. Data represent the means and SD of at least 5 individual replicates.

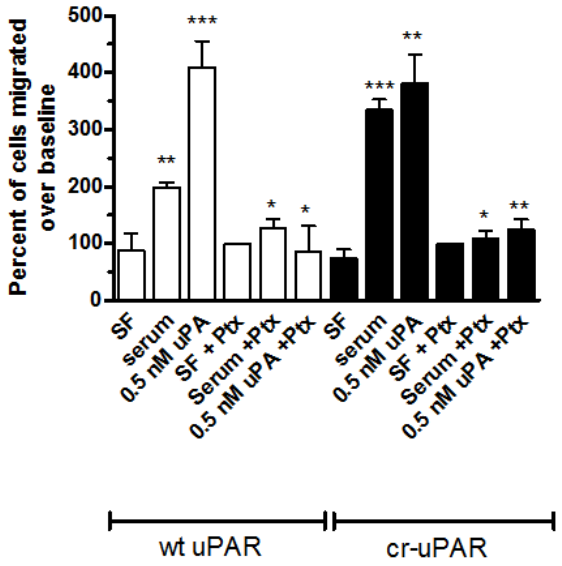

Fig 6.9. Inhibition of GPCR pathway prevents migration of u-PAR expressing cells. Suspended wt u-PAR (white bars) and cr-uPAR (black bars) cells which were pre-incubated in the presence or absence of PTX for 18 h. Cells were allowed to migrate over Vtn-coated chambers with no serum gradient (*SF*), pre-treated with SF DMEM and allowed to migrate toward 10% FCS (*serum*), or pre-treated with 0.5 nM tcu-PA and allowed to migrate toward 10% FCS (*0.5 nM tcu-PA*) for 2 h at 37°C. Data represent the means and SD of at least 3 individual replicates when compared to its SF counterpart (student's t test: *, p=n.s.; **, p <0.01; ***, p<0.001).

Table VI

Proliferation of 293 cells under normal conditions

Clones were harvested and analyzed as described in experimental procedures. Data are representative of the mean ± SD of 4 individual experiments

Cell line	293 wt u-PAR			293 cr-uPAR			293		
Clones	**2**	**11**	**13**	**4**	**7**	**8**	**Non-transfected**	**pcDNA 3.1(+)**	**mock**
Doubling Time (h)	38.2 ±4.4	41.0 ±8.1	38.3 ±4.3	25.8 ±4.6	24.1 ±7.6	23.8 ±2.3	39.0 ±1.9	37.6 ±1.8	39.8 ±4.2

CHAPTER 7: SUMMARY AND NEW DIRECTIONS

Upregulated expression of u-PAR on cancer cells as well as associated stromal and inflammatory cells occurs in a wide array of cancers and can correlate with increased metastasis, resistance to chemotherapy, and overall poor prognosis depending on the type of malignancy (Andreasen, Kjoller et al. 1997; Ge and Elghetany 2003). Elevated levels of cleaved u-PAR is an independent prognostic marker for several cancers as well (Pedersen, Schmitt et al. 1993; Sidenius, Sier et al. 2000; Garcia-Monco, Coleman et al. 2002). However, since cleaved u-PAR can promote cellular migration *in vitro*, it is unclear whether the presence of elevated serum soluble cleaved receptor in certain cancer patients merely reflects increased levels of u-PA activity or reflects a cleavage-mediated receptor activation mechanism. Confounding the interpretation of the clinicopathological data is that in certain highly invasive cancers, such as anaplastic thyroid carcinoma, overglycosylation of u-PAR allows u-PA-binding but hinders u-PA-dependent receptor cleavage (Montuori, Rossi et al. 1999). Nevertheless, because of its wide prognostic value, u-PAR has emerged as an attractive target for the development of small molecule antagonists. This emerging area of research highlights the need for a better understanding of the cellular biology of u-PAR and how its functions might be modulated by such small molecules.

Here we intended to discern the differences between the generation of cleaved u-PAR and the u-PAR activation post-exposure to u-PA. The studies shown here were performed using a mutant form of u-PAR, cr-uPAR, resistant to u-PA cleavage that resulted in a novel internalization profile, heightened cell proliferation, heightened cell migration, hyper-activated ERK and increased processes elongation, which were u-PA independent

at basal states. Cr-uPAR remained intact in the presence of vast stoichiometric excess of u-PA, suggesting that the ligand-induced receptor cleavage by non-specific proteases is unlikely. Overall, these studies showed an indiscriminant use of both a proteolytic and a non-proteolytic role by the generation of a cr-uPAR (Nieves and Manchanda 2010). These observations in combination with cellular and biological studies performed by other researchers suggest a series of conformational changes occur in different forms of u-PAR, i.e. unliganded or u-PA-bound. In addition to cellular studies, reported crystal structures in the presence of several binding molecules showed different conformational changes, reflective of a highly mobile linker region and domains. Our study gives novel insights into the events that are affected by the conformational state of the receptor. It would be intriguing to crystallize cr-uPAR to determine similarities with the u-PA bound u-PAR, since cr-uPAR activity resembles that of ligand-bound wt u-PAR. We observed cr-uPAR-expressing cells, in the absence u-PA, perform the functions of cellular migration and cellular proliferation to an extent similar to u-PA-treated cells expressing wt u-PAR.

There are two proposed models for u-PAR. One suggests binding of u-PA leads to a conformational change which exposes the chemotactic epitope, activating the receptor and initiating the correspondent cellular events. The second model suggests that binding of u-PA promotes cleavage and thus exposure of the linker region, leading to regulation of u-PAR's functions with the generation of the permanently active form of u-PAR. We challenged both models by preventing u-PAR cleavage and promoting the dysregulation of several key activities.

Our data are congruent with a functional model of u-PAR in which the receptor can be induced to adopt a range of activities based on the presence of ligand and the availability of co-receptors as defined by their membrane distribution. This functional model complements a recently described structural model in which unliganded u-PAR is proposed to be in dynamic equilibrium among several conformations as defined by the receptor's interdomain relationships. Some of these conformations have limited activity, such as moderate affinity for Vtn, while others are wholly inactive, and can be stabilized via small molecule u-PAR antagonists (Huai, Mazar et al. 2006; Madsen, Ferraris et al. 2007; De Souza, Matthews et al. 2011). In both models, fully active u-PAR is induced by u-PA-binding. Within this structural model, it may be possible for different protein-protein binding sites to exhibit dyssynchronous competencies in unliganded u-PAR, and it is only when u-PA is present to lock the receptor into a globally active conformation such that u-PAR's affinities for other co-receptors are fully revealed (Huai, Mazar et al. 2006; Xu, Gardsvoll et al. 2012). This dyssynchronous binding potential of unliganded u-PAR conformers could contribute to the differing degrees of pro-migratory versus pro-proliferative effects of cr-uPAR expression in the presence and absence of u-PA.

Our original goal was to dissect those functions that were exclusive to the intact receptor. We were surprised to discover that cr-uPAR retained all tested functions. These studies suggest a need for u-PAR cleavage to hinder the multiple events that are induced from over-stimulating the cell and dysregulating its normal functions. Removing the proteolytic sites of u-PAR caused an unexpected gain of cancer cell-like characteristics. Whether cr-uPAR leads to a stronger metastatic profile in a scid mouse model implanted with cells expressing human u-PAR in the presence or absence of human u-PA is yet to

be determined. In addition, at the geriatric state, u-PAR knockout mice have differences in leukocyte infiltration (Gueler, Rong et al. 2008). The fact that different mouse models have been used makes understanding the *in vivo* functions of u-PAR more difficult; however, it is feasible to use cr-uPAR as a tool to study regulation differences. The development of a knock-in human cr-uPAR mouse model can be generated to study the effects on auto-regulation of u-PAR functions. In addition, our molecule can potentially be used to isolate the molecular mechanisms underlying u-PAR's role in human malignancies. A confounding finding in our studies is the gain of interaction with LRP. Interestingly, the original function of u-PAR, the initiation of the plasminogen system, at first glance still occurs with cr-uPAR. However, a closer look at both receptor saturation and reversible inhibition demonstrated a crucial distinction between the two u-PAR variants used in this study. Again, these observations suggest that the lack of a regulation by proteolysis causes dysregulation of cr-uPAR activity. Additionally, cr-uPAR's ability to stimulate multiple pathways similar to both the intact and the cleaved form of u-PAR can be used to further isolate differences in the signaling pathways of the u-PA-bound u-PAR and the cleaved u-PAR, if they exist.

The regulation of u-PAR activity remains complex. While receptor cleavage does not appear to be a primary mechanism for initiating any of these functions, it is unknown whether cleavage is a physiologic means of receptor downregulation or perhaps a switch from matrix adhesion to stimulating migration. Moreover, ancillary observations on the cellular biology of cr-uPAR have yielded new testable hypotheses on the regulation of receptor activity by membrane trafficking. While dissection of these regulatory pathways is crucial to the development of anti-u-PAR therapeutic agents, the current data also

caution that u-PAR has the potential to be fixed in a uPA-independent, partially active state.

References:

Aguirre-Ghiso, J. A., D. Liu, et al. (2001). "Urokinase receptor and fibronectin regulate the ERK(MAPK) to p38(MAPK) activity ratios that determine carcinoma cell proliferation or dormancy in vivo." Mol Biol Cell **12**(4): 863-879.

Aguirre Ghiso, J. A. (2002). "Inhibition of FAK signaling activated by urokinase receptor induces dormancy in human carcinoma cells in vivo." Oncogene **21**(16): 2513-2524.

Aguirre Ghiso, J. A., K. Kovalski, et al. (1999). "Tumor dormancy induced by downregulation of urokinase receptor in human carcinoma involves integrin and MAPK signaling." J Cell Biol **147**(1): 89-104.

Alfano, D., P. Franco, et al. (2005). "The urokinase plasminogen activator and its receptor: role in cell growth and apoptosis." Thromb Haemost **93**(2): 205-211.

Alfano, D., I. Iaccarino, et al. (2006). "Urokinase signaling through its receptor protects against anoikis by increasing BCL-xL expression levels." J Biol Chem **281**(26): 17758-17767.

Anderson, R. G. (1994). "Functional specialization of the glycosylphosphatidylinositol membrane anchor." Semin Immunol **6**(2): 89-95.

Andreasen, P. A., L. Kjoller, et al. (1997). "The urokinase-type plasminogen activator system in cancer metastasis: a review." Int J Cancer **72**(1): 1-22.

Andreasen, P. A., L. Sottrup-Jensen, et al. (1994). "Receptor-mediated endocytosis of plasminogen activators and activator/inhibitor complexes." FEBS Lett **338**(3): 239-245.

Barinka, C., G. Parry, et al. (2006). "Structural basis of interaction between urokinase-type plasminogen activator and its receptor." J Mol Biol **363**(2): 482-495.

Barker, T. H., M. A. Pallero, et al. (2004). "Thrombospondin-1-induced focal adhesion disassembly in fibroblasts requires Thy-1 surface expression, lipid raft integrity, and Src activation." J Biol Chem **279**(22): 23510-23516.

Barnathan, E. S., A. Kuo, et al. (1990). "Characterization of human endothelial cell urokinase-type plasminogen activator receptor protein and messenger RNA." Blood **76**(9): 1795-1806.

Beaufort, N., D. Leduc, et al. (2004). "Proteolytic regulation of the urokinase receptor/CD87 on monocytic cells by neutrophil elastase and cathepsin G." J Immunol **172**(1): 540-549.

Behrendt, N., E. Ronne, et al. (1996). "Domain interplay in the urokinase receptor. Requirement for the third domain in high affinity ligand binding and demonstration of ligand contact sites in distinct receptor domains." J Biol Chem **271**(37): 22885-22894.

Behrendt, N., E. Ronne, et al. (1990). "The human receptor for urokinase plasminogen activator. NH2-terminal amino acid sequence and glycosylation variants." J Biol Chem **265**(11): 6453-6460.

Bernstein, A. M., S. S. Twining, et al. (2007). "Urokinase receptor cleavage: a crucial step in fibroblast-to-myofibroblast differentiation." Mol Biol Cell **18**(7): 2716-2727.

Besch, R., C. Berking, et al. (2007). "Inhibition of urokinase-type plasminogen activator receptor induces apoptosis in melanoma cells by activation of p53." Cell Death Differ **14**(4): 818-829.

Bifulco, K., I. Longanesi-Cattani, et al. (2011). "Involvement of the soluble urokinase receptor in chondrosarcoma cell mobilization." Sarcoma **2011**: 842842.

Blasi, F., N. Behrendt, et al. (1990). "The urokinase receptor and regulation of cell surface plasminogen activation." Cell Differ Dev **32**(3): 247-253.

Blasi, F. and P. Carmeliet (2002). "uPAR: a versatile signalling orchestrator." Nat Rev Mol Cell Biol **3**(12): 932-943.

Blasi, F., M. P. Stoppelli, et al. (1986). "The receptor for urokinase-plasminogen activator." J Cell Biochem **32**(3): 179-186.

Blasi, F., J. D. Vassalli, et al. (1987). "Urokinase-type plasminogen activator: proenzyme, receptor, and inhibitors." J Cell Biol **104**(4): 801-804.

Borglum, A. D., A. Byskov, et al. (1992). "Assignment of the urokinase-type plasminogen activator receptor gene (PLAUR) to chromosome 19q13.1-q13.2." Am J Hum Genet **50**(3): 492-497.

Bugge, T. H., T. T. Suh, et al. (1995). "The receptor for urokinase-type plasminogen activator is not essential for mouse development or fertility." J Biol Chem **270**(28): 16886-16894.

Cao, C., D. A. Lawrence, et al. (2006). "Endocytic receptor LRP together with tPA and PAI-1 coordinates Mac-1-dependent macrophage migration." EMBO Journal **25**(9): 1860-1870.

Carmeliet, P. (2000). "Mechanisms of angiogenesis and arteriogenesis." Nat Med **6**(4): 389-395.

Carriero, M. V., S. Del Vecchio, et al. (1997). "Vitronectin binding to urokinase receptor in human breast cancer." Clin Cancer Res **3**(8): 1299-1308.

Cavallo-Medved, D., J. Mai, et al. (2005). "Caveolin-1 mediates the expression and localization of cathepsin B, pro-urokinase plasminogen activator and their cell-surface receptors in human colorectal carcinoma cells." J Cell Sci **118**(Pt 7): 1493-1503.

Chapman, H. A. and Y. Wei (2001). "Protease crosstalk with integrins: the urokinase receptor paradigm." Thromb Haemost **86**(1): 124-129.

Chapman, H. A., Y. Wei, et al. (1999). "Role of urokinase receptor and caveolin in regulation of integrin signaling." Thromb Haemost **82**(2): 291-297.

Chen, C. Y. and A. B. Shyu (1995). "AU-rich elements: characterization and importance in mRNA degradation." Trends Biochem Sci **20**(11): 465-470.

Chillakuri, C. R., C. Jones, et al. (2010). "Heparin binding domain in vitronectin is required for oligomerization and thus enhances integrin mediated cell adhesion and spreading." FEBS Lett **584**(15): 3287-3291.

Cohen, R. L., X. P. Xi, et al. (1991). "Effects of urokinase receptor occupancy on plasmin generation and proteolysis of basement membrane by human tumor cells." Blood **78**(2): 479-487.

Conese, M., A. Nykjaer, et al. (1995). "alpha-2 Macroglobulin receptor/Ldl receptor-related protein(Lrp)-dependent internalization of the urokinase receptor." J Cell Biol **131**(6 Pt 1): 1609-1622.

Connolly, B. M., E. Y. Choi, et al. (2010). "Selective abrogation of the uPA-uPAR interaction in vivo reveals a novel role in suppression of fibrin-associated inflammation." Blood **116**(9): 1593-1603.

Cortese, K., M. Sahores, et al. (2008). "Clathrin and LRP-1-independent constitutive endocytosis and recycling of uPAR." PLoS ONE **3**(11): e3730.

Cunningham, O., A. Andolfo, et al. (2003). "Dimerization controls the lipid raft partitioning of uPAR/CD87 and regulates its biological functions." EMBO J **22**(22): 5994-6003.

Czekay, R. P., T. A. Kuemmel, et al. (2001). "Direct binding of occupied urokinase receptor (uPAR) to LDL receptor-related protein is required for endocytosis of uPAR and regulation of cell surface urokinase activity." Molecular Biology of the Cell **12**(5): 1467-1479.

Czekay, R. P., T. A. Kuemmel, et al. (2001). "Direct binding of occupied urokinase receptor (uPAR) to LDL receptor-related protein is required for endocytosis of uPAR and regulation of cell surface urokinase activity." Mol Biol Cell **12**(5): 1467-1479.

Czekay, R. P. and D. J. Loskutoff (2009). "Plasminogen activator inhibitors regulate cell adhesion through a uPAR-dependent mechanism." J Cell Physiol **220**(3): 655-663.

D'Alessio, S. and F. Blasi (2009). "The urokinase receptor as an entertainer of signal transduction." Front Biosci **14**: 4575-4587.

D'Alessio, S., F. Margheri, et al. (2004). "Antisense oligodeoxynucleotides for urokinase-plasminogen activator receptor have anti-invasive and anti-proliferative effects in vitro and inhibit spontaneous metastases of human melanoma in mice." Int J Cancer **110**(1): 125-133.

Dang, J., D. Boyd, et al. (1999). "A region between -141 and -61 bp containing a proximal AP-1 is essential for constitutive expression of urokinase-type plasminogen activator receptor." Eur J Biochem **264**(1): 92-99.

Dano K., N. Behrendt, et al. "The urokinase receptor. protein structure and role in plasminogen activation and cancer invasion." Fibrinolysis: 189-203.

Dass, C. R., A. P. Nadesapillai, et al. (2005). "Downregulation of uPAR confirms link in growth and metastasis of osteosarcoma." Clin Exp Metastasis **22**(8): 643-652.

Dass, K., A. Ahmad, et al. (2007). "Evolving role of uPA/uPAR system in human cancers." Cancer Treat Rev.

De Souza, M., H. Matthews, et al. (2011). "Small molecule antagonists of the urokinase (uPA): urokinase receptor (uPAR) interaction with high reported potencies show only weak effects in cell-based competition assays employing the native uPAR ligand." Bioorg Med Chem **19**(8): 2549-2556.

de Witte, J. H., J. A. Foekens, et al. (2001). "Prognostic impact of urokinase-type plasminogen activator receptor (uPAR) in cytosols and pellet extracts derived from primary breast tumours." Br J Cancer **85**(1): 85-92.

Declerck, P. J., M. De Mol, et al. (1992). "Identification of a conformationally distinct form of plasminogen activator inhibitor-1, acting as a noninhibitory substrate for tissue-type plasminogen activator." J Biol Chem **267**(17): 11693-11696.

Degryse, B. (2011). "The urokinase receptor system as strategic therapeutic target: challenges for the 21st century." Curr Pharm Des **17**(19): 1872-1873.

Degryse, B., S. Orlando, et al. (2001). "Urokinase/urokinase receptor and vitronectin/alpha(v)beta(3) integrin induce chemotaxis and cytoskeleton reorganization through different signaling pathways." Oncogene **20**(16): 2032-2043.

Degryse, B., M. Resnati, et al. (1999). "Src-dependence and pertussis-toxin sensitivity of urokinase receptor-dependent chemotaxis and cytoskeleton reorganization in rat smooth muscle cells." Blood **94**(2): 649-662.

Duffy, M. J., D. Reilly, et al. (1990). "Urokinase-plasminogen activator, a new and independent prognostic marker in breast cancer." Cancer Res **50**(21): 6827-6829.

Dumler, I., A. Weis, et al. (1998). "The Jak/Stat pathway and urokinase receptor signaling in human aortic vascular smooth muscle cells." J Biol Chem **273**(1): 315-321.

Ellis, V., N. Behrendt, et al. (1991). "Plasminogen activation by receptor-bound urokinase. A kinetic study with both cell-associated and isolated receptor." J Biol Chem **266**(19): 12752-12758.

Ellis, V., S. A. Whawell, et al. (1999). "Assembly of urokinase receptor-mediated plasminogen activation complexes involves direct, non-active-site interactions between urokinase and plasminogen." Biochemistry **38**(2): 651-659.

Erickson, L. A., R. R. Schleef, et al. (1985). "The fibrinolytic system of the vascular wall." Clin Haematol **14**(2): 513-530.

Estreicher, A., J. Muhlhauser, et al. (1990). "The receptor for urokinase type plasminogen activator polarizes expression of the protease to the leading edge of migrating monocytes and promotes degradation of enzyme inhibitor complexes." J Cell Biol **111**(2): 783-792.

Estreicher, A., A. Wohlwend, et al. (1989). "Characterization of the cellular binding site for the urokinase-type plasminogen activator." Journal of Biological Chemistry **264**(2): 1180-1189.

Estreicher, A., A. Wohlwend, et al. (1989). "Characterization of the cellular binding site for the urokinase-type plasminogen activator." J Biol Chem **264**(2): 1180-1189.

Fazioli, F., M. Resnati, et al. (1997). "A urokinase-sensitive region of the human urokinase receptor is responsible for its chemotactic activity." EMBO J **16**(24): 7279-7286.

Fernebro, E., R. R. Madsen, et al. (2001). "Prognostic importance of the soluble plasminogen activator receptor, suPAR, in plasma from rectal cancer patients." Eur J Cancer **37**(4): 486-491.

Fiore, M. M., P. F. Neuenschwander, et al. (1992). "An unusual antibody that blocks tissue factor/factor VIIa function by inhibiting cleavage only of macromolecular substrates." Blood **80**(12): 3127-3134.

Fong, S., M. V. Doyle, et al. (2002). "Random peptide bacteriophage display as a probe for urokinase receptor ligands." Biol Chem **383**(1): 149-158.

Garcia-Monco, J. C., J. L. Coleman, et al. (2002). "Soluble urokinase receptor (uPAR, CD 87) is present in serum and cerebrospinal fluid in patients with neurologic diseases." J Neuroimmunol **129**(1-2): 216-223.

Gardsvoll, H. and M. Ploug (2007). "Mapping of the vitronectin-binding site on the urokinase receptor: involvement of a coherent receptor interface consisting of

residues from both domain I and the flanking interdomain linker region." J Biol Chem **282**(18): 13561-13572.
Gargiulo, L., I. Longanesi-Cattani, et al. (2005). "Cross-talk between fMLP and vitronectin receptors triggered by urokinase receptor-derived SRSRY peptide." J Biol Chem **280**(26): 25225-25232.
Ge, Y. and M. T. Elghetany (2003). "Urokinase plasminogen activator receptor (CD87): something old, something new." Lab Hematol **9**(2): 67-71.
Giancotti, F. G. and E. Ruoslahti (1999). "Integrin signaling." Science **285**(5430): 1028-1032.
Ginsburg, D., R. Zeheb, et al. (1986). "cDNA cloning of human plasminogen activator-inhibitor from endothelial cells." J Clin Invest **78**(6): 1673-1680.
Gondi, C. S., N. Kandhukuri, et al. (2007). "Down-regulation of uPAR and uPA activates caspase-mediated apoptosis and inhibits the PI3K/AKT pathway." Int J Oncol **31**(1): 19-27.
Gondi, C. S., S. S. Lakka, et al. (2004). "Adenovirus-mediated expression of antisense urokinase plasminogen activator receptor and antisense cathepsin B inhibits tumor growth, invasion, and angiogenesis in gliomas." Cancer Res **64**(12): 4069-4077.
Griffith, M. J., L. Breitkreutz, et al. (1985). "Characterization of the clotting activities of structurally different forms of activated factor IX. Enzymatic properties of normal human factor IXa alpha, factor IXa beta, and activated factor IX Chapel Hill." J Clin Invest **75**(1): 4-10.
Grondahl-Hansen, J., H. A. Peters, et al. (1995). "Prognostic significance of the receptor for urokinase plasminogen activator in breast cancer." Clin Cancer Res **1**(10): 1079-1087.
Gueler, F., S. Rong, et al. (2008). "Renal urokinase-type plasminogen activator (uPA) receptor but not uPA deficiency strongly attenuates ischemia reperfusion injury and acute kidney allograft rejection." J Immunol **181**(2): 1179-1189.
Gyetko, M. R., R. F. Todd, 3rd, et al. (1994). "The urokinase receptor is required for human monocyte chemotaxis in vitro." J Clin Invest **93**(4): 1380-1387.
Hanahan, D. and R. A. Weinberg (2000). "The hallmarks of cancer." Cell **100**(1): 57-70.
Henic, E., M. Sixt, et al. (2006). "EGF-stimulated migration in ovarian cancer cells is associated with decreased internalization, increased surface expression, and increased shedding of the urokinase plasminogen activator receptor." Gynecologic Oncology **101**(1): 28-39.
Hillig, T., L. H. Engelholm, et al. (2008). "A composite role of vitronectin and urokinase in the modulation of cell morphology upon expression of the urokinase receptor." J Biol Chem **283**(22): 15217-15223.
Horn, I. R., B. M. van den Berg, et al. (1997). "Molecular analysis of ligand binding to the second cluster of complement-type repeats of the low density lipoprotein receptor-related protein. Evidence for an allosteric component in receptor-associated protein-mediated inhibition of ligand binding." J Biol Chem **272**(21): 13608-13613.
Hoyer-Hansen, G., N. Behrendt, et al. (1997). "The intact urokinase receptor is required for efficient vitronectin binding: receptor cleavage prevents ligand interaction." FEBS Lett **420**(1): 79-85.

Hoyer-Hansen, G., U. Pessara, et al. (2001). "Urokinase-catalysed cleavage of the urokinase receptor requires an intact glycolipid anchor." Biochemical Journal **358**(Pt 3): 673-679.

Hoyer-Hansen, G., U. Pessara, et al. (2001). "Urokinase-catalysed cleavage of the urokinase receptor requires an intact glycolipid anchor." Biochem J **358**(Pt 3): 673-679.

Hoyer-Hansen, G., M. Ploug, et al. (1997). "Cell-surface acceleration of urokinase-catalyzed receptor cleavage." Eur J Biochem **243**(1-2): 21-26.

Hoyer-Hansen, G., E. Ronne, et al. (1992). "Urokinase plasminogen activator cleaves its cell surface receptor releasing the ligand-binding domain." J Biol Chem **267**(25): 18224-18229.

Huai, Q., A. P. Mazar, et al. (2006). "Structure of human urokinase plasminogen activator in complex with its receptor." Science **311**(5761): 656-659.

Huai, Q., A. Zhou, et al. (2008). "Crystal structures of two human vitronectin, urokinase and urokinase receptor complexes." Nat Struct Mol Biol **15**(4): 422-423.

Jain, R. K. and P. F. Carmeliet (2001). "Vessels of death or life." Sci Am **285**(6): 38-45.

Janicke, F., M. Schmitt, et al. (1991). "Clinical relevance of the urokinase-type and tissue-type plasminogen activators and of their type 1 inhibitor in breast cancer." Semin Thromb Hemost **17**(3): 303-312.

Jedrychowski, M. P., C. A. Gartner, et al. (2010). "Proteomic analysis of GLUT4 storage vesicles reveals LRP1 to be an important vesicle component and target of insulin signaling." J Biol Chem **285**(1): 104-114.

Jo, M., S. Takimoto, et al. (2009). "The Urokinase Receptor Promotes Cancer Metastasis Independently of Urokinase-Type Plasminogen Activator in Mice." Am J Pathol.

Jo, M., K. S. Thomas, et al. (2005). "Dynamic assembly of the urokinase-type plasminogen activator signaling receptor complex determines the mitogenic activity of urokinase-type plasminogen activator." J Biol Chem **280**(17): 17449-17457.

Jo, M., K. S. Thomas, et al. (2003). "Epidermal growth factor receptor-dependent and -independent cell-signaling pathways originating from the urokinase receptor." J Biol Chem **278**(3): 1642-1646.

Juhan-Vague, I., M. C. Alessi, et al. (1991). "Increased plasma plasminogen activator inhibitor 1 levels. A possible link between insulin resistance and atherothrombosis." Diabetologia **34**(7): 457-462.

Kasperska-Zajac, A. and B. Rogala (2005). "Circulating levels of urokinase-type plasminogen activator (uPA) and its soluble receptor (suPAR) in patients with atopic eczema/dermatitis syndrome." Inflammation **29**(2-3): 90-93.

Kettner, C. and E. Shaw (1979). "The susceptibility of urokinase to affinity labeling by peptides of arginine chloromethyl ketone." Biochimica et Biophysica Acta **569**(1): 31-40.

Kiyan, J., R. Kiyan, et al. (2005). "Urokinase-induced signaling in human vascular smooth muscle cells is mediated by PDGFR-beta." EMBO J **24**(10): 1787-1797.

Kjoller, L. and A. Hall (2001). "Rac mediates cytoskeletal rearrangements and increased cell motility induced by urokinase-type plasminogen activator receptor binding to vitronectin." J Cell Biol **152**(6): 1145-1157.

Korty, P. E., C. Brando, et al. (1991). "CD59 functions as a signal-transducing molecule for human T cell activation." J Immunol **146**(12): 4092-4098.

Koshelnick, Y., M. Ehart, et al. (1997). "Urokinase receptor is associated with the components of the JAK1/STAT1 signaling pathway and leads to activation of this pathway upon receptor clustering in the human kidney epithelial tumor cell line TCL-598." J Biol Chem **272**(45): 28563-28567.

Kotzsch, M., A. M. Sieuwerts, et al. (2008). "Urokinase receptor splice variant uPAR-del4/5-associated gene expression in breast cancer: identification of rab31 as an independent prognostic factor." Breast Cancer Res Treat **111**(2): 229-240.

Kounnas, M. Z., F. C. Church, et al. (1996). "Cellular internalization and degradation of antithrombin III-thrombin, heparin cofactor II-thrombin, and alpha 1-antitrypsin-trypsin complexes is mediated by the low density lipoprotein receptor-related protein." J Biol Chem **271**(11): 6523-6529.

Kunigal, S., S. S. Lakka, et al. (2007). "RNAi-mediated downregulation of urokinase plasminogen activator receptor and matrix metalloprotease-9 in human breast cancer cells results in decreased tumor invasion, angiogenesis and growth." Int J Cancer **121**(10): 2307-2316.

Laemmli, U. K. (1970). "Cleavage of structural proteins during the assembly of the head of bacteriophage T4." Nature **227**(5259): 680-685.

Lakka, S. S., R. Rajagopal, et al. (2001). "Adenovirus-mediated antisense urokinase-type plasminogen activator receptor gene transfer reduces tumor cell invasion and metastasis in non-small cell lung cancer cell lines." Clin Cancer Res **7**(4): 1087-1093.

Lengyel, E., E. Stepp, et al. (1995). "Involvement of a mitogen-activated protein kinase signaling pathway in the regulation of urokinase promoter activity by c-Ha-ras." J Biol Chem **270**(39): 23007-23012.

Li, H., A. Kuo, et al. (1994). "Endocytosis of urokinase-plasminogen activator inhibitor type 1 complexes bound to a chimeric transmembrane urokinase receptor." Journal of Biological Chemistry **269**(11): 8153-8158.

Lindberg, P., A. Larsson, et al. (2006). "Expression of plasminogen activator inhibitor-1, urokinase receptor and laminin gamma-2 chain is an early coordinated event in incipient oral squamous cell carcinoma." Int J Cancer **118**(12): 2948-2956.

Liu, D., J. Aguirre Ghiso, et al. (2002). "EGFR is a transducer of the urokinase receptor initiated signal that is required for in vivo growth of a human carcinoma." Cancer Cell **1**(5): 445-457.

Liu, K., Y. X. Liu, et al. (1997). "Temporal expression of urokinase type plasminogen activator, tissue type plasminogen activator, plasminogen activator inhibitor type 1 in rhesus monkey corpus luteum during the luteal maintenance and regression." Mol Cell Endocrinol **133**(2): 109-116.

Llinas, P., M. H. Le Du, et al. (2005). "Crystal structure of the human urokinase plasminogen activator receptor bound to an antagonist peptide." EMBO J **24**(9): 1655-1663.

Ma, Z., K. S. Thomas, et al. (2002). "Regulation of Rac1 activation by the low density lipoprotein receptor-related protein." Journal of Cell Biology **159**(6): 1061-1070.

Ma, Z., D. J. Webb, et al. (2001). "Endogenously produced urokinase-type plasminogen activator is a major determinant of the basal level of activated ERK/MAP kinase

and prevents apoptosis in MDA-MB-231 breast cancer cells." J Cell Sci **114**(Pt 18): 3387-3396.

Madsen, C. D., G. M. Ferraris, et al. (2007). "uPAR-induced cell adhesion and migration: vitronectin provides the key." J Cell Biol **177**(5): 927-939.

Madsen, C. D. and N. Sidenius (2008). "The interaction between urokinase receptor and vitronectin in cell adhesion and signalling." Eur J Cell Biol **87**(8-9): 617-629.

Manchanda, N. and B. S. Schwartz (1990). "Lipopolysaccharide-induced modulation of human monocyte urokinase production and activity." J Immunol **145**(12): 4174-4180.

Manchanda, N. and B. S. Schwartz (1991). "Single chain urokinase. Augmentation of enzymatic activity upon binding to monocytes." J Biol Chem **266**(22): 14580-14584.

Manchanda, N. and B. S. Schwartz (1991). "Single chain urokinase. Augmentation of enzymatic activity upon binding to monocytes." Journal of Biological Chemistry **266**(22): 14580-14584.

Margheri, F., S. D'Alessio, et al. (2005). "Effects of blocking urokinase receptor signaling by antisense oligonucleotides in a mouse model of experimental prostate cancer bone metastases." Gene Ther **12**(8): 702-714.

Margheri, F., M. Manetti, et al. (2006). "Domain 1 of the urokinase-type plasminogen activator receptor is required for its morphologic and functional, beta2 integrin-mediated connection with actin cytoskeleton in human microvascular endothelial cells: failure of association in systemic sclerosis endothelial cells." Arthritis Rheum **54**(12): 3926-3938.

Mazar, A. P. (2001). "The urokinase plasminogen activator receptor (uPAR) as a target for the diagnosis and therapy of cancer." Anticancer Drugs **12**(5): 387-400.

Mazzieri, R. and F. Blasi (2005). "The urokinase receptor and the regulation of cell proliferation." Thromb Haemost **93**(4): 641-646.

Mazzieri, R., S. D'Alessio, et al. (2006). "An uncleavable uPAR mutant allows dissection of signaling pathways in uPA-dependent cell migration." Mol Biol Cell **17**(1): 367-378.

Miles, L. A., E. G. Levin, et al. (1988). "Plasminogen receptors, urokinase receptors, and their modulation on human endothelial cells." Blood **72**(2): 628-635.

Miles, L. A. and E. F. Plow (1987). "Receptor mediated binding of the fibrinolytic components, plasminogen and urokinase, to peripheral blood cells." Thromb Haemost **58**(3): 936-942.

Mitra, S. K. and D. D. Schlaepfer (2006). "Integrin-regulated FAK-Src signaling in normal and cancer cells." Curr Opin Cell Biol **18**(5): 516-523.

Mohan, P. M., S. S. Lakka, et al. (1999). "Downregulation of the urokinase-type plasminogen activator receptor through inhibition of translation by antisense oligonucleotide suppresses invasion of human glioblastoma cells." Clin Exp Metastasis **17**(7): 617-621.

Moller, L. B., M. Ploug, et al. (1992). "Structural requirements for glycosyl-phosphatidylinositol-anchor attachment in the cellular receptor for urokinase plasminogen activator." Eur J Biochem **208**(2): 493-500.

Moller, L. B., J. Pollanen, et al. (1993). "N-linked glycosylation of the ligand-binding domain of the human urokinase receptor contributes to the affinity for its ligand." J Biol Chem **268**(15): 11152-11159.

Montuori, N., M. V. Carriero, et al. (2002). "The cleavage of the urokinase receptor regulates its multiple functions." J Biol Chem **277**(49): 46932-46939.

Montuori, N., M. V. Carriero, et al. (2002). "The cleavage of the urokinase receptor regulates its multiple functions." Journal of Biological Chemistry **277**(49): 46932-46939.

Montuori, N., A. Mattiello, et al. (2001). "Urokinase-type plasminogen activator up-regulates the expression of its cellular receptor through a post-transcriptional mechanism." FEBS Lett **508**(3): 379-384.

Montuori, N., A. Mattiello, et al. (2003). "Urokinase-mediated posttranscriptional regulation of urokinase-receptor expression in non small cell lung carcinoma." Int J Cancer **105**(3): 353-360.

Montuori, N., G. Rossi, et al. (1999). "Cleavage of urokinase receptor regulates its interaction with integrins in thyroid cells." FEBS Lett **460**(1): 32-36.

Montuori, N., G. Rossi, et al. (1999). "Cleavage of urokinase receptor regulates its interaction with integrins in thyroid cells." FEBS Letters **460**(1): 32-36.

Mukhina, S., V. Stepanova, et al. (2000). "The chemotactic action of urokinase on smooth muscle cells is dependent on its kringle domain. Characterization of interactions and contribution to chemotaxis." J Biol Chem **275**(22): 16450-16458.

Murphy, L. O., S. Smith, et al. (2002). "Molecular interpretation of ERK signal duration by immediate early gene products." Nat Cell Biol **4**(8): 556-564.

Mustjoki, S., R. Alitalo, et al. (1999). "Blast cell-surface and plasma soluble urokinase receptor in acute leukemia patients: relationship to classification and response to therapy." Thromb Haemost **81**(5): 705-710.

Mustjoki, S., N. Sidenius, et al. (2000). "Soluble urokinase receptor levels correlate with number of circulating tumor cells in acute myeloid leukemia and decrease rapidly during chemotherapy." Cancer Res **60**(24): 7126-7132.

Nau, F., C. Guerin-Dubiard, et al. (2003). "Cloning and characterization of HEP21, a new member of the uPAR/Ly6 protein superfamily predominantly expressed in hen egg white." Poult Sci **82**(2): 242-250.

Needham, G. K., S. Nicholson, et al. (1988). "Relationship of membrane-bound tissue type and urokinase type plasminogen activators in human breast cancers to estrogen and epidermal growth factor receptors." Cancer Res **48**(22): 6603-6607.

Nguyen, D. H., I. M. Hussaini, et al. (1998). "Binding of urokinase-type plasminogen activator to its receptor in MCF-7 cells activates extracellular signal-regulated kinase 1 and 2 which is required for increased cellular motility." Journal of Biological Chemistry **273**(14): 8502-8507.

Nguyen, D. H., I. M. Hussaini, et al. (1998). "Binding of urokinase-type plasminogen activator to its receptor in MCF-7 cells activates extracellular signal-regulated kinase 1 and 2 which is required for increased cellular motility." J Biol Chem **273**(14): 8502-8507.

Nguyen, D. H., D. J. Webb, et al. (2000). "Urokinase-type plasminogen activator stimulates the Ras/Extracellular signal-regulated kinase (ERK) signaling pathway and MCF-7 cell migration by a mechanism that requires focal adhesion kinase,

Src, and Shc. Rapid dissociation of GRB2/Sps-Shc complex is associated with the transient phosphorylation of ERK in urokinase-treated cells." J Biol Chem **275**(25): 19382-19388.

Nielsen, L. S., G. M. Kellerman, et al. (1988). "A 55,000-60,000 Mr receptor protein for urokinase-type plasminogen activator. Identification in human tumor cell lines and partial purification." J Biol Chem **263**(5): 2358-2363.

Nieves, E. C. and N. Manchanda (2010). "A cleavage-resistant urokinase plasminogen activator receptor exhibits dysregulated cell-surface clearance." J Biol Chem **285**(17): 12595-12603.

Nykaer, A. c., E.; Vorum, H.; Hager, H.; Petersen, C.; Roigaard, H.; Min, H.; Vilhardt, F.; Moller, L.; Kornfeld, S.; Gliemann, J. (1998). "Mannose 6-phosphate/insulin-like growth factor-II receptor targets the urokinase recptor to lysosomes via a novel binding interaction." J. Cell Biology **141**(3): 815-828.

Nykjaer, A., M. Conese, et al. (1997). "Recycling of the urokinase receptor upon internalization of the uPA:serpin complexes." EMBO J **16**(10): 2610-2620.

Nykjaer, A., L. Kjoller, et al. (1994). "Regions involved in binding of urokinase-type-1 inhibitor complex and pro-urokinase to the endocytic alpha 2-macroglobulin receptor/low density lipoprotein receptor-related protein. Evidence that the urokinase receptor protects pro-urokinase against binding to the endocytic receptor." J Biol Chem **269**(41): 25668-25676.

Nykjaer, A., L. Kjoller, et al. (1994). "Regions involved in binding of urokinase-type-1 inhibitor complex and pro-urokinase to the endocytic alpha 2-macroglobulin receptor/low density lipoprotein receptor-related protein. Evidence that the urokinase receptor protects pro-urokinase against binding to the endocytic receptor." Journal of Biological Chemistry **269**(41): 25668-25676.

Ossowski, L. (1988). "In vivo invasion of modified chorioallantoic membrane by tumor cells: the role of cell surface-bound urokinase." J Cell Biol **107**(6 Pt 1): 2437-2445.

Ossowski, L. and J. A. Aguirre-Ghiso (2000). "Urokinase receptor and integrin partnership: coordination of signaling for cell adhesion, migration and growth." Curr Opin Cell Biol **12**(5): 613-620.

Ossowski, L., G. Clunie, et al. (1991). "In vivo paracrine interaction between urokinase and its receptor: effect on tumor cell invasion." J Cell Biol **115**(4): 1107-1112.

Pedersen, H., N. Brunner, et al. (1994). "Prognostic impact of urokinase, urokinase receptor, and type 1 plasminogen activator inhibitor in squamous and large cell lung cancer tissue." Cancer Res **54**(17): 4671-4675.

Pedersen, N., M. Schmitt, et al. (1993). "A ligand-free, soluble urokinase receptor is present in the ascitic fluid from patients with ovarian cancer." J Clin Invest **92**(5): 2160-2167.

Piccolella, M., C. Festuccia, et al. (2008). "suPAR, a soluble form of urokinase plasminogen activator receptor, inhibits human prostate cancer cell growth and invasion." Int J Oncol **32**(1): 185-191.

Picone, R., E. L. Kajtaniak, et al. (1989). "Regulation of urokinase receptors in monocytelike U937 cells by phorbol ester phorbol myristate acetate." J Cell Biol **108**(2): 693-702.

Plesner, T., E. Ralfkiaer, et al. (1994). "Expression of the receptor for urokinase-type plasminogen activator in normal and neoplastic blood cells and hematopoietic tissue." Am J Clin Pathol **102**(6): 835-841.

Ploug, M. (1998). "Identification of specific sites involved in ligand binding by photoaffinity labeling of the receptor for the urokinase-type plasminogen activator. Residues located at equivalent positions in uPAR domains I and III participate in the assembly of a composite ligand-binding site." Biochemistry **37**(47): 16494-16505.

Ploug, M. (2003). "Structure-function relationships in the interaction between the urokinase-type plasminogen activator and its receptor." Curr Pharm Des **9**(19): 1499-1528.

Ploug, M. and V. Ellis (1994). "Structure-function relationships in the receptor for urokinase-type plasminogen activator. Comparison to other members of the Ly-6 family and snake venom alpha-neurotoxins." FEBS Lett **349**(2): 163-168.

Ploug, M., V. Ellis, et al. (1994). "Ligand interaction between urokinase-type plasminogen activator and its receptor probed with 8-anilino-1-naphthalenesulfonate. Evidence for a hydrophobic binding site exposed only on the intact receptor." Biochemistry **33**(30): 8991-8997.

Ploug, M., M. Kjalke, et al. (1993). "Localization of the disulfide bonds in the NH2-terminal domain of the cellular receptor for human urokinase-type plasminogen activator. A domain structure belonging to a novel superfamily of glycolipid-anchored membrane proteins." J Biol Chem **268**(23): 17539-17546.

Ploug, M., H. Rahbek-Nielsen, et al. (1998). "Glycosylation profile of a recombinant urokinase-type plasminogen activator receptor expressed in Chinese hamster ovary cells." J Biol Chem **273**(22): 13933-13943.

Plow, E. F., D. E. Freaney, et al. (1986). "The plasminogen system and cell surfaces: evidence for plasminogen and urokinase receptors on the same cell type." J Cell Biol **103**(6 Pt 1): 2411-2420.

Preissner, K. T., S. M. Kanse, et al. (1999). "The dual role of the urokinase receptor system in pericellular proteolysis and cell adhesion: implications for cardiovascular function." Basic Res Cardiol **94**(5): 315-321.

Pyke, C., P. Kristensen, et al. (1991). "Urokinase-type plasminogen activator is expressed in stromal cells and its receptor in cancer cells at invasive foci in human colon adenocarcinomas." Am J Pathol **138**(5): 1059-1067.

Ragno, P., N. Montuori, et al. (1998). "Differential expression of a truncated form of the urokinase-type plasminogen-activator receptor in normal and tumor thyroid cells." Cancer Res **58**(6): 1315-1319.

Rasch, M. G., I. K. Lund, et al. (2008). "Intact and cleaved uPAR forms: diagnostic and prognostic value in cancer." Front Biosci **13**: 6752-6762.

Resnati, M., M. Guttinger, et al. (1996). "Proteolytic cleavage of the urokinase receptor substitutes for the agonist-induced chemotactic effect." EMBO J **15**(7): 1572-1582.

Resnati, M., I. Pallavicini, et al. (2002). "The fibrinolytic receptor for urokinase activates the G protein-coupled chemotactic receptor FPRL1/LXA4R." Proc Natl Acad Sci U S A **99**(3): 1359-1364.

Reuning, U., S. P. Little, et al. (1993). "Molecular cloning of cDNA for the bovine urokinase-type plasminogen activator receptor." Thromb Res **72**(1): 59-70.

Riisbro, R., I. J. Christensen, et al. (2005). "Preoperative plasma soluble urokinase plasminogen activator receptor as a prognostic marker in rectal cancer patients. An EORTC-Receptor and Biomarker Group collaboration." Int J Biol Markers **20**(2): 93-102.

Rodenburg, K. W., L. Kjoller, et al. (1998). "Binding of urokinase-type plasminogen activator-plasminogen activator inhibitor-1 complex to the endocytosis receptors alpha2-macroglobulin receptor/low-density lipoprotein receptor-related protein and very-low-density lipoprotein receptor involves basic residues in the inhibitor." Biochem J **329 (Pt 1)**: 55-63.

Ronne, E., N. Behrendt, et al. (1991). "Cell-induced potentiation of the plasminogen activation system is abolished by a monoclonal antibody that recognizes the NH2-terminal domain of the urokinase receptor." FEBS Lett **288**(1-2): 233-236.

Rothberg, K. G., J. E. Heuser, et al. (1992). "Caveolin, a protein component of caveolae membrane coats." Cell **68**(4): 673-682.

Saksela, O. and D. B. Rifkin (1988). "Cell-associated plasminogen activation: regulation and physiological functions." Annu Rev Cell Biol **4**: 93-126.

Sambrook, J. and D. W. Russell (2006). "SDS-Polyacrylamide Gel Electrophoresis of Proteins." CSH Protoc **2006**(4).

Shetty, S. (2005). "Protein synthesis and urokinase mRNA metabolism." Mol Cell Biochem **271**(1-2): 13-22.

Shetty, S. and S. Idell (1998). "A urokinase receptor mRNA binding protein-mRNA interaction regulates receptor expression and function in human pleural mesothelioma cells." Arch Biochem Biophys **356**(2): 265-279.

Shetty, S., A. Kumar, et al. (1997). "Posttranscriptional regulation of urokinase receptor mRNA: identification of a novel urokinase receptor mRNA binding protein in human mesothelioma cells." Mol Cell Biol **17**(3): 1075-1083.

Shetty, S., H. Muniyappa, et al. (2004). "Regulation of urokinase receptor expression by phosphoglycerate kinase." Am J Respir Cell Mol Biol **31**(1): 100-106.

Shetty, S., G. N. Rao, et al. (2006). "Urokinase induces activation of STAT3 in lung epithelial cells." Am J Physiol Lung Cell Mol Physiol **291**(4): L772-780.

Sidenius, N. and F. Blasi (2000). "Domain 1 of the urokinase receptor (uPAR) is required for uPAR-mediated cell binding to vitronectin." FEBS Lett **470**(1): 40-46.

Sidenius, N. and F. Blasi (2003). "The urokinase plasminogen activator system in cancer: recent advances and implication for prognosis and therapy." Cancer Metastasis Rev **22**(2-3): 205-222.

Sidenius, N., C. F. Sier, et al. (2000). "Shedding and cleavage of the urokinase receptor (uPAR): identification and characterisation of uPAR fragments in vitro and in vivo." FEBS Lett **475**(1): 52-56.

Sidenius, N., C. F. Sier, et al. (2000). "Serum level of soluble urokinase-type plasminogen activator receptor is a strong and independent predictor of survival in human immunodeficiency virus infection." Blood **96**(13): 4091-4095.

Sier, C. F., I. Nicoletti, et al. (2004). "Metabolism of tumour-derived urokinase receptor and receptor fragments in cancer patients and xenografted mice." Thromb Haemost **91**(2): 403-411.

Simon, D. I., Y. Wei, et al. (2000). "Identification of a urokinase receptor-integrin interaction site. Promiscuous regulator of integrin function." J Biol Chem **275**(14): 10228-10234.
Sivaraman, V. S., H. Wang, et al. (1997). "Hyperexpression of mitogen-activated protein kinase in human breast cancer." J Clin Invest **99**(7): 1478-1483.
Skriver, L., L. I. Larsson, et al. (1984). "Immunocytochemical localization of urokinase-type plasminogen activator in Lewis lung carcinoma." J Cell Biol **99**(2): 753-757.
Smith, H. W. and C. J. Marshall (2010). "Regulation of cell signalling by uPAR." Nat Rev Mol Cell Biol **11**(1): 23-36.
Soravia, E., A. Grebe, et al. (1995). "A conserved TATA-less proximal promoter drives basal transcription from the urokinase-type plasminogen activator receptor gene." Blood **86**(2): 624-635.
Stahl, A. and B. M. Mueller (1995). "The urokinase-type plasminogen activator receptor, a GPI-linked protein, is localized in caveolae." J Cell Biol **129**(2): 335-344.
Stan, R. V. (2007). "Endothelial stomatal and fenestral diaphragms in normal vessels and angiogenesis." J Cell Mol Med **11**(4): 621-643.
Stefanova, I., V. Horejsi, et al. (1991). "GPI-anchored cell-surface molecules complexed to protein tyrosine kinases." Science **254**(5034): 1016-1019.
Stepanova, V. V. and V. A. Tkachuk (2002). "Urokinase as a multidomain protein and polyfunctional cell regulator." Biochemistry (Mosc) **67**(1): 109-118.
Stephens, R. W., H. J. Nielsen, et al. (1999). "Plasma urokinase receptor levels in patients with colorectal cancer: relationship to prognosis." J Natl Cancer Inst **91**(10): 869-874.
Stoppelli, M. P., A. Corti, et al. (1985). "Differentiation-enhanced binding of the amino-terminal fragment of human urokinase plasminogen activator to a specific receptor on U937 monocytes." Proc Natl Acad Sci U S A **82**(15): 4939-4943.
Tang, P. F., G. A. Burke, et al. (2009). "Patients with long bone fracture have altered Caveolin-1 expression in their peripheral blood mononuclear cells." Arch Orthop Trauma Surg **129**(9): 1287-1292.
Temerinac, S., S. Klippel, et al. (2000). "Cloning of PRV-1, a novel member of the uPAR receptor superfamily, which is overexpressed in polycythemia rubra vera." Blood **95**(8): 2569-2576.
Tkachuk, V. A., V. V. Stepanova, et al. (1998). "[Involvement of urokinase and its receptor in the remodeling of normal and pathological tissue]." Vestn Ross Akad Med Nauk(8): 36-41.
Tran, H., F. Maurer, et al. (2003). "Stabilization of urokinase and urokinase receptor mRNAs by HuR is linked to its cytoplasmic accumulation induced by activated mitogen-activated protein kinase-activated protein kinase 2." Mol Cell Biol **23**(20): 7177-7188.
Tummalapalli, P., C. S. Gondi, et al. (2007). "RNA interference-mediated targeting of urokinase plasminogen activator receptor and matrix metalloproteinase-9 gene expression in the IOMM-lee malignant meningioma cell line inhibits tumor growth, tumor cell invasion and angiogenesis." Int J Oncol **31**(1): 5-17.
Vassalli, J. D., D. Baccino, et al. (1985). "A cellular binding site for the Mr 55,000 form of the human plasminogen activator, urokinase." J Cell Biol **100**(1): 86-92.

Wahlberg, K., G. Hoyer-Hansen, et al. (1998). "Soluble receptor for urokinase plasminogen activator in both full-length and a cleaved form is present in high concentration in cystic fluid from ovarian cancer." Cancer Res **58**(15): 3294-3298.

Waltz, D. A. and H. A. Chapman (1994). "Reversible cellular adhesion to vitronectin linked to urokinase receptor occupancy." J Biol Chem **269**(20): 14746-14750.

Waltz, D. A., L. R. Natkin, et al. (1997). "Plasmin and plasminogen activator inhibitor type 1 promote cellular motility by regulating the interaction between the urokinase receptor and vitronectin." J Clin Invest **100**(1): 58-67.

Wang, G. J., M. Collinge, et al. (1998). "Posttranscriptional regulation of urokinase plasminogen activator receptor messenger RNA levels by leukocyte integrin engagement." Proc Natl Acad Sci U S A **95**(11): 6296-6301.

Wang, H. Y., L. Ma, et al. (2001). "The role of nitric oxide on cigarette smoke-induced programmed cell death in the gastric mucosa." Scand J Gastroenterol **36**(3): 235-240.

Wang, Y. (2001). "The role and regulation of urokinase-type plasminogen activator receptor gene expression in cancer invasion and metastasis." Med Res Rev **21**(2): 146-170.

Wang, Y., J. Dang, et al. (2000). "Identification of a novel nuclear factor-kappaB sequence involved in expression of urokinase-type plasminogen activator receptor." Eur J Biochem **267**(11): 3248-3254.

Wang, Y., B. Mao, et al. (2001). "[Expression and significance of urokinase-type plasminogen activator in medulloblastoma]." Hua Xi Yi Ke Da Xue Xue Bao **32**(3): 376-378.

Weber, J. D., W. Hu, et al. (1997). "Ras-stimulated extracellular signal-related kinase 1 and RhoA activities coordinate platelet-derived growth factor-induced G1 progression through the independent regulation of cyclin D1 and p27." J Biol Chem **272**(52): 32966-32971.

Wei, Y., R. P. Czekay, et al. (2005). "Regulation of alpha5beta1 integrin conformation and function by urokinase receptor binding." J Cell Biol **168**(3): 501-511.

Wei, Y., J. A. Eble, et al. (2001). "Urokinase receptors promote beta1 integrin function through interactions with integrin alpha3beta1." Mol Biol Cell **12**(10): 2975-2986.

Wei, Y., M. Lukashev, et al. (1996). "Regulation of integrin function by the urokinase receptor." Science **273**(5281): 1551-1555.

Wei, Y., C. H. Tang, et al. (2007). "Urokinase receptors are required for alpha 5 beta 1 integrin-mediated signaling in tumor cells." J Biol Chem **282**(6): 3929-3939.

Wei, Y., D. A. Waltz, et al. (1994). "Identification of the urokinase receptor as an adhesion receptor for vitronectin." J Biol Chem **269**(51): 32380-32388.

Wei, Y., X. Yang, et al. (1999). "A role for caveolin and the urokinase receptor in integrin-mediated adhesion and signaling." J Cell Biol **144**(6): 1285-1294.

Wei, Y. L., Matvey; Simon, Daniel I.; Bodary, Sarah C.; Chapman, H. A. (1996). "Regulation of Integrin Function by the Urokinase receptor." Science **273**(5281): 1551-1555.

Williams, S. E., J. D. Ashcom, et al. (1992). "A novel mechanism for controlling the activity of alpha 2-macroglobulin receptor/low density lipoprotein receptor-

related protein. Multiple regulatory sites for 39-kDa receptor-associated protein." J Biol Chem **267**(13): 9035-9040.

Wu, L. and S. L. Gonias (2005). "The low-density lipoprotein receptor-related protein-1 associates transiently with lipid rafts." J Cell Biochem **96**(5): 1021-1033.

Xu, X., H. Gardsvoll, et al. (2012). "Crystal structure of the urokinase receptor in a ligand-free form." J Mol Biol **416**(5): 629-641.

Yamamoto, M., R. Sawaya, et al. (1994). "Expression and localization of urokinase-type plasminogen activator receptor in human gliomas." Cancer Res **54**(18): 5016-5020.

Yanamandra, N., S. D. Konduri, et al. (2000). "Downregulation of urokinase-type plasminogen activator receptor (uPAR) induces caspase-mediated cell death in human glioblastoma cells." Clin Exp Metastasis **18**(7): 611-615.

Yebra, M., L. Goretzki, et al. (1999). "Urokinase-type plasminogen activator binding to its receptor stimulates tumor cell migration by enhancing integrin-mediated signal transduction." Exp Cell Res **250**(1): 231-240.

Yu, W., J. Kim, et al. (1997). "Reduction in surface urokinase receptor forces malignant cells into a protracted state of dormancy." J Cell Biol **137**(3): 767-777.

Yuan, C. and M. Huang (2007). "Does the urokinase receptor exist in a latent form?" Cell Mol Life Sci **64**(9): 1033-1037.

Zhang, J., S. Sud, et al. (2011). "Activation of urokinase plasminogen activator and its receptor axis is essential for macrophage infiltration in a prostate cancer mouse model." Neoplasia **13**(1): 23-30.

Zhang, J. C., R. Sakthivel, et al. (1998). "The low density lipoprotein receptor-related protein/alpha2-macroglobulin receptor regulates cell surface plasminogen activator activity on human trophoblast cells." J Biol Chem **273**(48): 32273-32280.